

10

Waveguides and Cavity Resonators

10-1 Introduction

In the preceding chapter we studied the characteristic properties of transverse electromagnetic (TEM) waves guided by transmission lines. The TEM mode of guided waves is one in which the electric and magnetic fields are perpendicular to each other and both are transverse to the direction of propagation along the guiding line. One of the salient properties of TEM waves guided by conducting lines of negligible resistance is that the velocity of propagation of a wave of any frequency is the same as that in an unbounded dielectric medium. This was pointed out in connection with Eq. (9-21) and was reinforced by Eq. (9-72).

TEM waves, however, are not the only mode of guided waves that can propagate on transmission lines; nor are the three types of transmission lines (parallel-plate, two-wire, and coaxial) mentioned in Section 9-1 the only possible wave-guiding structures. As a matter of fact, we see from Eqs. (9-55) and (9-63) that the attenuation constant resulting from the finite conductivity of the lines increases with R , the resistance per unit line length, which, in turn, is proportional to \sqrt{f} in accordance with Tables 9-1 and 9-2. Hence the attenuation of TEM waves tends to increase monotonically with frequency and would be prohibitively high in the microwave range.

In this chapter we first present a general analysis of the characteristics of the waves propagating along uniform guiding structures. Waveguiding structures are called *waveguides*, of which the three types of transmission lines are special cases. The basic governing equations will be examined. We will see that, in addition to *transverse electromagnetic (TEM) waves*, which have no field components in the direction of propagation, both *transverse magnetic (TM) waves* with a longitudinal electric-field component and *transverse electric (TE) waves* with a longitudinal magnetic-field component can also exist. Both TM and TE modes have characteristic *cutoff frequencies*. Waves of frequencies below the cutoff frequency of a particular mode cannot propagate, and power and signal transmission at that mode is possible

only for frequencies higher than the cutoff frequency. Thus waveguides operating in TM and TE modes are like high-pass filters.

Also in this chapter we will reexamine the field and wave characteristics of parallel-plate waveguides with emphasis on TM and TE modes and show that all transverse field components can be expressed in terms of E_z (z being the direction of propagation) for TM waves and in terms of H_z for TE waves. The attenuation constants resulting from imperfectly conducting walls will be determined for TM and TE waves, and we will find that the attenuation constant depends, in a complicated way, on the mode of the propagating wave, as well as on frequency. For some modes the attenuation may decrease as the frequency increases; for other modes the attenuation may reach a minimum as the frequency exceeds the cutoff frequency by a certain amount.

Electromagnetic waves can propagate through hollow metal pipes of an arbitrary cross section. Without electromagnetic theory it would not be possible to explain the properties of hollow waveguides. We will see that single-conductor waveguides cannot support TEM waves. We will examine in detail the fields, the current and charge distributions, and the propagation and attenuation characteristics of rectangular and circular cylindrical waveguides. Both TM and TE modes will be discussed.

Electromagnetic waves can also be guided by an open dielectric-slab waveguide. The fields are essentially confined within the dielectric region and decay rapidly away from the slab surface in the transverse plane. For this reason the waves supported by a dielectric-slab waveguide are called *surface waves*. Both TM and TE modes are possible. We will examine the field characteristics and cutoff frequencies of those surface waves. Cylindrical optical fibers will also be discussed.

At microwave frequencies, ordinary lumped-parameter elements (such as inductances and capacitances) connected by wires are no longer practical as circuit elements or as resonant circuits because the dimensions of the elements would have to be extremely small, because the resistance of the wire circuits becomes very high as a result of the skin effect, and because of radiation. We will briefly discuss irises and posts as waveguide reactive elements. A hollow conducting box with proper dimensions can be used as a resonant device. The box walls provide large areas for current flow, and losses are extremely small. Consequently, an enclosed conducting box can be a resonator of a very high Q . Such a box, which is essentially a segment of a waveguide with closed end faces, is called a *cavity resonator*. We will discuss the different mode patterns of the fields inside rectangular as well as circular cylindrical cavity resonators.

10-2 General Wave Behaviors along Uniform Guiding Structures

In this section we examine some general characteristics for waves propagating along straight guiding structures with a uniform cross section. We will assume that the waves propagate in the $+z$ -direction with a propagation constant $\gamma = \alpha + j\beta$ that is yet to be determined. For harmonic time dependence with an angular frequency ω , the dependence on z and t for all field components can be described by the exponential

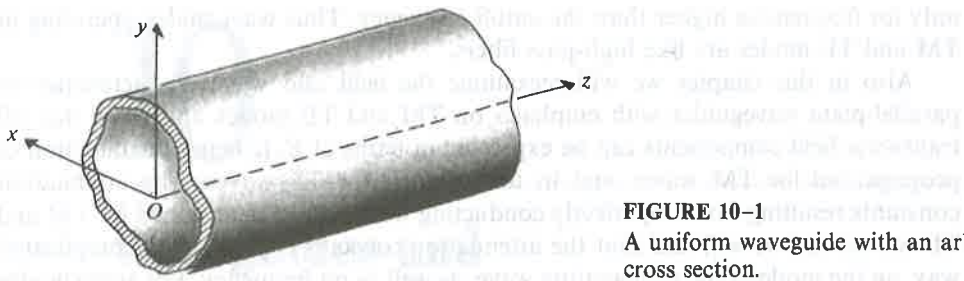


FIGURE 10-1
A uniform waveguide with an arbitrary cross section.

factor

$$e^{-\gamma z} e^{j\omega t} = e^{(j\omega t - \gamma z)} = e^{-\alpha z} e^{j(\omega t - \beta z)}. \quad (10-1)$$

As an example, for a cosine reference we may write the instantaneous expression for the \mathbf{E} field in Cartesian coordinates as

$$\mathbf{E}(x, y, z; t) = \Re[e^0(x, y)e^{(j\omega t - \gamma z)}], \quad (10-2)$$

where $E^0(x, y)$ is a two-dimensional vector phasor that depends only on the cross-sectional coordinates. The instantaneous expression for the \mathbf{H} field can be written in a similar way. Hence, in using a phasor representation in equations relating field quantities we may replace partial derivatives with respect to t and z simply by products with $(j\omega)$ and $(-\gamma)$, respectively; the common factor $e^{(j\omega t - \gamma z)}$ can be dropped.

We consider a straight waveguide in the form of a dielectric-filled metal tube having an arbitrary cross section and lying along the z -axis, as shown in Fig. 10-1. According to Eqs. (7-105) and (7-106), the electric and magnetic field intensities in the charge-free dielectric region inside satisfy the following homogeneous vector Helmholtz's equations:

$$\nabla^2 \mathbf{E} + k^2 \mathbf{E} = 0 \quad (10-3)$$

and

$$\nabla^2 \mathbf{H} + k^2 \mathbf{H} = 0, \quad (10-4)$$

where \mathbf{E} and \mathbf{H} are three-dimensional vector phasors, and k is the wavenumber:

$$k = \omega \sqrt{\mu \epsilon}. \quad (10-5)$$

The three-dimensional Laplacian operator ∇^2 may be broken into two parts: $\nabla_{u_1 u_2}^2$ for the cross-sectional coordinates and ∇_z^2 for the longitudinal coordinate. For waveguides with a rectangular cross section we use Cartesian coordinates:

$$\begin{aligned} \nabla^2 \mathbf{E} &= (\nabla_{xy}^2 + \nabla_z^2) \mathbf{E} = \left(\nabla_{xy}^2 + \frac{\partial^2}{\partial z^2} \right) \mathbf{E} \\ &= \nabla_{xy}^2 \mathbf{E} + \gamma^2 \mathbf{E}. \end{aligned} \quad (10-6)$$

Combination of Eqs. (10-3) and (10-6) gives

$$\nabla_{xy}^2 \mathbf{E} + (\gamma^2 + k^2) \mathbf{E} = 0. \quad (10-7)$$

Similarly, from Eq. (10-4) we have

$$\nabla_{xy}^2 \mathbf{H} + (\gamma^2 + k^2) \mathbf{H} = 0. \quad (10-8)$$

We note that each of Eqs. (10-7) and (10-8) is really three second-order partial differential equations, one for each component of \mathbf{E} and \mathbf{H} . The exact solution of these component equations depends on the cross-sectional geometry and the boundary conditions that a particular field component must satisfy at conductor-dielectric interfaces. We note further that by writing $\nabla_{r\phi}^2$ for the transversal operator ∇_{xy}^2 , Eqs. (10-7) and (10-8) become the governing equations for waveguides with a circular cross section.

Of course, the various components of \mathbf{E} and \mathbf{H} are not all independent, and it is not necessary to solve all six second-order partial differential equations for the six components of \mathbf{E} and \mathbf{H} . Let us examine the interrelationships among the six components in Cartesian coordinates by expanding the two source-free curl equations, Eqs. (7-104a) and (7-104b):

From $\nabla \times \mathbf{E} = -j\omega\mu\mathbf{H}$:	From $\nabla \times \mathbf{H} = j\omega\epsilon\mathbf{E}$:
$\frac{\partial E_z^0}{\partial y} + \gamma E_y^0 = -j\omega\mu H_x^0 \quad (10-9a)$	$\frac{\partial H_z^0}{\partial y} + \gamma H_y^0 = j\omega\epsilon E_x^0 \quad (10-10a)$
$-\gamma E_x^0 - \frac{\partial E_z^0}{\partial x} = -j\omega\mu H_y^0 \quad (10-9b)$	$-\gamma H_x^0 - \frac{\partial H_z^0}{\partial x} = j\omega\epsilon E_y^0 \quad (10-10b)$
$\frac{\partial E_y^0}{\partial x} - \frac{\partial E_x^0}{\partial y} = -j\omega\mu H_z^0 \quad (10-9c)$	$\frac{\partial H_y^0}{\partial x} - \frac{\partial H_x^0}{\partial y} = j\omega\epsilon E_z^0 \quad (10-10c)$

Note that partial derivatives with respect to z have been replaced by multiplications by $(-\gamma)$. All the component field quantities in the equations above are phasors that depend only on x and y , the common $e^{-\gamma z}$ factor for z -dependence having been omitted. By manipulating these equations we can express the transverse field components H_x^0 , H_y^0 , and E_x^0 , and E_y^0 in terms of the two longitudinal components E_z^0 and H_z^0 . For instance, Eqs. (10-9a) and (10-10b) can be combined to eliminate E_y^0 and obtain H_x^0 in terms of E_z^0 and H_z^0 . We have

$$H_x^0 = -\frac{1}{h^2} \left(\gamma \frac{\partial H_z^0}{\partial x} - j\omega\epsilon \frac{\partial E_z^0}{\partial y} \right), \quad (10-11)$$

$$H_y^0 = -\frac{1}{h^2} \left(\gamma \frac{\partial H_z^0}{\partial y} + j\omega\epsilon \frac{\partial E_z^0}{\partial x} \right), \quad (10-12)$$

$$E_x^0 = -\frac{1}{h^2} \left(\gamma \frac{\partial E_z^0}{\partial x} + j\omega\mu \frac{\partial H_z^0}{\partial y} \right), \quad (10-13)$$

$$E_y^0 = -\frac{1}{h^2} \left(\gamma \frac{\partial E_z^0}{\partial y} - j\omega\mu \frac{\partial H_z^0}{\partial x} \right), \quad (10-14)$$

where

$$h^2 = \gamma^2 + k^2. \quad (10-15)$$

The wave behavior in a waveguide can be analyzed by solving Eqs. (10-7) and (10-8) for the longitudinal components, E_z^0 and H_z^0 , respectively, subject to the required boundary conditions, and then by using Eqs. (10-11) through (10-14) to determine the other components.

It is convenient to classify the propagating waves in a uniform waveguide into three types according to whether E_z or H_z exists.

1. *Transverse electromagnetic (TEM) waves.* These are waves that contain neither E_z nor H_z . We encountered TEM waves in Chapter 8 when we discussed plane waves and in Chapter 9 on waves along transmission lines.
2. *Transverse magnetic (TM) waves.* These are waves that contain a nonzero E_z but $H_z = 0$.
3. *Transverse electric (TE) waves.* These are waves that contain a nonzero H_z but $E_z = 0$.

The propagation characteristics of the various types of waves are different; they will be discussed in subsequent subsections.

10-2.1 TRANSVERSE ELECTROMAGNETIC WAVES

Since $E_z = 0$ and $H_z = 0$ for TEM waves within a guide, we see that Eqs. (10-11) through (10-14) constitute a set of trivial solutions (all field components vanish) unless the denominator h^2 also equals zero. In other words, TEM waves exist only when

$$\gamma_{\text{TEM}}^2 + k^2 = 0 \quad (10-16)$$

or

$$\gamma_{\text{TEM}} = jk = j\omega\sqrt{\mu\epsilon}, \quad (10-17)$$

which is exactly the same expression for the propagation constant of a uniform plane wave in an unbounded medium characterized by constitutive parameters ϵ and μ . We recall that Eq. (10-17) also holds for a TEM wave on a lossless transmission line. It follows that the velocity of propagation (phase velocity) for TEM waves is

$$u_{p(\text{TEM})} = \frac{\omega}{k} = \frac{1}{\sqrt{\mu\epsilon}} \quad (\text{m/s}). \quad (10-18)$$

We can obtain the ratio between E_x^0 and H_y^0 from Eqs. (10-9b) and (10-10a) by setting E_z and H_z to zero. This ratio is called the *wave impedance*. We have

$$Z_{\text{TEM}} = \frac{E_x^0}{H_y^0} = \frac{j\omega\mu}{\gamma_{\text{TEM}}} = \frac{\gamma_{\text{TEM}}}{j\omega\epsilon}, \quad (10-19)$$

(10-15)

(10-7) and (10-8)
to the required
to determine

waveguide into

contain neither
discussed planenonzero E_z but
nonzero H_z but

erent; they will

t Eqs. (10-11)
ponents vanish)
aves exist only

(10-16)

(10-17)

uniform plane
eters ϵ and μ .
s transmission
TEM waves is

(10-18)

d (10-10a) by
e have

(10-19)

which becomes, in view of Eq. (10-17),

$$Z_{\text{TEM}} = \sqrt{\frac{\mu}{\epsilon}} = \eta \quad (\Omega). \quad (10-20)$$

We note that Z_{TEM} is the same as the intrinsic impedance of the dielectric medium, as given in Eq. (8-30). Equations (10-18) and (10-20) assert that *the phase velocity and the wave impedance for TEM waves are independent of the frequency of the waves.*

Letting $E_z^0 = 0$ in Eq. (10-9a) and $H_z^0 = 0$ in Eq. (10-10b), we obtain

$$\frac{E_y^0}{H_x^0} = -Z_{\text{TEM}} = -\sqrt{\frac{\mu}{\epsilon}}. \quad (10-21)$$

Equations (10-19) and (10-21) can be combined to obtain the following formula for a TEM wave propagating in the $+z$ -direction:

$$\mathbf{H} = \frac{1}{Z_{\text{TEM}}} \mathbf{a}_z \times \mathbf{E} \quad (\text{A/m}), \quad (10-22)$$

which again reminds us of a similar relation for a uniform plane wave in an unbounded medium—see Eq. (8-29).

Single-conductor waveguides cannot support TEM waves. In Section 6-2 we pointed out that magnetic flux lines always close upon themselves. Hence if a TEM wave were to exist in a waveguide, the field lines of \mathbf{B} and \mathbf{H} would form closed loops in a transverse plane. However, the generalized Ampère's circuital law, Eq. (7-54b), requires that the line integral of the magnetic field (the magnetomotive force) around any closed loop in a transverse plane must equal the sum of the longitudinal conduction and displacement currents through the loop. Without an inner conductor there is no longitudinal conduction current inside the waveguide. By definition, a TEM wave does not have an E_z -component; consequently, there is no longitudinal displacement current. The total absence of a longitudinal current inside a waveguide leads to the conclusion that there can be no closed loops of magnetic field lines in any transverse plane. Therefore, we conclude that *TEM waves cannot exist in a single-conductor hollow (or dielectric-filled) waveguide of any shape*. On the other hand, *assuming perfect conductors*, a coaxial transmission line having an inner conductor *can* support TEM waves; so can a two-conductor stripline and a two-wire transmission line. When the conductors have losses, waves along transmission lines are strictly no longer TEM, as noted in Section 9-2.

10-2.2 TRANSVERSE MAGNETIC WAVES

Transverse magnetic (TM) waves do not have a component of the magnetic field in the direction of propagation, $H_z = 0$. The behavior of TM waves can be analyzed

by solving Eq. (10-7) for E_z subject to the boundary conditions of the guide and using Eqs. (10-11) through (10-14) to determine the other components. Writing Eq. (10-7) for E_z , we have

$$\nabla_{xy}^2 E_z^0 + (\gamma^2 + k^2) E_z^0 = 0 \quad (10-23)$$

or

$$\boxed{\nabla_{xy}^2 E_z^0 + h^2 E_z^0 = 0.} \quad (10-24)$$

Equation (10-24) is a second-order partial differential equation, which can be solved for E_z^0 . In this section we wish to discuss only the general properties of the various wave types. The actual solution of Eq. (10-24) will wait until subsequent sections when we examine particular waveguides.

For TM waves we set $H_z = 0$ in Eqs. (10-11) through (10-14) to obtain

$$H_x^0 = \frac{j\omega\epsilon}{h^2} \frac{\partial E_z^0}{\partial y}, \quad (10-25)$$

$$H_y^0 = -\frac{j\omega\epsilon}{h^2} \frac{\partial E_z^0}{\partial x}, \quad (10-26)$$

$$E_x^0 = -\frac{\gamma}{h^2} \frac{\partial E_z^0}{\partial x}, \quad (10-27)$$

$$E_y^0 = -\frac{\gamma}{h^2} \frac{\partial E_z^0}{\partial y}. \quad (10-28)$$

It is convenient to combine Eqs. (10-27) and (10-28) and write

$$\boxed{(\mathbf{E}_T^0)_{TM} = \mathbf{a}_x E_x^0 + \mathbf{a}_y E_y^0 = -\frac{\gamma}{h^2} \nabla_T E_z^0 \quad (V/m),} \quad (10-29)$$

where

$$\nabla_T E_z^0 = \left(\mathbf{a}_x \frac{\partial}{\partial x} + \mathbf{a}_y \frac{\partial}{\partial y} \right) E_z^0 \quad (10-30)$$

denotes the gradient of E_z^0 in the transverse plane. Equation (10-29) is a concise formula for finding E_x^0 and E_y^0 from E_z^0 .

The transverse components of magnetic field intensity, H_x^0 and H_y^0 , can be determined simply from E_x^0 and E_y^0 on the introduction of the wave impedance for the TM mode. We have, from Eqs. (10-25) through (10-28),

$$\boxed{Z_{TM} = \frac{E_x^0}{H_y^0} = -\frac{E_y^0}{H_x^0} = \frac{\gamma}{j\omega\epsilon} \quad (\Omega).} \quad (10-31)$$

It is important to note that Z_{TM} is *not* equal to $j\omega\mu/\gamma$, because γ for TM waves, unlike γ_{TEM} , is *not* equal to $j\omega\sqrt{\mu\epsilon}$. The following relation between the electric and magnetic

the guide and
s. Writing Eq.

(10-23)

can be solved
of the various
quent sections

obtain

(10-25)

(10-26)

(10-27)

(10-28)

(10-29)

(10-30)

9) is a concise

, can be deter-
edance for the

(10-31)

M waves, unlike
ic and magnetic

field intensities holds for TM waves:

$$\mathbf{H} = \frac{1}{Z_{\text{TM}}} (\mathbf{a}_z \times \mathbf{E}) \quad (\text{A/m}). \quad (10-32)$$

Equation (10-32) is seen to be of the same form as Eq. (10-22) for TEM waves.

When we undertake to solve the two-dimensional homogeneous Helmholtz equation, Eq. (10-24), subject to the boundary conditions of a given waveguide, we will discover that solutions are possible only for *discrete values of h*. There may be an infinity of these discrete values, but solutions are not possible for all values of h. The values of h for which a solution of Eq. (10-24) exists are called the **characteristic values** or **eigenvalues** of the boundary-value problem. Each of the eigenvalues determines the characteristic properties of a particular TM mode of the given waveguide.

In the following sections we will also discover that the eigenvalues of the various waveguide problems are real numbers. From Eq. (10-15) we have

$$\begin{aligned} \gamma &= \sqrt{h^2 - k^2} \\ &= \sqrt{h^2 - \omega^2 \mu \epsilon}. \end{aligned} \quad (10-33)$$

Two distinct ranges of the values for the propagation constant are noted, the dividing point being $\gamma = 0$, where

$$\omega_c^2 \mu \epsilon = h^2 \quad (10-34)$$

or

$$f_c = \frac{h}{2\pi\sqrt{\mu\epsilon}} \quad (\text{Hz}). \quad (10-35)$$

The frequency, f_c , at which $\gamma = 0$ is called a **cutoff frequency**. The value of f_c for a particular mode in a waveguide depends on the eigenvalue of this mode. Using Eq. (10-35), we can write Eq. (10-33) as

$$\gamma = h \sqrt{1 - \left(\frac{f}{f_c}\right)^2}. \quad (10-36)$$

The two distinct ranges of γ can be defined in terms of the ratio $(f/f_c)^2$ as compared to unity.

a) $\left(\frac{f}{f_c}\right)^2 > 1$, or $f > f_c$. In this range, $\omega^2 \mu \epsilon > h^2$ and γ is imaginary. We have, from Eq. (10-33),

$$\gamma = j\beta = jk \sqrt{1 - \left(\frac{h}{k}\right)^2} = jk \sqrt{1 - \left(\frac{f_c}{f}\right)^2}. \quad (10-37)$$

It is a propagating mode with a phase constant β :

$$\beta = k \sqrt{1 - \left(\frac{f_c}{f}\right)^2} \quad (\text{rad/m}). \quad (10-38)$$

The corresponding wavelength in the guide is

$$\lambda_g = \frac{2\pi}{\beta} = \frac{\lambda}{\sqrt{1 - (f_c/f)^2}} > \lambda, \quad (10-39)$$

where

$$\lambda = \frac{2\pi}{k} = \frac{1}{f\sqrt{\mu\epsilon}} = \frac{u}{f} \quad (10-40)$$

is the wavelength of a plane wave with a frequency f in an unbounded dielectric medium characterized by μ and ϵ , and $u = 1/\sqrt{\mu\epsilon}$ is the velocity of light in the medium. Equation (10-39) can be rearranged to give a simple relation connecting λ , the guide wavelength λ_g , and the cutoff wavelength $\lambda_c = u/f_c$:

$$\frac{1}{\lambda^2} = \frac{1}{\lambda_g^2} + \frac{1}{\lambda_c^2}. \quad (10-41)$$

The phase velocity of the propagating wave in the guide is

$$u_p = \frac{\omega}{\beta} = \frac{u}{\sqrt{1 - (f_c/f)^2}} = \frac{\lambda_g}{\lambda} u > u. \quad (10-42)$$

We see from Eq. (10-42) that the phase velocity within a waveguide is always higher than that in an unbounded medium and is frequency-dependent. Hence **single-conductor waveguides are dispersive transmission systems**, although an unbounded lossless dielectric medium is nondispersive. The group velocity for a propagating wave in a waveguide can be determined by using Eq. (8-72):

$$u_g = \frac{1}{d\beta/d\omega} = u \sqrt{1 - \left(\frac{f_c}{f}\right)^2} = \frac{\lambda}{\lambda_g} u < u. \quad (10-43)$$

Thus,

$$u_g u_p = u^2. \quad (10-44)$$

For air dielectric, $u = c$, Eq. (10-44) becomes $u_g u_p = c^2$. In a lossless waveguide the velocity of signal propagation (the *velocity of energy transport*) is equal to the group velocity. An illustration of this statement can be found later, in Subsection 10-3.3.

Substitution of Eq. (10-37) in Eq. (10-31) yields

$$Z_{TM} = \eta \sqrt{1 - \left(\frac{f_c}{f}\right)^2} \quad (\Omega). \quad (10-45)$$

(10-38)

(10-39)

(10-40)

(10-41)

(10-42)

undielectric
y of light in the
ation connecting

guide is always
dependent. Hence
ns, although an
up velocity for a
Eq. (8-72):

(10-43)

(10-44)

ssless waveguide
(*rt*) is equal to the
er, in Subsection

(10-45)

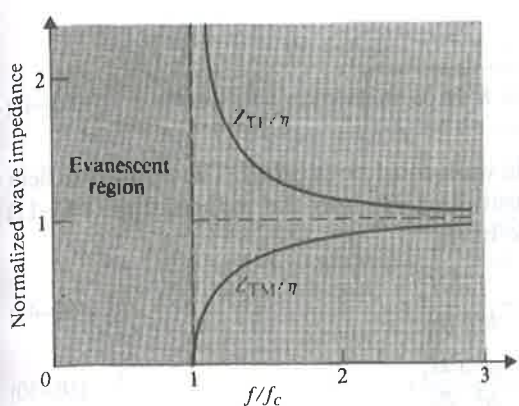


FIGURE 10-2
Normalized wave impedances for propagating TM and TE waves.

The wave impedance of propagating TM modes in a waveguide with a lossless dielectric is purely resistive and is always less than the intrinsic impedance of the dielectric medium. The variation of Z_{TM} versus f/f_c for $f > f_c$ is sketched in Fig. 10-2.

b) $\left(\frac{f}{f_c}\right)^2 < 1$, or $f < f_c$. When the operating frequency is lower than the cutoff frequency, γ is real and Eq. (10-36) can be written as

$$\gamma = \alpha = h \sqrt{1 - \left(\frac{f}{f_c}\right)^2}, \quad f < f_c, \quad (10-46)$$

which is, in fact, an attenuation constant. Since all field components contain the propagation factor $e^{-\gamma z} = e^{-\alpha z}$, the wave diminishes rapidly with z and is said to be *evanescent*. Therefore, **a waveguide exhibits the property of a high-pass filter**. For a given mode, only waves with a frequency higher than the cutoff frequency of the mode can propagate in the guide.

Substitution of Eq. (10-46) in Eq. (10-31) gives the wave impedance of TM modes for $f < f_c$:

$$Z_{\text{TM}} = -j \frac{h}{\omega \epsilon} \sqrt{1 - \left(\frac{f}{f_c}\right)^2}, \quad f < f_c. \quad (10-47)$$

Thus, the wave impedance of evanescent TM modes at frequencies below cutoff is purely reactive, indicating that there is no power flow associated with evanescent waves.

10-2.3 TRANSVERSE ELECTRIC WAVES

Transverse electric (TE) waves do not have a component of the electric field in the direction of propagation, $E_z = 0$. The behavior of TE waves can be analyzed by first

solving Eq. (10-8) for H_z :

$$\nabla_{xy}^2 H_z + h^2 H_z = 0. \quad (10-48)$$

Proper boundary conditions at the guide walls must be satisfied. The transverse field components can then be found by substituting H_z into the reduced Eqs. (10-11) through (10-14) with E_z set to zero. We have

$$H_x^0 = -\frac{\gamma}{h^2} \frac{\partial H_z^0}{\partial x}, \quad (10-49)$$

$$H_y^0 = -\frac{\gamma}{h^2} \frac{\partial H_z^0}{\partial y}, \quad (10-50)$$

$$E_x^0 = -\frac{j\omega\mu}{h^2} \frac{\partial H_z^0}{\partial y}, \quad (10-51)$$

$$E_y^0 = \frac{j\omega\mu}{h^2} \frac{\partial H_z^0}{\partial x}. \quad (10-52)$$

Combining Eqs. (10-49) and (10-50), we obtain

$$(\mathbf{H}_T^0)_{TE} = \mathbf{a}_x H_x^0 + \mathbf{a}_y H_y^0 = -\frac{\gamma}{h^2} \nabla_T H_z^0 \quad (\text{A/m}). \quad (10-53)$$

We note that Eq. (10-53) is entirely similar to Eq. (10-29) for TM modes.

The transverse components of electric field intensity, E_x^0 and E_y^0 , are related to those of magnetic field intensity through the wave impedance. We have, from Eqs. (10-49) through (10-52),

$$Z_{TE} = \frac{E_x^0}{H_y^0} = -\frac{E_y^0}{H_x^0} = \frac{j\omega\mu}{\gamma} \quad (\Omega). \quad (10-54)$$

Note that Z_{TE} in Eq. (10-54) is quite different from Z_{TM} in Eq. (10-31) because γ for TE waves, unlike γ_{TEM} , is *not* equal to $j\omega\sqrt{\mu\epsilon}$. Equations (10-51), (10-52), and (10-54) can now be combined to give the following vector formula:

$$\mathbf{E} = -Z_{TE}(\mathbf{a}_z \times \mathbf{H}) \quad (\text{V/m}). \quad (10-55)$$

Inasmuch as we have not changed the relation between γ and h , Eqs. (10-33) through (10-44) pertaining to TM waves also apply to TE waves. There are also two distinct ranges of γ , depending on whether the operating frequency is higher or lower than the cutoff frequency, f_c , given in Eq. (10-35).

(10-48)

- a) $\left(\frac{f}{f_c}\right)^2 > 1$, or $f > f_c$. In this range, γ is imaginary, and we have a propagating mode. The expression for γ is the same as that given in Eq. (10-37):

$$\gamma = j\beta = jk \sqrt{1 - \left(\frac{f_c}{f}\right)^2}. \quad (10-56)$$

transverse field
Eqs. (10-11)

(10-49)

(10-50)

(10-51)

(10-52)

(10-53)

modes.
 η , are related to
have, from Eqs.

(10-54)

10-31) because γ
51), (10-52), and
:

(10-55)

and h , Eqs. (10-33)
es. There are also
frequency is higher or

Consequently, the formulas for β , λ_g , u_p , and u_g in Eqs. (10-38), (10-39), (10-42), and (10-43), respectively, also hold for TE waves. Using Eq. (10-56) in Eq. (10-54), we obtain

$$Z_{TE} = \frac{\eta}{\sqrt{1 - (f_c/f)^2}} \quad (\Omega), \quad (10-57)$$

which is obviously different from the expression for Z_{TM} in Eq. (10-45). Equation (10-57) indicates that *the wave impedance of propagating TE modes in a waveguide with a lossless dielectric is purely resistive and is always larger than the intrinsic impedance of the dielectric medium*. The variation of Z_{TE} versus f/f_c for $f > f_c$ is also sketched in Fig. 10-2.

- b) $\left(\frac{f}{f_c}\right)^2 < 1$, or $f < f_c$. In this case, γ is real and we have an evanescent or non-propagating mode:

$$\gamma = \alpha = h \sqrt{1 - \left(\frac{f}{f_c}\right)^2}, \quad f < f_c. \quad (10-58)$$

Substitution of Eq. (10-58) in Eq. (10-54) gives the wave impedance of TE modes for $f < f_c$:

$$Z_{TE} = j \frac{\omega \mu}{h \sqrt{1 - (f/f_c)^2}}, \quad f < f_c, \quad (10-59)$$

which is purely reactive, indicating again that there is no power flow for evanescent waves at $f < f_c$.

EXAMPLE 10-1 (a) Determine the wave impedance and guide wavelength at a frequency equal to twice the cutoff frequency in a waveguide for TM and TE modes. (b) Repeat part (a) for a frequency equal to one-half of the cutoff frequency. (c) What are the wave impedance and guide wavelength for the TEM mode?

Solution

- a) At $f = 2f_c$, which is above the cutoff frequency, we have propagating modes. The appropriate formulas are Eqs. (10-45), (10-57), and (10-39).

For $f = 2f_c$, $(f_c/f)^2 = \frac{1}{4}$, $\sqrt{1 - (f_c/f)^2} = \sqrt{3}/2 = 0.866$. Thus,

$$Z_{TM} = 0.866\eta < \eta, \quad \lambda_{TM} = 1.155\lambda > \lambda, \\ Z_{TE} = 1.155\eta > \eta, \quad \lambda_{TE} = 1.155\lambda > \lambda,$$

TABLE 10-1
Wave Impedances and Guide Wavelengths for $f > f_c$

Mode	Wave Impedance, Z	Guide Wavelength, λ_g
TEM	$\eta = \sqrt{\frac{\mu}{\epsilon}}$	$\lambda = \frac{1}{f\sqrt{\mu\epsilon}}$
TM	$\eta \sqrt{1 - \left(\frac{f_c}{f}\right)^2}$	$\frac{\lambda}{\sqrt{1 - (f_c/f)^2}}$
TE	$\frac{\eta}{\sqrt{1 - (f_c/f)^2}}$	$\frac{\lambda}{\sqrt{1 - (f_c/f)^2}}$

where η is the intrinsic impedance of the guide medium. These results are summarized in Table 10-1.

- b) At $f = f_c/2 < f_c$, the waveguide modes are evanescent, and guide wavelength has no significance. We now have

$$Z_{TM} = -j \frac{h}{\omega\epsilon} \sqrt{1 - \left(\frac{f}{f_c}\right)^2} = -j0.276h/f_c\epsilon,$$

$$Z_{TE} = j \frac{\omega\mu}{h\sqrt{1 - (f/f_c)^2}} = j3.63f_c\mu/h.$$

We note that both Z_{TM} and Z_{TE} become imaginary (reactive) for evanescent modes at $f < f_c$; their values depend on the eigenvalue h , which is a characteristic of the particular TM or TE mode.

- c) The TEM mode does not exhibit a cutoff property and $h = 0$. The wave impedance and guide wavelength are independent of frequency. From Eqs. (10-20) and (10-18) we have

$$Z_{TEM} = \eta$$

and

$$\lambda_{TEM} = \lambda.$$

For propagating modes, $\gamma = j\beta$ and the variation of β versus frequency determines the characteristics of a wave along a guide. It is therefore useful to plot and examine an $\omega-\beta$ diagram.[†] Figure 10-3 is such a diagram in which the dashed line through the origin represents the $\omega-\beta$ relationship for TEM mode. The constant slope of this straight line is $\omega/\beta = u = 1/\sqrt{\mu\epsilon}$, which is the same as the velocity of light in an unbounded dielectric medium with constitutive parameters μ and ϵ .

[†] Also referred to as a *Brillouin diagram*.

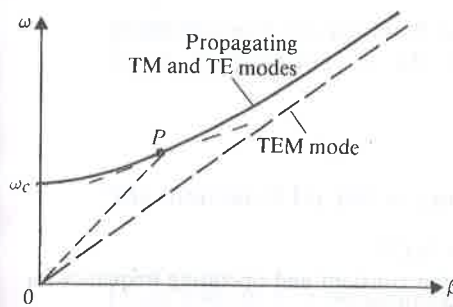


FIGURE 10-3
 ω - β diagram for waveguide.

The solid curve above the dashed line depicts a typical ω - β relation for either a TM or a TE propagating mode, given by Eq. (10-38). We can write

$$\omega = \frac{\beta u}{\sqrt{1 - (\omega_c/\omega)^2}}. \quad (10-60)$$

The ω - β curve intersects the ω -axis ($\beta = 0$) at $\omega = \omega_c$. The slope of the line joining the origin and any point, such as P , on the curve is equal to the phase velocity, u_p , for a particular mode having a cutoff frequency f_c and operating at a particular frequency. The local slope of the ω - β curve at P is the group velocity, u_g . We note that, for propagating TM and TE waves in a waveguide, $u_p > u$, $u_g < u$, and Eq. (10-44) holds. As the operating frequency increases much above the cutoff frequency, both u_p and u_g approach u asymptotically. The exact value of ω_c depends on the eigenvalue h in Eq. (10-35)—that is, on the particular TM or TE mode in a waveguide of a given cross section. Methods for determining h will be discussed when we examine different types of waveguides. We recall that the ω - β graph for wave propagation in an ionized medium (Fig. 8-7) was quite similar to the ω - β diagram for a waveguide shown in Fig. 10-3.

EXAMPLE 10-2 Obtain a graph showing the relation between the attenuation constant α and the operating frequency f for evanescent modes in a waveguide.

Solution For evanescent TM or TE modes, $f < f_c$ and Eq. (10-46) or (10-58) applies. We have

$$\left(\frac{f_c}{h} \alpha\right)^2 + f^2 = f_c^2. \quad (10-61)$$

Hence the graph of $(f_c \alpha/h)$ plotted versus f is a circle centered at the origin and having a radius f_c . This is shown in Fig. 10-4. The value of α for any $f < f_c$ can be found from this quarter of a circle.

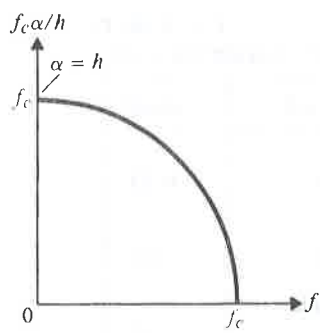


FIGURE 10-4
Relation between attenuation constant and operating frequency for evanescent modes (Example 10-2).

10-3 Parallel-Plate Waveguide

In Section 9-2 we discussed the characteristics of TEM waves propagating along a parallel-plate transmission line. It was then pointed out, and again emphasized in Subsection 10-2.1, that the field behavior for TEM modes bears a very close resemblance to that for uniform plane waves in an unbounded dielectric medium. However, TEM modes are not the only type of waves that can propagate along perfectly conducting parallel-plates separated by a dielectric. A parallel-plate waveguide can also support TM and TE waves. The characteristics of these waves are examined separately in following subsections.

10-3.1 TM WAVES BETWEEN PARALLEL PLATES

Consider the parallel-plate waveguide of two perfectly conducting plates separated by a dielectric medium with constitutive parameters ϵ and μ , as shown in Fig. 10-5. The plates are assumed to be infinite in extent in the x -direction. This is tantamount to assuming that the fields do not vary in the x -direction and that edge effects are negligible. Let us suppose that TM waves ($H_z = 0$) propagate in the $+z$ -direction. For harmonic time dependence it is expedient to work with equations relating field

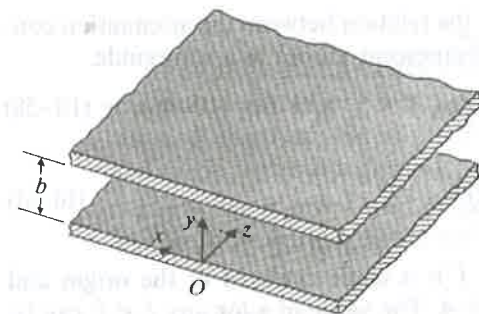


FIGURE 10-5
An infinite parallel-plate waveguide.

quantities with the common factor $e^{(j\omega t - \gamma z)}$ omitted. We write the phasor $E_z(y, z)$ as $E_z^0(y)e^{-\gamma z}$. Equation (10-24) then becomes

$$\frac{d^2 E_z^0(y)}{dy^2} + h^2 E_z^0(y) = 0. \quad (10-62)$$

The solution of Eq. (10-62) must satisfy the boundary conditions

$$E_z^0(y) = 0 \quad \text{at } y = 0 \quad \text{and} \quad y = b.$$

From Section 4-5 we conclude that $E_z^0(y)$ must be of the following form ($h = n\pi/b$):

$$E_z^0(y) = A_n \sin\left(\frac{n\pi y}{b}\right), \quad (10-63)$$

where the amplitude A_n depends on the strength of excitation of the particular TM wave. The only other nonzero field components are obtained from Eqs. (10-25) and (10-28). Keeping in mind that $\partial E_z/\partial x = 0$ and omitting the $e^{-\gamma z}$ factor, we have

$$H_x^0(y) = \frac{j\omega\epsilon}{h} A_n \cos\left(\frac{n\pi y}{b}\right), \quad (10-64)$$

$$E_y^0(y) = -\frac{\gamma}{h} A_n \cos\left(\frac{n\pi y}{b}\right). \quad (10-65)$$

The γ in Eq. (10-65) is the propagation constant that can be determined from Eq. (10-33):

$$\gamma = \sqrt{\left(\frac{n\pi}{b}\right)^2 - \omega^2 \mu\epsilon}. \quad (10-66)$$

The cutoff frequency is the frequency that makes $\gamma = 0$. We have

$$f_c = \frac{n}{2b\sqrt{\mu\epsilon}} \quad (\text{Hz}), \quad (10-67)$$

which, of course, checks with Eq. (10-35). Waves with $f > f_c$ propagate with a phase constant β , given in Eq. (10-38); and waves with $f \leq f_c$ are evanescent.

Depending on the values of n , there are different possible propagating TM modes (eigenmodes) corresponding to the different eigenvalues h . Thus there are the TM_1 mode ($n = 1$) with cutoff frequency $(f_c)_1 = 1/2b\sqrt{\mu\epsilon}$, the TM_2 mode ($n = 2$) with $(f_c)_2 = 1/b\sqrt{\mu\epsilon}$, and so on. Each mode has its own characteristic phase constant, guide wavelength, phase velocity, group velocity, and wave impedance; they can be determined from Eqs. (10-38), (10-39), (10-42), (10-43), and (10-45), respectively. When $n = 0$, $E_z = 0$ and only the transverse components H_x and E_y exist. Hence TM_0 mode is the TEM mode, for which $f_c = 0$. The mode having the lowest cutoff frequency is called the *dominant mode* of the waveguide. **For parallel-plate waveguides the dominant mode is the TEM mode.**

EXAMPLE 10-3 (a) Write the instantaneous field expressions for TM₁ mode in a parallel-plate waveguide. (b) Sketch the electric and magnetic field lines in the *yz*-plane.

Solution

a) The instantaneous field expressions for the TM₁ mode are obtained by multiplying the phasor expressions in Eqs. (10-63), (10-64), and (10-65) with $e^{j(\omega t - \beta z)}$ and taking the real part of the product. We have, for $n = 1$,

$$E_z(y, z; t) = A_1 \sin\left(\frac{\pi y}{b}\right) \cos(\omega t - \beta z), \quad (10-68)$$

$$E_y(y, z; t) = \frac{\beta b}{\pi} A_1 \cos\left(\frac{\pi y}{b}\right) \sin(\omega t - \beta z), \quad (10-69)$$

$$H_x(y, z; t) = -\frac{\omega \epsilon b}{\pi} A_1 \cos\left(\frac{\pi y}{b}\right) \sin(\omega t - \beta z), \quad (10-70)$$

where

$$\beta = \sqrt{\omega^2 \mu \epsilon - \left(\frac{\pi}{b}\right)^2}. \quad (10-71)$$

b) In the *yz*-plane, \mathbf{E} has both a *y*- and a *z*-component, and the equation of the electric field lines at a given *t* can be found from the relation

$$\frac{dy}{E_y} = \frac{dz}{E_z}. \quad (10-72)$$

For example, at *t* = 0, Eq. (10-72) can be written as

$$\frac{dy}{dz} = \frac{E_y(y, z; 0)}{E_z(y, z; 0)} = -\frac{\beta b}{\pi} \cot\left(\frac{\pi y}{b}\right) \tan \beta z, \quad (10-73)$$

which gives the slope of the electric field lines. Equation (10-73) can be integrated to give

$$\cos\left(\frac{\pi y}{b}\right) \cos \beta z = \text{Constant}, \quad 0 \leq y \leq b. \quad (10-74)^{\dagger}$$

[†] Equation (10-73) can be rearranged as

$$\frac{dy}{dz} = -\left(\frac{\beta b}{\pi}\right) \frac{\cos(\pi y/b) \sin \beta z}{\sin(\pi y/b) \cos \beta z}$$

or

$$\frac{(\pi/b) \sin(\pi y/b) dy}{\cos(\pi y/b)} = -\frac{\beta \sin \beta z dz}{\cos \beta z}$$

or

$$-\frac{d[\cos(\pi y/b)]}{\cos(\pi y/b)} = \frac{d(\cos \beta z)}{\cos \beta z}.$$

Integration gives

$$-\ln[\cos(\pi y/b)] = \ln(\cos \beta z) + c_1$$

or

$$\cos(\pi y/b) \cos \beta z = c_2,$$

which is Eq. (10-74). c_1 and c_2 are constants.

or TM_1 mode in a
field lines in the yz -

obtained by multi-
(10-65) with $e^{j(\omega t - \beta z)}$

$$(10-68)$$

$$(10-69)$$

$$(10-70)$$

$$(10-71)$$

the equation of the

$$(10-72)$$

$$(10-73)$$

can be integrated

$$(10-74)^{\dagger}$$

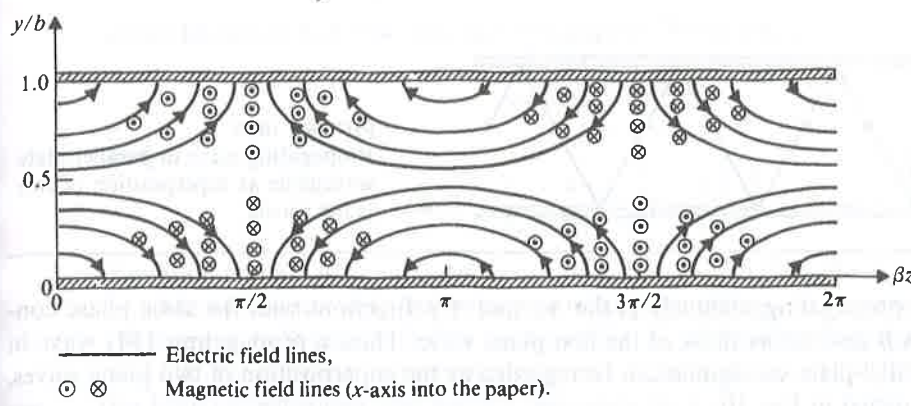


FIGURE 10-6
Field lines for TM_1 mode in parallel-plate waveguide.

Several such electric field lines are drawn in Fig. 10-6. The field lines repeat themselves for every change of 2π (rad) in βz and reverse their directions for every change of π (rad).

Since \mathbf{H} has only an x -component, the magnetic field lines are everywhere perpendicular to the yz -plane. For the TM_1 mode at $t = 0$, Eq. (10-70) becomes

$$H_x(y, z; 0) = \frac{\omega \epsilon b}{\pi} A_1 \cos\left(\frac{\pi y}{b}\right) \sin \beta z. \quad (10-75)$$

The density of H_x lines varies as $\cos(\pi y/b)$ in the y -direction and as $\sin \beta z$ in the z -direction. This is also sketched in Fig. 10-6. At the conducting plates ($y = 0$ and $y = b$) there are surface currents because of a discontinuity in the tangential magnetic field, and surface charges because of the presence of a normal electric field. (Problem P.10-4). ■

EXAMPLE 10-4 Show that the field solution of a propagating TM_1 wave in a parallel-plate waveguide can be interpreted as the superposition of two plane waves bouncing back and forth obliquely between the two conducting plates.

Solution This can be seen readily by writing the phasor expression of $E_z^0(y)$ from Eq. (10-63) for $n = 1$ and with the factor $e^{-j\beta z}$ restored. We have

$$\begin{aligned} E_z(y, z) &= A_1 \sin\left(\frac{\pi y}{b}\right) e^{-j\beta z} = \frac{A_1}{2j} (e^{j\pi y/b} - e^{-j\pi y/b}) e^{-j\beta z} \\ &= \frac{A_1}{2j} [e^{-j(\beta z - \pi y/b)} - e^{-j(\beta z + \pi y/b)}]. \end{aligned} \quad (10-76)$$

From Chapter 8 we recognize that the first term on the right side of Eq. (10-76) represents a plane wave propagating obliquely in the $+z$ and $-y$ directions with phase constants β and π/b , respectively. Similarly, the second term represents a plane

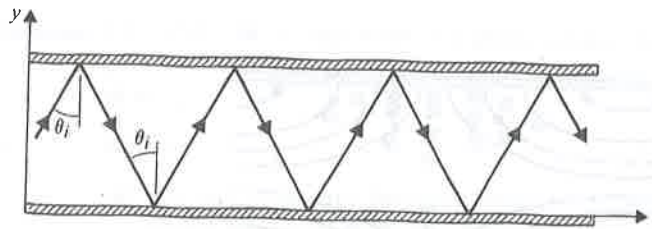


FIGURE 10-7
Propagating wave in parallel-plate waveguide as superposition of two plane waves.

wave propagating obliquely in the $+z$ and $+y$ directions with the same phase constants β and π/b as those of the first plane wave. Thus, a propagating TM_1 wave in a parallel-plate waveguide can be regarded as the superposition of two plane waves, as depicted in Fig. 10-7.

In Subsection 8-7.2 on reflection of a parallelly polarized (TM) plane wave incident obliquely at a conducting boundary plane, we obtained an expression for the longitudinal component of the total E_1 field that is the sum of the longitudinal components of the incident E_i and the reflected E_r . To adapt the coordinate designations of Fig. 8-13 to those of Fig. 10-5, x and z must be changed to z and $-y$, respectively. We rewrite E_x of Eq. (8-128) as

$$E_z(y, z) = E_{i0} \cos \theta_i (e^{j\beta_1 y \cos \theta_i} - e^{-j\beta_1 y \cos \theta_i}) e^{-j\beta_1 z \sin \theta_i}.$$

Comparing the exponents of the terms in this equation with those in Eq. (10-76), we obtain two equations:

$$\beta_1 \sin \theta_i = \beta, \quad (10-77)$$

$$\beta_1 \cos \theta_i = \frac{\pi}{b}. \quad (10-78)$$

(The field amplitudes involved in these equations are of no importance in the present consideration.) Solution of Eqs. (10-77) and (10-78) gives

$$\beta = \sqrt{\beta_1^2 - \left(\frac{\pi}{b}\right)^2} = \sqrt{\omega^2 \mu \epsilon - \left(\frac{\pi}{b}\right)^2},$$

which is the same as Eq. (10-71), and

$$\cos \theta_i = \frac{\pi}{\beta_1 b} = \frac{\lambda}{2b}, \quad (10-79)$$

where $\lambda = 2\pi/\beta_1$ is the wavelength in the unbounded dielectric medium.

We observe that a solution of Eq. (10-79) for θ_i exists only when $\lambda/2b \leq 1$. At $\lambda/2b = 1$, or $f = u/\lambda = 1/2b\sqrt{\mu\epsilon}$, which is the cutoff frequency in Eq. (10-67) for $n = 1$, $\cos \theta_i = 1$, and $\theta_i = 0$. This corresponds to the case in which the waves bounce back and forth in the y -direction, normal to the parallel plates, and there is no propagation in the z -direction ($\beta = \beta_1 \sin \theta_i = 0$). Propagation of TM_1 mode is possible only when $\lambda < \lambda_c = 2b$ or $f > f_c$. Both $\cos \theta_i$ and $\sin \theta_i$ can be expressed in terms of

cutoff frequency f_c . From Eqs. (10-79) and (10-77) we have

$$\cos \theta_i = \frac{\lambda}{\lambda_c} = \frac{f_c}{f} \quad (10-80)$$

and

$$\sin \theta_i = \frac{\lambda}{\lambda_g} = \frac{u}{u_p} = \sqrt{1 - \left(\frac{f_c}{f}\right)^2}. \quad (10-81)$$

Equation (10-81) is in agreement with Eqs. (10-39) and (10-42).

We studied traveling waves in a parallel-plate waveguide in terms of bouncing plane waves in Section 8-7 with the aid of Fig. 8-12. We note here that Eqs. (10-79) and (10-81) are consistent respectively with Eqs. (8-119) and (8-120), which hold for both perpendicular and parallel polarizations.

10-3.2 TE WAVES BETWEEN PARALLEL PLATES

For transverse electric waves, $E_z = 0$, we solve the following equation for $H_z^0(y)$, which is a simplified version of Eq. (10-48) with no x -dependence:

$$\frac{d^2 H_z^0(y)}{dy^2} + h^2 H_z^0(y) = 0. \quad (10-82)$$

We note that $H_z(y, z) = H_z^0(y)e^{-\gamma z}$. The boundary conditions to be satisfied by $H_z^0(y)$ are obtained from Eq. (10-51). Since E_x must vanish at the surfaces of the conducting plates, we require

$$\frac{dH_z^0(y)}{dy} = 0 \quad \text{at } y = 0 \quad \text{and} \quad y = b.$$

Therefore the proper solution of Eq. (10-82) is of the form

$$H_z^0(y) = B_n \cos\left(\frac{n\pi y}{b}\right), \quad (10-83)$$

where the amplitude B_n depends on the strength of excitation of the particular TE wave. We obtain the only other nonzero field components from Eqs. (10-50) and (10-51), keeping in mind that $\partial H_z / \partial x = 0$:

$$H_y^0(y) = \frac{\gamma}{h} B_n \sin\left(\frac{n\pi y}{b}\right), \quad (10-84)$$

$$E_x^0(y) = \frac{j\omega\mu}{h} B_n \sin\left(\frac{n\pi y}{b}\right). \quad (10-85)$$

The propagation constant γ in Eq. (10-84) is the same as that for TM waves given in Eq. (10-66). Inasmuch as cutoff frequency is the frequency that makes $\gamma = 0$, **the cutoff frequency for the TE_n mode in a parallel-plate waveguide is exactly the same as that for the TM_n mode given in Eq. (10-67)**. For $n = 0$, both H_y and E_x vanish; hence the TE_0 mode does not exist in a parallel-plate waveguide.

EXAMPLE 10-5 (a) Write the instantaneous field expressions for the TE₁ mode in a parallel-plate waveguide. (b) Sketch the electric and magnetic field lines in the yz -plane.

Solution

a) The instantaneous field expressions for the TE₁ mode are obtained by taking the real part of the products of the phasor expressions in Eqs. (10-83), (10-84), and (10-85) with $e^{j(\omega t - \beta z)}$. We have, for $n = 1$,

$$H_z(y, z; t) = B_1 \cos\left(\frac{\pi y}{b}\right) \cos(\omega t - \beta z), \quad (10-86)$$

$$H_y(y, z; t) = -\frac{\beta b}{\pi} B_1 \sin\left(\frac{\pi y}{b}\right) \sin(\omega t - \beta z), \quad (10-87)$$

$$E_x(y, z; t) = -\frac{\omega \mu b}{\pi} B_1 \sin\left(\frac{\pi y}{b}\right) \sin(\omega t - \beta z), \quad (10-88)$$

where the phase constant β is given by Eq. (10-71), same as that for the TM₁ mode.

b) The electric field has only an x -component. At $t = 0$, Eq. (10-88) becomes

$$E_x(y, z; 0) = \frac{\omega \mu b}{\pi} B_1 \sin\left(\frac{\pi y}{b}\right) \sin \beta z. \quad (10-89)$$

Thus the density of E_x lines varies as $\sin(\pi y/b)$ in the y direction and as $\sin \beta z$ in the z direction; E_x lines are sketched as dots and crosses in Fig. 10-8.

The magnetic field has both a y - and a z -component. The equation of the magnetic field lines at $t = 0$ can be found from the following relation:

$$\frac{dy}{dz} = \frac{H_y(y, z; 0)}{H_z(y, z; 0)} = \frac{\beta b}{\pi} \tan\left(\frac{\pi y}{b}\right) \tan \beta z. \quad (10-90)$$

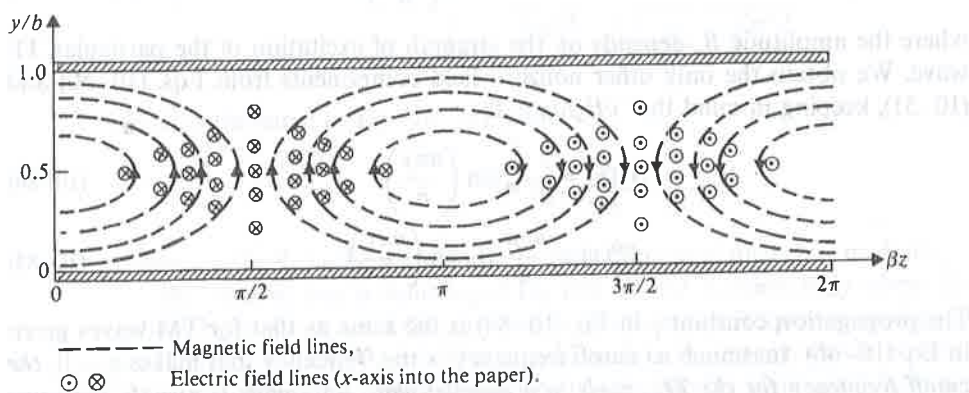


FIGURE 10-8
Field lines for TE₁ mode in parallel-plate waveguide.

TE₁ mode in a
in the *yz*-plane.

ined by taking
(10-83), (10-84),

(10-86)
(10-87)

(10-88)

at for the TM₁
(10-89)

and as $\sin \beta z$
g. 10-8.
equation of the
tion:

(10-90)

Using the procedure illustrated in Example 10-3, we can integrate Eq. (10-90) to obtain

$$\sin\left(\frac{\pi y}{b}\right) \cos \beta z = \text{Constant}, \quad 0 \leq y \leq b, \quad (10-91)$$

which is the equation for magnetic field lines in the *yz*-plane at *t* = 0. The constant in Eq. (10-91) lies between -1 and +1. According to Eq. (10-86), the density of the *H_z* line varies as $|\cos(\pi y/b)|$. Several magnetic field lines are drawn in Fig. 10-8. The lines repeat themselves for every change of 2π (rad) in βz .

10-3.3 ENERGY-TRANSPORT VELOCITY

In Subsections 10-2.2 and 10-2.3 we noted that signals having a frequency higher than the cutoff frequency will propagate in a waveguide with a phase velocity *u_p* given by Eq. (10-42) and a group velocity *u_g* given by Eq. (10-43). When the concept of group velocity was introduced in Section 8-4, it was defined as the velocity of the envelope of a narrow-band signal. For signals with a broad frequency spectrum, such as pulses of short durations, group velocity loses its significance because the low-frequency components may be below cutoff (therefore cannot propagate) and the high-frequency components will travel with widely different velocities. These wideband signals will then be badly distorted, and no single group velocity can represent the signal-propagation velocity. In such cases we examine the velocity at which energy propagates along a waveguide, or *energy-transport velocity*.

For signal transmission in a lossless waveguide we define energy-transport velocity, *u_{en}*, as the ratio of the time-average propagated power to the time-average stored energy per unit guide length:

$$u_{en} = \frac{(P_z)_{av}}{W'_{av}} \quad (\text{m/s}), \quad (10-92)$$

where the time-average power $(P_z)_{av}$ is equal to the time-average Poynting vector \mathcal{P}_{av} integrated over the guide cross section:

$$(P_z)_{av} = \int_S \mathcal{P}_{av} \cdot ds, \quad (10-93)$$

and the time-average stored energy per unit length W'_{av} is the sum of the time-average stored electric energy density $(w_e)_{av}$ and the time-average stored magnetic energy density $(w_m)_{av}$ integrated over the guide cross section:

$$W'_{av} = \int_S [(w_e)_{av} + (w_m)_{av}] ds. \quad (10-94)$$

For a particular mode of propagation in a waveguide we calculate $(P_z)_{av}$ and W'_{av} from Eqs. (10-93) and (10-94), respectively, and substitute into Eq. (10-92) to find energy-transport velocity.

EXAMPLE 10-6 Determine the energy-transport velocity of the TM_n mode in a lossless parallel-plate waveguide.

Solution We first obtain the time-average Poynting vector by using Eqs. (8-96), (10-63), (10-64), and (10-65):

$$\begin{aligned}\mathcal{P}_{av} &= \frac{1}{2} \mathcal{R}_e (\mathbf{E} \times \mathbf{H}^*) \\ &= \frac{1}{2} \mathcal{R}_e (-\mathbf{a}_z E_y^0 H_x^{0*} + \mathbf{a}_y E_z^0 H_x^{0*}).\end{aligned}\quad (10-95)$$

Thus,

$$\begin{aligned}\mathcal{P}_{av} \cdot \mathbf{a}_z &= -\frac{1}{2} \mathcal{R}_e (E_y^0 H_x^{0*}) \\ &= \frac{\omega \epsilon \beta}{2h^2} A_n^2 \cos^2 \left(\frac{n\pi y}{b} \right),\end{aligned}\quad (10-96)$$

where we have replaced γ by $j\beta$. For a unit width of the parallel-plate waveguide, substitution of Eq. (10-96) in Eq. (10-93) yields

$$\begin{aligned}(P_z)_{av} &= \int_0^b \mathcal{P}_{av} \cdot \mathbf{a}_z dy \\ &= \frac{\omega \epsilon \beta b}{4h^2} A_n^2.\end{aligned}\quad (10-97)$$

Following the procedure leading to Eq. (8-96) from Eq. (8-83), we can readily prove from Eqs. (8-85) and (8-86) that

$$(w_e)_{av} = \frac{\epsilon}{4} \mathcal{R}_e (\mathbf{E} \cdot \mathbf{E}^*), \quad (10-98)$$

and

$$(w_m)_{av} = \frac{\mu}{4} \mathcal{R}_e (\mathbf{H} \cdot \mathbf{H}^*). \quad (10-99)$$

Substituting Eqs. (10-63) and (10-65) in Eq. (10-98), we have

$$(w_e)_{av} = \frac{\epsilon}{4} A_n^2 \left[\sin^2 \left(\frac{n\pi y}{b} \right) + \frac{\beta^2}{h^2} \cos^2 \left(\frac{n\pi y}{b} \right) \right] \quad (10-100)$$

and

$$\begin{aligned}\int_0^b (w_e)_{av} dy &= \frac{\epsilon b}{8} A_n^2 \left[1 + \frac{\beta^2}{h^2} \right] \\ &= \frac{\epsilon b}{8h^2} k^2 A_n^2,\end{aligned}\quad (10-101)$$

where Eq. (10-15) has been used to replace $\beta^2 + h^2$ by k^2 . Similarly, using Eq. (10-64) in Eq. (10-99), we obtain

$$(w_m)_{av} = \frac{\mu}{4} \left(\frac{\omega^2 \epsilon^2}{h^2} \right) A_n^2 \cos^2 \left(\frac{n\pi y}{b} \right) \quad (10-102)$$

and

$$\int_0^b (w_m)_{av} dy = \frac{\mu b}{8h^2} (\omega^2 \epsilon^2) A_n^2 = \frac{\epsilon b}{8h^2} k^2 A_n^2, \quad (10-103)$$

TM_n mode in a
ng Eqs. (8-96),

(10-95)

(10-96)

late waveguide,

(10-97)

we can readily

(10-98)

(10-99)

(10-100)

using Eq. (10-64)

(10-102)

(10-103)

which is seen to be equal to the time-average stored electric energy per unit guide width obtained in Eq. (10-101).

We are now ready to find u_{en} from Eq. (10-92) by dividing $(P_z)_{av}$ in Eq. (10-97) by the sum of the stored energies in Eqs. (10-101) and (10-103):

$$\begin{aligned} u_{en} &= \frac{\omega\beta}{k^2} = \frac{\omega}{k} \left(\frac{\beta}{k} \right) \\ &= u \sqrt{1 - \left(\frac{f_c}{f} \right)^2}, \end{aligned} \quad (10-104)$$

where we have made use of Eqs. (10-5) and (10-38). We recognize that the energy-transport velocity in Eq. (10-104) is equal to the group velocity given in Eq. (10-43).

10-3.4 ATTENUATION IN PARALLEL-PLATE WAVEGUIDES

Attenuation in any waveguide (not just the parallel-plate waveguide) arises from two sources: lossy dielectric and imperfectly conducting walls. Losses modify the electric and magnetic fields within the guide, making exact solutions difficult to obtain. However, in practical waveguides the losses are usually very small, and we will assume that the transverse field patterns of the propagating modes are not affected by them. A real part of the propagation constant now appears as the attenuation constant, which accounts for power losses. The attenuation constant consists of two parts:

$$\alpha = \alpha_d + \alpha_c, \quad (10-105)$$

where α_d is the attenuation constant due to losses in the dielectric and α_c is that due to ohmic power loss in the imperfectly conducting walls.

We will now consider the attenuation constants for TEM, TM, and TE modes separately.

TEM Modes The attenuation constant for TEM modes on a parallel-plate transmission line has been discussed in Subsection 9-3.4. From Eq. (9-90) and Table 9-1 we have approximately

$$\alpha_d = \frac{G}{2} R_0 = \frac{\sigma}{2} \sqrt{\frac{\mu}{\epsilon}} = \frac{\sigma}{2} \eta \quad (\text{Np/m}), \quad (10-106)$$

where ϵ , μ , and σ are the permittivity, permeability, and conductivity, respectively, of the dielectric medium. In Eq. (10-106), $\eta = \sqrt{\mu/\epsilon}$ is the intrinsic impedance of the dielectric if the dielectric is lossless. If the losses in the dielectric are represented by the imaginary part, $-\epsilon''$, of a complex permittivity as in Eq. (7-111), we may replace σ by $\omega\epsilon''$ and write Eq. (10-106) alternatively as

$$\alpha_d \cong \frac{\omega\epsilon''}{2} \eta \quad (\text{Np/m}). \quad (10-107)$$

Also from Eq. (9-90) and Table 9-1 we have

$$\alpha_c = \frac{R}{2R_0} = \frac{1}{b} \sqrt{\frac{\pi f \epsilon}{\sigma_c}} \quad (\text{Np/m}), \quad (10-108)$$

where σ_c is the conductivity of the metal plates. We note that, for TEM modes, α_d is independent of frequency, and α_c is proportional to \sqrt{f} . We note further that $\alpha_d \rightarrow 0$ as $\sigma \rightarrow 0$ and that $\alpha_c \rightarrow 0$ as $\sigma_c \rightarrow \infty$, as expected.

TM Modes The attenuation constant due to losses in the dielectric at frequencies above f_c can be found from Eq. (10-66) by substituting $\epsilon_d = \epsilon + (\sigma/j\omega)$ for ϵ . We have

$$\begin{aligned} \gamma &= j \left[\omega^2 \mu \epsilon \left(1 - \frac{j\sigma}{\omega \epsilon} \right) - \left(\frac{n\pi}{b} \right)^2 \right]^{1/2} \\ &= j \sqrt{\omega^2 \mu \epsilon - \left(\frac{n\pi}{b} \right)^2} \left\{ 1 - j \omega \mu \sigma \left[\omega^2 \mu \epsilon - \left(\frac{n\pi}{b} \right)^2 \right]^{-1} \right\}^{1/2} \\ &\approx j \sqrt{\omega^2 \mu \epsilon - \left(\frac{n\pi}{b} \right)^2} \left\{ 1 - \frac{j \omega \mu \sigma}{2} \left[\omega^2 \mu \epsilon - \left(\frac{n\pi}{b} \right)^2 \right]^{-1} \right\}. \end{aligned} \quad (10-109)$$

Only the first two terms in the binomial expansion for the second line in Eq. (10-109) are retained in the third line under the assumption that

$$\omega \mu \sigma \ll \omega^2 \mu \epsilon - \left(\frac{n\pi}{b} \right)^2.$$

From Eq. (10-67) we see that

$$\frac{n\pi}{b} = 2\pi f_c \sqrt{\mu \epsilon},$$

which enables us to write

$$\begin{aligned} \sqrt{\omega^2 \mu \epsilon - \left(\frac{n\pi}{b} \right)^2} &= \omega \sqrt{\mu \epsilon} \sqrt{1 - (\omega_c/\omega)^2} \\ &= \omega \sqrt{\mu \epsilon} \sqrt{1 - (f_c/f)^2}. \end{aligned}$$

With the above relation, Eq. (10-109) becomes

$$\gamma = \alpha_d + j\beta = \frac{\sigma}{2} \sqrt{\frac{\mu}{\epsilon}} \frac{1}{\sqrt{1 - (f_c/f)^2}} + j\omega \sqrt{\mu \epsilon} \sqrt{1 - (f_c/f)^2},$$

from which we obtain

$$\alpha_d = \frac{\sigma \eta}{2 \sqrt{1 - (f_c/f)^2}} \quad (\text{Np/m}) \quad (10-110)$$

and

$$\beta = \omega \sqrt{\mu \epsilon} \sqrt{1 - (f_c/f)^2} \quad (\text{rad/m}). \quad (10-111)$$

Thus, α_d for TM modes decreases when frequency increases.

(10-108)

TEM modes, α_d is rather than $\alpha_d \rightarrow 0$ ric at frequencies ω for ϵ . We have

(10-109)

e in Eq. (10-109)

To find the attenuation constant due to losses in the imperfectly conducting plates, we use Eq. (9-88), which was derived from the law of conservation of energy. Thus,

$$\alpha_c = \frac{P_L(z)}{2P(z)}, \quad (10-112)$$

where $P(z)$ is the time-average power flowing through a cross section (say, of width w) of the waveguide, and $P_L(z)$ is the time-average power lost in the two plates per unit length. For TM modes we use Eqs. (10-64) and (10-65):

$$\begin{aligned} P(z) &= w \int_0^b -\frac{1}{2}(E_y^0)(H_x^0)^* dy \\ &= \frac{w\omega\epsilon\beta}{2} \left(\frac{bA_n}{n\pi} \right)^2 \int_0^b \cos^2 \left(\frac{n\pi y}{b} \right) dy \\ &= w\omega\epsilon\beta b \left(\frac{bA_n}{2n\pi} \right)^2. \end{aligned} \quad (10-113)$$

The surface current densities on the upper and lower plates have the same magnitude. On the lower plate where $y = 0$ we have

$$|J_{sz}^0| = |H_x^0(y=0)| = \frac{\omega\epsilon b A_n}{n\pi}.$$

The total power loss per unit length in two plates of width w is

$$P_L(z) = 2w \left(\frac{1}{2} |J_{sz}^0|^2 R_s \right) = w \left(\frac{\omega\epsilon b A_n}{n\pi} \right)^2 R_s. \quad (10-114)$$

Substitution of Eqs. (10-113) and (10-114) in Eq. (10-112) yields

$$\alpha_c = \frac{2\omega\epsilon R_s}{\beta b} = \frac{2R_s}{\eta b \sqrt{1 - (f_c/f)^2}} \quad (\text{Np/m}), \quad (10-115)$$

where, from Eq. (9-26b),

$$R_s = \sqrt{\frac{\pi f \mu_c}{\sigma_c}} \quad (\Omega). \quad (10-116)$$

The use of Eq. (10-116) in Eq. (10-115) gives the explicit dependence of α_c on f for TM modes:

$$\alpha_c = \frac{2}{\eta b} \sqrt{\frac{\pi \mu_c f_c}{\sigma_c}} \frac{1}{\sqrt{(f_c/f)[1 - (f_c/f)^2]}}. \quad (10-117)$$

A sketch of the normalized α_c is shown in Fig. 10-9, which reveals the existence of a minimum.

TE Modes In Subsection 10-3.2 we noted that the expression for the propagation constant for TE waves between parallel plates is the same as that for TM waves. It follows that the formula for α_d in Eq. (10-110) holds for TE modes as well.

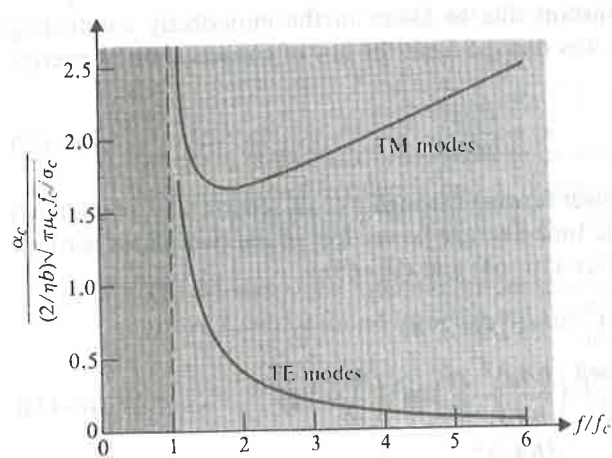


FIGURE 10-9
Normalized attenuation constant due to finite conductivity of the plates in parallel-plate waveguide.

In order to determine the attenuation constant α_c due to losses in the imperfectly conducting plates, we again apply Eq. (10-112). Of course, the field expressions in Eqs. (10-83), (10-84), and (10-85) for TE modes must now be used. We have

$$\begin{aligned} P(z) &= w \int_0^b \frac{1}{2} (E_x^0)(H_y^0)^* dy \\ &= \frac{w\omega\mu\beta}{2} \left(\frac{bB_n}{n\pi} \right)^2 \int_0^b \sin^2 \left(\frac{n\pi y}{b} \right) dy \\ &= w\omega\mu\beta b \left(\frac{bB_n}{2n\pi} \right)^2 \end{aligned} \quad (10-118)$$

and

$$\begin{aligned} P_L(z) &= 2w \left(\frac{1}{2} |J_{sx}^0|^2 R_s \right) \\ &= w |H_z^0(y=0)|^2 R_z = w B_n^2 R_s. \end{aligned} \quad (10-119)$$

Consequently,

$$\begin{aligned} \alpha_c &= \frac{P_L(z)}{2P(z)} = \frac{2R_s}{\omega\mu\beta b} \left(\frac{n\pi}{b} \right)^2 \\ &= \frac{2R_s f_c^2}{\eta b f^2 \sqrt{1 - (f_e/f)^2}}. \end{aligned} \quad (10-120)$$

A normalized α_c curve based on Eq. (10-120) is also sketched in Fig. 10-9. Unlike α_c for TM modes, α_c for TE modes does not have a minimum but decreases monotonically as f increases.

10-4 Rectangular Waveguides

The analysis of parallel-plate waveguides in Section 10-3 assumed the plates to be of an infinite extent in the transverse x direction; that is, the fields do not vary with x . In practice, these plates are always finite in width, with fringing fields at the edges. Electromagnetic energy will leak through the sides of the guide and create undesirable stray couplings to other circuits and systems. Thus practical waveguides are usually uniform structures of a cross section of the enclosed variety. The simplest of such cross sections, in terms of ease both in analysis and in manufacture, are rectangular and circular. In this section we will analyze the wave behavior in hollow rectangular waveguides. Circular waveguides will be treated in the next section. Rectangular waveguides are more commonly used in practice than circular waveguides.

In the following discussion we draw on the material in Section 10-2 concerning general wave behaviors along uniform guiding structures. Propagation of time-harmonic waves in the $+z$ direction with a propagation constant γ is considered. TM and TE modes will be discussed separately. As we have noted previously, TEM waves cannot exist in a single-conductor hollow or dielectric-filled waveguide.

10-4.1 TM WAVES IN RECTANGULAR WAVEGUIDES

Consider the waveguide sketched in Fig. 10-10, with its rectangular cross section of sides a and b . The enclosed dielectric medium is assumed to have constitutive parameters ϵ and μ . For TM waves, $H_z = 0$ and E_z is to be solved from Eq. (10-24). Writing $E_z(x, y, z)$ as

$$E_z(x, y, z) = E_z^0(x, y)e^{-\gamma z}, \quad (10-121)$$

we solve the following second-order partial differential equation:

$$\left(\frac{\partial^2}{\partial x^2} + \frac{\partial^2}{\partial y^2} + h^2 \right) E_z^0(x, y) = 0. \quad (10-122)$$

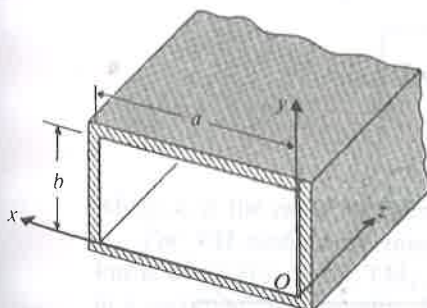


FIGURE 10-10
A rectangular waveguide.

(10-118)

(10-119)

(10-120)

10-9. Unlike
increases mono-

Here we use the method of separation of variables discussed in Section 4-5 by letting

$$E_z^0(x, y) = X(x)Y(y). \quad (10-123)$$

Substituting Eq. (10-123) in Eq. (10-122) and dividing the resulting equation by $X(x)Y(y)$, we have

$$-\frac{1}{X(x)} \frac{d^2 X(x)}{dx^2} = \frac{1}{Y(y)} \frac{d^2 Y(y)}{dy^2} + h^2. \quad (10-124)$$

Now we argue that, since the left side of Eq. (10-124) is a function of x only and the right side is a function of y only, both sides must equal a constant in order for the equation to hold for all values of x and y . Calling this constant (separation constant) k_x^2 , we obtain two separate ordinary differential equations:

$$\frac{d^2 X(x)}{dx^2} + k_x^2 X(x) = 0, \quad (10-125)$$

$$\frac{d^2 Y(y)}{dy^2} + k_y^2 Y(y) = 0, \quad (10-126)$$

where

$$k_y^2 = h^2 - k_x^2. \quad (10-127)$$

The possible solutions of Eqs. (10-125) and (10-126) are listed in Table 4-1, Section 4-5. The appropriate forms to be chosen must satisfy the following boundary conditions.

1. In the x -direction:

$$E_z^0(0, y) = 0, \quad (10-128)$$

$$E_z^0(a, y) = 0. \quad (10-129)$$

2. In the y -direction:

$$E_z^0(x, 0) = 0, \quad (10-130)$$

$$E_z^0(x, b) = 0. \quad (10-131)$$

Obviously, then, we must choose:

$X(x)$ in the form of $\sin k_x x$,

$$k_x = \frac{m\pi}{a}, \quad m = 1, 2, 3, \dots$$

$Y(y)$ in the form of $\sin k_y y$,

$$k_y = \frac{n\pi}{b}, \quad n = 1, 2, 3, \dots$$

and the proper solution for $E_z^0(x, y)$ is

$$E_z^0(x, y) = E_0 \sin\left(\frac{m\pi}{a}x\right) \sin\left(\frac{n\pi}{b}y\right) \quad (\text{V/m}).$$

(10-132)

in 4-5 by letting
 (10-123)
 equation by
 (10-124)

x only and the
 n order for the
 ation constant)

(10-125)

(10-126)

(10-127)

in Table 4-1,
 wing boundary

(10-128)

(10-129)

(10-130)

(10-131)

(10-132)

From Eq. (10-127) we have

$$h^2 = \left(\frac{m\pi}{a}\right)^2 + \left(\frac{n\pi}{b}\right)^2. \quad (10-133)$$

The other field components are obtained from Eqs. (10-25) through (10-28):

$$E_x^0(x, y) = -\frac{\gamma}{h^2} \left(\frac{m\pi}{a}\right) E_0 \cos\left(\frac{m\pi}{a} x\right) \sin\left(\frac{n\pi}{b} y\right), \quad (10-134)$$

$$E_y^0(x, y) = -\frac{\gamma}{h^2} \left(\frac{n\pi}{b}\right) E_0 \sin\left(\frac{m\pi}{a} x\right) \cos\left(\frac{n\pi}{b} y\right), \quad (10-135)$$

$$H_x^0(x, y) = \frac{j\omega\epsilon}{h^2} \left(\frac{n\pi}{b}\right) E_0 \sin\left(\frac{m\pi}{a} x\right) \cos\left(\frac{n\pi}{b} y\right), \quad (10-136)$$

$$H_y^0(x, y) = -\frac{j\omega\epsilon}{h^2} \left(\frac{m\pi}{a}\right) E_0 \cos\left(\frac{m\pi}{a} x\right) \sin\left(\frac{n\pi}{b} y\right), \quad (10-137)$$

where

$$\gamma = j\beta = j \sqrt{\omega^2 \mu \epsilon - \left(\frac{m\pi}{a}\right)^2 - \left(\frac{n\pi}{b}\right)^2}. \quad (10-138)$$

Every combination of the integers m and n defines a possible mode that may be designated as the TM_{mn} mode; thus there are a double infinite number of TM modes. The first subscript denotes the number of half-cycle variations of the fields in the x -direction, and the second subscript denotes the number of half-cycle variations of the fields in the y -direction. The cutoff of a particular mode is the condition that makes γ vanish. For the TM_{mn} mode the cutoff frequency is

$$(f_c)_{mn} = \frac{1}{2\sqrt{\mu\epsilon}} \sqrt{\left(\frac{m\pi}{a}\right)^2 + \left(\frac{n\pi}{b}\right)^2} \quad (\text{Hz}), \quad (10-139)$$

which checks with Eq. (10-35). Alternatively, we may write

$$(\lambda_c)_{mn} = \frac{2}{\sqrt{\left(\frac{m\pi}{a}\right)^2 + \left(\frac{n\pi}{b}\right)^2}} \quad (\text{m}), \quad (10-140)$$

where λ_c is the *cutoff wavelength*.

For TM modes in rectangular waveguides, neither m nor n can be zero. (Do you know why?) Hence, the TM_{11} mode has the lowest cutoff frequency of all TM modes in a rectangular waveguide. The expressions for the phase constant β and the wave impedance Z_{TM} for propagating modes in Eqs. (10-38) and (10-45), respectively, apply here directly.

EXAMPLE 10-7 (a) Write the instantaneous field expressions for the TM_{11} mode in a rectangular waveguide of sides a and b . (b) Sketch the electric and magnetic field lines in a typical xy -plane and in a typical yz -plane.

Solution

a) The instantaneous field expressions for the TM_{11} mode are obtained by multiplying the phasor expressions in Eqs. (10-132) and (10-134) through (10-137) with $e^{j(\omega t - \beta z)}$ and then taking the real part of the product. We have, for $m = n = 1$,

$$E_x(x, y, z; t) = \frac{\beta}{h^2} \left(\frac{\pi}{a} \right) E_0 \cos \left(\frac{\pi}{a} x \right) \sin \left(\frac{\pi}{b} y \right) \sin (\omega t - \beta z), \quad (10-141)$$

$$E_y(x, y, z; t) = \frac{\beta}{h^2} \left(\frac{\pi}{b} \right) E_0 \sin \left(\frac{\pi}{a} x \right) \cos \left(\frac{\pi}{b} y \right) \sin (\omega t - \beta z), \quad (10-142)$$

$$E_z(x, y, z; t) = E_0 \sin \left(\frac{\pi}{a} x \right) \sin \left(\frac{\pi}{b} y \right) \cos (\omega t - \beta z), \quad (10-143)$$

$$H_x(x, y, z; t) = -\frac{\omega \epsilon}{h^2} \left(\frac{\pi}{b} \right) E_0 \sin \left(\frac{\pi}{a} x \right) \cos \left(\frac{\pi}{b} y \right) \sin (\omega t - \beta z), \quad (10-144)$$

$$H_y(x, y, z; t) = \frac{\omega \epsilon}{h^2} \left(\frac{\pi}{a} \right) E_0 \cos \left(\frac{\pi}{a} x \right) \sin \left(\frac{\pi}{b} y \right) \sin (\omega t - \beta z), \quad (10-145)$$

$$H_z(x, y, z; t) = 0, \quad (10-146)$$

where

$$\beta = \sqrt{k^2 - h^2} = \sqrt{\omega^2 \mu \epsilon - \left(\frac{\pi}{a} \right)^2 - \left(\frac{\pi}{b} \right)^2}. \quad (10-147)$$

b) In a typical xy -plane, the slopes of the electric field and magnetic field lines are

$$\left(\frac{dy}{dx} \right)_E = \frac{a}{b} \tan \left(\frac{\pi}{a} x \right) \cot \left(\frac{\pi}{b} y \right), \quad (10-148)$$

$$\left(\frac{dy}{dx} \right)_H = -\frac{b}{a} \cot \left(\frac{\pi}{a} x \right) \tan \left(\frac{\pi}{b} y \right). \quad (10-149)$$

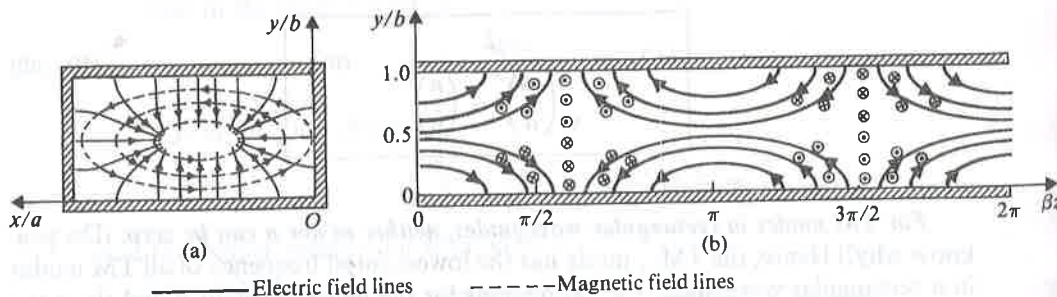


FIGURE 10-11
Field lines for TM_{11} mode in rectangular waveguide.

TM₁₁ mode in magnetic field

ined by multi-
ough (10-137)
for $m = n = 1$,

(10-141)

(10-142)

(10-143)

βz , (10-144)

(10-145)

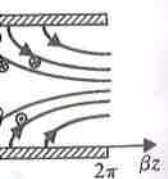
(10-146)

(10-147)

: field lines are

(10-148)

(10-149)



These equations are quite similar to Eq. (10-73) and can be used to sketch the **E** and **H** lines shown in Fig. 10-11(a). Note that from Eqs. (10-148) and (10-149),

$$\left(\frac{dy}{dx}\right)_E \left(\frac{dy}{dx}\right)_H = -1, \quad (10-150)$$

indicating that **E** and **H** lines are everywhere perpendicular to one another. Note also that **E** lines are normal and that **H** lines are parallel to conducting guide walls.

Similarly, in a typical *yz*-plane, say, for $x = a/2$ or $\sin(\pi x/a) = 1$ and $\cos(\pi x/a) = 0$, we have

$$\left(\frac{dy}{dz}\right)_E = \frac{\beta}{h^2} \left(\frac{\pi}{b}\right) \cot\left(\frac{\pi}{b} y\right) \tan(\omega t - \beta z), \quad (10-151)$$

and **H** has only an *x*-component. Some typical **E** and **H** lines are drawn in Fig. 10-11(b) for $t = 0$.

10-4.2 TE WAVES IN RECTANGULAR WAVEGUIDES

For transverse electric waves, $E_z = 0$, we solve Eq. (10-48) for H_z . We write

$$H_z(x, y, z) = H_z^0(x, y)e^{-\gamma z}, \quad (10-152)$$

where $H_z^0(x, z)$ satisfies the following second-order partial differential equation:

$$\left(\frac{\partial^2}{\partial x^2} + \frac{\partial^2}{\partial y^2} + h^2\right) H_z^0(x, y) = 0. \quad (10-153)$$

Equation (10-153) is seen to be of exactly the same form as Eq. (10-122). The solution for $H_z^0(x, y)$ must satisfy the following boundary conditions.

1. In the *x*-direction:

$$\frac{\partial H_z^0}{\partial x} = 0 \quad (E_y = 0) \quad \text{at } x = 0, \quad (10-154)$$

$$\frac{\partial H_z^0}{\partial x} = 0 \quad (E_y = 0) \quad \text{at } x = a. \quad (10-155)$$

2. In the *y*-direction:

$$\frac{\partial H_z^0}{\partial y} = 0 \quad (E_x = 0) \quad \text{at } y = 0, \quad (10-156)$$

$$\frac{\partial H_z^0}{\partial y} = 0 \quad (E_x = 0) \quad \text{at } y = b. \quad (10-157)$$

It is readily verified that the appropriate solution for $H_z^0(x, y)$ is

$$H_z^0(x, y) = H_0 \cos\left(\frac{m\pi}{a}x\right) \cos\left(\frac{n\pi}{b}y\right) \quad (\text{A/m}). \quad (10-158)$$

The relation between the eigenvalue h and $(m\pi/a)$ and $(n\pi/b)$ is the same as that given in Eq. (10-133) for TM modes.

The other field components are obtained from Eqs. (10-49) through (10-52):

$$E_x^0(x, y) = \frac{j\omega\mu}{h^2} \left(\frac{n\pi}{b} \right) H_0 \cos \left(\frac{m\pi}{a} x \right) \sin \left(\frac{n\pi}{b} y \right), \quad (10-159)$$

$$E_y^0(x, y) = -\frac{j\omega\mu}{h^2} \left(\frac{m\pi}{a} \right) H_0 \sin \left(\frac{m\pi}{a} x \right) \cos \left(\frac{n\pi}{b} y \right), \quad (10-160)$$

$$H_x^0(x, y) = \frac{\gamma}{h^2} \left(\frac{m\pi}{a} \right) H_0 \sin \left(\frac{m\pi}{a} x \right) \cos \left(\frac{n\pi}{b} y \right), \quad (10-161)$$

$$H_y^0(x, y) = \frac{\gamma}{h^2} \left(\frac{n\pi}{b} \right) H_0 \cos \left(\frac{m\pi}{a} x \right) \sin \left(\frac{n\pi}{b} y \right), \quad (10-162)$$

where γ has the same expression as that given in Eq. (10-138) for TM modes.

Equation (10-139) for cutoff frequency also applies here. For TE modes, either m or n (but not both) can be zero. If $a > b$, the cutoff frequency is the *lowest* when $m = 1$ and $n = 0$:

$$(f_c)_{TE_{10}} = \frac{1}{2a\sqrt{\mu\epsilon}} = \frac{u}{2a} \quad (\text{Hz}). \quad (10-163)$$

The corresponding cutoff wavelength is

$$(\lambda_c)_{TE_{10}} = 2a \quad (\text{m}). \quad (10-164)$$

Hence **the TE_{10} mode is the dominant mode of a rectangular waveguide with $a > b$.** Because the TE_{10} mode has the lowest attenuation of all modes in a rectangular waveguide and its electric field is definitely polarized in one direction everywhere, it is of particular practical importance (see Subsection 10-4.3).

EXAMPLE 10-8 (a) Write the instantaneous field expressions for the TE_{10} mode in a rectangular waveguide having sides a and b . (b) Sketch the electric and magnetic field lines in typical xy -, yz -, and xz -planes. (c) Sketch the surface currents on the guide walls.

Solution

- a) The instantaneous field expressions for the dominant TE_{10} mode are obtained by multiplying the phasor expressions in Eqs. (10-158) through (10-162) with $e^{j(\omega t - \beta z)}$ and then taking the real part of the product. We have, for $m = 1$ and $n = 0$,

$$E_x(x, y, z; t) = 0, \quad (10-165)$$

as that given
ugh (10-52):

$$(10-159) \quad E_y(x, y, z; t) = \frac{\omega\mu}{h^2} \left(\frac{\pi}{a}\right) H_0 \sin\left(\frac{\pi}{a}x\right) \sin(\omega t - \beta z),$$

$$(10-160) \quad E_z(x, y, z; t) = 0,$$

$$(10-161) \quad H_x(x, y, z; t) = -\frac{\beta}{h^2} \left(\frac{\pi}{a}\right) H_0 \sin\left(\frac{\pi}{a}x\right) \sin(\omega t - \beta z),$$

where

$$(10-162) \quad H_y(x, y, z; t) = H_0 \cos\left(\frac{\pi}{a}x\right) \cos(\omega t - \beta z),$$

M modes.
S modes, either
the lowest when

$$(10-163)$$

$$(10-164)$$

de with $a > b$.
a rectangular
everywhere, it

TE₁₀ mode in
and magnetic
currents on the

are obtained
(10-162) with
for $m = 1$ and

$$(10-165)$$

$$E_y(x, y, z; t) = \frac{\omega\mu}{h^2} \left(\frac{\pi}{a}\right) H_0 \sin\left(\frac{\pi}{a}x\right) \sin(\omega t - \beta z), \quad (10-166)$$

$$E_z(x, y, z; t) = 0, \quad (10-167)$$

$$H_x(x, y, z; t) = -\frac{\beta}{h^2} \left(\frac{\pi}{a}\right) H_0 \sin\left(\frac{\pi}{a}x\right) \sin(\omega t - \beta z), \quad (10-168)$$

$$H_y(x, y, z; t) = 0, \quad (10-169)$$

$$H_z(x, y, z; t) = H_0 \cos\left(\frac{\pi}{a}x\right) \cos(\omega t - \beta z), \quad (10-170)$$

where

$$\beta = \sqrt{k^2 - h^2} = \sqrt{\omega^2 \mu \epsilon - \left(\frac{\pi}{a}\right)^2}. \quad (10-171)$$

- b) We see from Eqs. (10-165) through (10-170) that the TE₁₀ mode has only three nonzero field components—namely, E_y , H_x , and H_z . In a typical xy -plane, say, when $\sin(\omega t - \beta z) = 1$, both E_y and H_x vary as $\sin(\pi x/a)$ and are independent of y , as shown in Fig. 10-12(a).

In a typical yz -plane, for example at $x = a/2$ or $\sin(\pi x/a) = 1$ and $\cos(\pi x/a) = 0$, we only have E_y and H_x , both of which vary sinusoidally with βz . A sketch of E_y and H_x at $t = 0$ is given in Fig. 10-12(b).

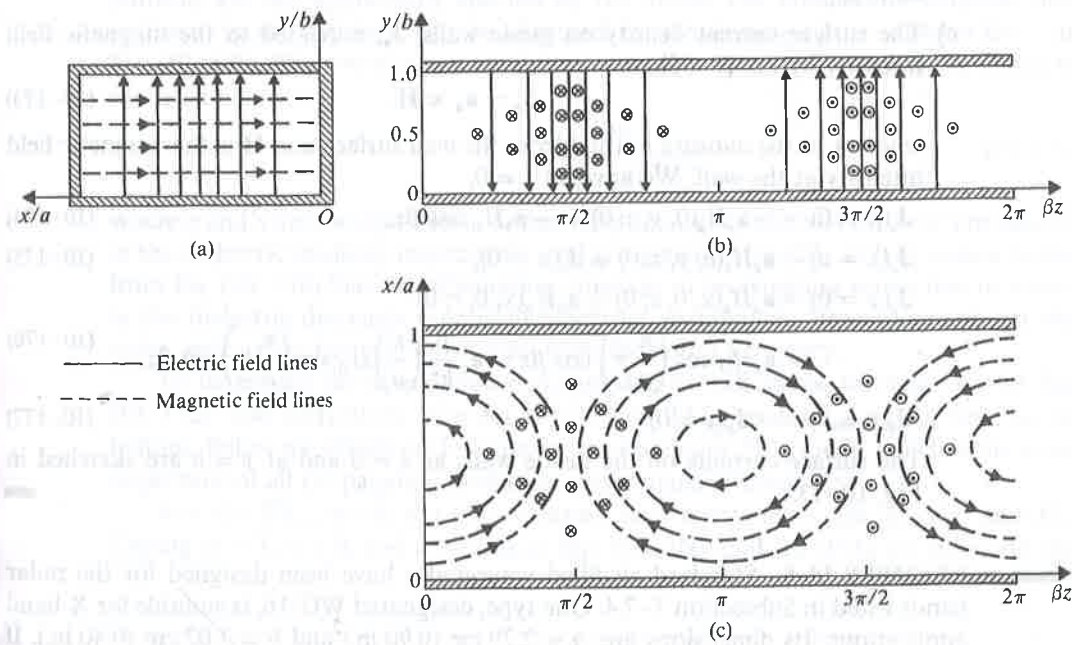


FIGURE 10-12
Field lines for TE₁₀ mode in rectangular waveguide.

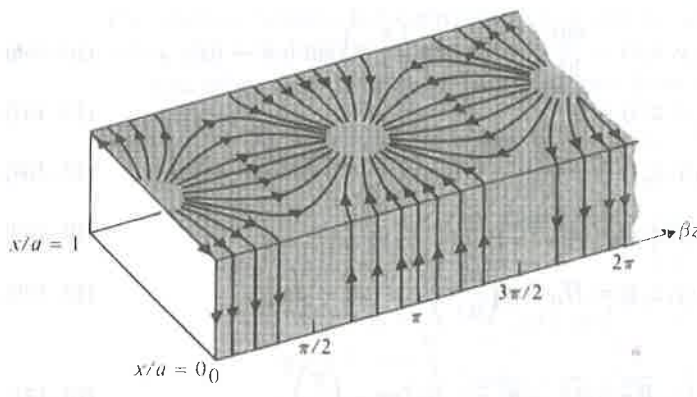


FIGURE 10-13
Surface currents on guide walls
for TE_{10} mode in rectangular
waveguide.

The sketch in an xz -plane will show all three nonzero field components— E_y , H_x , and H_z . The slope of the \mathbf{H} lines at $t = 0$ is governed by the following equation:

$$\left(\frac{dx}{dz}\right)_{\mathbf{H}} = \frac{\beta}{h^2} \left(\frac{\pi}{a}\right) \tan\left(\frac{\pi}{a}x\right) \tan\beta z, \quad (10-172)$$

which can be used to draw the \mathbf{H} lines in Fig. 10-12(c). These lines are independent of y .

- c) The surface current density on guide walls, \mathbf{J}_s , is related to the magnetic field intensity by Eq. (7-66b):

$$\mathbf{J}_s = \mathbf{a}_n \times \mathbf{H}, \quad (10-173)$$

where \mathbf{a}_n is the *outward* normal from the wall surface and \mathbf{H} is the magnetic field intensity at the wall. We have, at $t = 0$,

$$\mathbf{J}_s(x = 0) = -\mathbf{a}_y H_z(0, y, z; 0) = -\mathbf{a}_y H_0 \cos\beta z, \quad (10-174)$$

$$\mathbf{J}_s(x = a) = \mathbf{a}_y H_z(a, y, z; 0) = \mathbf{J}_s(x = 0), \quad (10-175)$$

$$\begin{aligned} \mathbf{J}_s(y = 0) &= \mathbf{a}_x H_z(x, 0, z; 0) - \mathbf{a}_z H_x(x, 0, z; 0) \\ &= \mathbf{a}_x H_0 \cos\left(\frac{\pi}{a}x\right) \cos\beta z - \mathbf{a}_z \frac{\beta}{h^2} \left(\frac{\pi}{a}\right) H_0 \sin\left(\frac{\pi}{a}x\right) \sin\beta z, \end{aligned} \quad (10-176)$$

$$\mathbf{J}_s(y = b) = -\mathbf{J}_s(y = 0). \quad (10-177)$$

The surface currents on the inside walls at $x = 0$ and at $y = b$ are sketched in Fig. 10-13.

EXAMPLE 10-9 Standard air-filled waveguides have been designed for the radar bands listed in Subsection 7-7.4. One type, designated WG-16, is suitable for X-band applications. Its dimensions are: $a = 2.29$ cm (0.90 in.) and $b = 1.02$ cm (0.40 in.). If it is desired that a WG-16 waveguide operate only in the dominant TE_{10} mode and

that the operating frequency be at least 25% above the cutoff frequency of the TE_{10} mode but no higher than 95% of the next higher cutoff frequency, what is the allowable operating-frequency range?

Solution For $a = 2.29 \times 10^{-2}$ (m) and $b = 1.02 \times 10^{-2}$ (m), the two modes having the lowest cutoff frequencies are TE_{10} and TE_{20} . Using Eq. (10-139), we find

$$(f_c)_{10} = \frac{c}{2a} = \frac{3 \times 10^8}{2 \times 2.29 \times 10^{-2}} = 6.55 \times 10^9 \text{ (Hz)},$$

$$(f_c)_{20} = \frac{c}{a} = 13.10 \times 10^9 \text{ (Hz).}^{\dagger}$$

Thus the allowable operating-frequency range under the specified conditions is

$$1.25(f_c)_{\text{TE}_{10}} \leq f \leq 0.95(f_c)_{\text{TE}_{20}}$$

or

$$8.19 \text{ (GHz)} \leq f \leq 12.45 \text{ (GHz).}$$

10-4.3 ATTENUATION IN RECTANGULAR WAVEGUIDES

Attenuation for propagating modes results when there are losses in the dielectric and in the imperfectly conducting guide walls. Because these losses are usually very small, we will assume, as in the case of parallel-plate waveguides, that the transverse field patterns are not appreciably affected by the losses. The attenuation constant due to losses in the dielectric can be obtained by substituting $\epsilon_d = \epsilon + (\sigma/j\omega)$ for ϵ in Eq. (10-138). The result is exactly the same as that given in Eq. (10-110), which is repeated below:

$$\alpha_d = \frac{\sigma\eta}{2\sqrt{1 - (f_c/f)^2}}, \quad (10-178)$$

where σ and η are the equivalent conductivity (see Eq. 7-112) and intrinsic impedance of the dielectric medium, respectively, and f_c is given by Eq. (10-139). It is easy to see from Eq. (10-178) that the attenuation constant of propagating waves due to losses in the dielectric decreases monotonically from an infinitely large value toward the value $\sigma\eta/2$ as the frequency increases from the cutoff frequency.

To determine the attenuation constant due to wall losses, we make use of Eq. (10-112). The derivations of α_c for the general TM_{mn} and TE_{mn} modes tend to be tedious. Below we obtain the formula for the dominant TE_{10} mode, which is the most important of all propagating modes in a rectangular waveguide.

For the TE_{10} mode the only nonzero field components are E_y , H_x , and H_z . Letting $m = 1$, $n = 0$, and $h = (\pi/a)$ in Eqs. (10-160) and (10-161), we calculate the

[†] Note that $(f_c)_{01} = (c/2b) > (f_c)_{20}$ and $(f_c)_{11} = (c/2a)\sqrt{1 + (a/b)^2} > (f_c)_{20}$.

time-average power flowing through a cross section of the waveguide:

$$\begin{aligned} P(z) &= \int_0^b \int_0^a -\frac{1}{2}(E_y^0)(H_x^0)^* dx dy \\ &= \frac{1}{2} \omega \mu \beta \left(\frac{a}{\pi}\right)^2 H_0^2 \int_0^b \int_0^a \sin^2 \left(\frac{\pi}{a} x\right) dx dy \\ &= \omega \mu \beta ab \left(\frac{a H_0}{2\pi}\right)^2. \end{aligned} \quad (10-179)$$

In order to calculate the time-average power lost in the conducting walls per unit length, we must consider all four walls. From Eqs. (10-173), (10-158), and (10-161) we see that

$$\mathbf{J}_s^0(x = 0) = \mathbf{J}_s^0(x = a) = -\mathbf{a}_y H_z^0(x = 0) = -\mathbf{a}_y H_0 \quad (10-180)$$

and

$$\begin{aligned} \mathbf{J}_s^0(y = 0) &= -\mathbf{J}_s^0(y = b) = \mathbf{a}_x H_z^0(y = 0) - \mathbf{a}_z H_x^0(y = 0) \\ &= \mathbf{a}_x H_0 \cos \left(\frac{\pi}{a} x\right) - \mathbf{a}_z \frac{\beta a}{\pi} H_0 \sin \left(\frac{\pi}{a} x\right). \end{aligned} \quad (10-181)$$

The total power loss is then double the sum off the losses in the walls at $x = 0$ and at $y = 0$. We have

$$P_L(z) = 2[P_L(z)]_{x=0} + 2[P_L(z)]_{y=0}, \quad (10-182)$$

where

$$[P_L(z)]_{x=0} = \int_0^b \frac{1}{2} |J_s^0(x = 0)|^2 R_s dy = \frac{b}{2} H_0^2 R_s \quad (10-183)$$

and

$$\begin{aligned} [P_L(z)]_{y=0} &= \int_0^a \frac{1}{2} [|J_{sx}^0(y = 0)|^2 + |J_{sz}^0(y = 0)|^2] R_s dx \\ &= \frac{a}{4} \left[1 + \left(\frac{\beta a}{\pi}\right)^2 \right] H_0^2 R_s. \end{aligned} \quad (10-184)$$

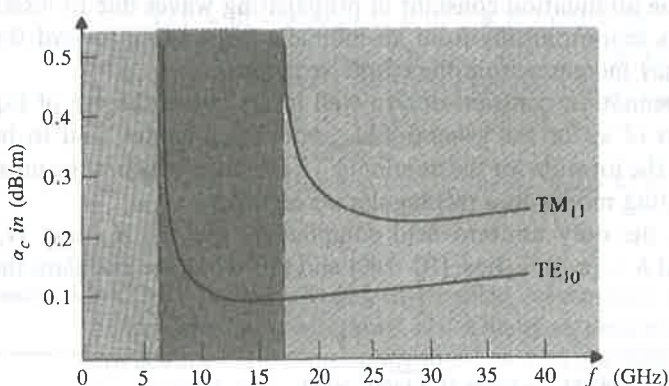


FIGURE 10-14
Attenuation due to wall losses in rectangular copper waveguide for TE_{10} and TM_{11} modes.
 $a = 2.29$ (cm), $b = 1.02$ (cm).

de:

(10-179)

ducting walls per
(10-158), and

(10-180)

$\left(\frac{\pi}{a}x\right). \quad (10-181)$

alls at $x = 0$ and

(10-182)

(10-183)

(10-184)

to wall losses in
er waveguide for
modes.
 $= 1.02 \text{ (cm)}$

Substitution of Eqs. (10-183) and (10-184) in Eq. (10-182) yields

$$\begin{aligned} P_L(z) &= \left\{ b + \frac{a}{2} \left[1 + \left(\frac{\beta a}{\pi} \right)^2 \right] \right\} H_0^2 R_s \\ &= \left[b + \frac{a}{2} \left(\frac{f}{f_c} \right)^2 \right] H_0^2 R_s. \end{aligned} \quad (10-185)$$

The last expression is the result of recognizing that

$$\beta = \sqrt{\omega^2 \mu \epsilon - \left(\frac{\pi}{a} \right)^2} = \omega \sqrt{\mu \epsilon} \sqrt{1 - \left(\frac{f_c}{f} \right)^2}. \quad (10-186)$$

Inserting Eqs. (10-179) and (10-185) in Eq. (10-112), we obtain

$$\begin{aligned} (\alpha_c)_{TE_{10}} &= \frac{R_s [1 + (2b/a)(f_c/f)^2]}{\eta b \sqrt{1 - (f_c/f)^2}} \\ &= \frac{1}{\eta b} \sqrt{\frac{\pi f \mu_c}{\sigma_c [1 - (f_c/f)^2]}} \left[1 + \frac{2b}{a} \left(\frac{f_c}{f} \right)^2 \right] \quad (\text{Np/m}). \end{aligned} \quad (10-187)$$

Equation (10-187) reveals a rather complicated dependence of $(\alpha_c)_{TE_{10}}$ on the ratio (f_c/f) . It tends to infinity when f is close to the cutoff frequency, decreases toward a minimum as f increases, and increases again steadily for further increases in f .

For a given guide width a , the attenuation decreases as b increases. However, increasing b also decreases the cutoff frequency of the next higher-order mode TE_{11} (or TM_{11}), with the consequence that the available bandwidth for the dominant TE_{10} mode (the range of frequencies over which TE_{10} is the only possible propagating mode) is reduced. The usual compromise is to choose the ratio b/a in the neighborhood of $\frac{1}{2}$.

If we follow a similar procedure that led to Eq. (10-187), the attenuation constant due to wall losses for TM modes can be derived. For the TM_{11} mode we obtain

$$(\alpha_c)_{TM_{11}} = \frac{2R_s(b/a^2 + a/b^2)}{\eta ab \sqrt{1 - (f_c/f)^2}(1/a^2 + 1/b^2)}. \quad (10-188)$$

In Fig. 10-14 are plotted the graphs of $(\alpha_c)_{TE_{10}}$ and $(\alpha_c)_{TM_{11}}$ for a standard air-filled WR-16 rectangular copper waveguide with $a = 2.29 \text{ (cm)}$ and $b = 1.02 \text{ (cm)}$. From Eq. (10-139) we find $(f_c)_{10} = 6.55 \text{ (GHz)}$ and $(f_c)_{11} = 16.10 \text{ (GHz)}$. The curves show that the attenuation constant increases rapidly toward infinity as the operating frequency approaches the cutoff frequency. In the operating range ($f > f_c$), both curves possess a broad minimum. The attenuation constant of the TE_{10} mode is everywhere lower than that of the TM_{11} mode. These facts have direct relevance in the choice of operating modes and frequencies.

EXAMPLE 10-10 A TE₁₀ wave at 10 (GHz) propagates in a brass— $\sigma_c = 1.57 \times 10^7$ (S/m)—rectangular waveguide with inner dimensions $a = 1.5$ (cm) and $b = 0.6$ (cm), which is filled with polyethylene— $\epsilon_r = 2.25$, $\mu_r = 1$, loss tangent = 4×10^{-4} . Determine (a) the phase constant, (b) the guide wavelength, (c) the phase velocity, (d) the wave impedance, (e) the attenuation constant due to loss in the dielectric, and (f) the attenuation constant due to loss in the guide walls.

Solution At $f = 10^{10}$ (Hz) the wavelength in unbounded polyethylene is

$$\lambda = \frac{u}{f} = \frac{3 \times 10^8}{\sqrt{2.25 \times 10^{10}}} = \frac{2 \times 10^8}{10^{10}} = 0.02 \text{ (m).}$$

The cutoff frequency for the TE₁₀ mode is, from Eq. (10-163),

$$f_c = \frac{u}{2a} = \frac{2 \times 10^8}{2 \times (1.5 \times 10^{-2})} = 0.667 \times 10^{10} \text{ (Hz).}$$

a) The phase constant is, from Eq. (10-186),

$$\begin{aligned} \beta &= \frac{\omega}{u} \sqrt{1 - \left(\frac{f_c}{f}\right)^2} = \frac{2\pi 10^{10}}{2 \times 10^8} \sqrt{1 - 0.667^2} \\ &= 74.5\pi = 234 \text{ (rad/m).} \end{aligned}$$

b) The guide wavelength is, from Eq. (10-39),

$$\lambda_g = \frac{\lambda}{\sqrt{1 - (f_c/f)^2}} = \frac{0.02}{\sqrt{1 - (f_c/f)^2}} = \frac{0.02}{0.745} = 0.0268 \text{ (m).}$$

c) The phase velocity is, from Eq. (10-42),

$$u_p = \frac{u}{\sqrt{1 - (f_c/f)^2}} = \frac{2 \times 10^8}{0.745} = 2.68 \times 10^8 \text{ (m/s).}$$

d) The wave impedance is, from Eq. (10-57),

$$(Z_{TE})_{10} = \frac{\sqrt{\mu/\epsilon}}{\sqrt{1 - (f_c/f)^2}} = \frac{377/\sqrt{2.25}}{0.745} = 337.4 \text{ (\Omega).}$$

e) The attenuation constant due to loss in dielectric is obtained from Eq. (10-178).

The effective conductivity for polyethylene at 10 (GHz) can be determined from the given loss tangent by using Eq. (7-115):

$$\begin{aligned} \sigma &= 4 \times 10^{-4} \omega \epsilon = 4 \times 10^{-4} \times (2\pi \times 10^{10}) \times \left(\frac{2.25}{36\pi} \times 10^{-9} \right) \\ &= 5 \times 10^{-4} \text{ (S/m).} \end{aligned}$$

Thus,

$$\begin{aligned} \alpha_d &= \frac{\sigma}{2} Z_{TE} = \frac{5 \times 10^{-4}}{2} \times 337.4 = 0.084 \text{ (Np/m)} \\ &= 0.73 \text{ (dB/m).} \end{aligned}$$

- f) The attenuation constant due to loss in the guide walls is found from Eq. (10-187). We have, from Eq. (9-26b),

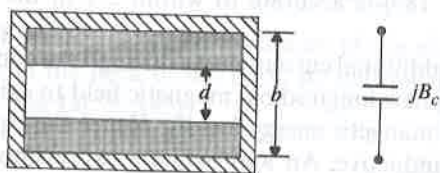
$$R_s = \sqrt{\frac{\pi f \mu_c}{\sigma_c}} = \sqrt{\frac{\pi 10^{10} (4\pi 10^{-7})}{1.57 \times 10^7}} = 0.0501 \text{ } (\Omega),$$

$$\alpha_c = \frac{R_s [1 + (2b/a)(f_c/f)^2]}{\eta b \sqrt{1 - (f_c/f)^2}} = \frac{0.0501 [1 + (1.2/1.5)(0.667)^2]}{251 \times 0.006 \times 0.745} = 0.0605 \text{ } (\text{Np/m})$$

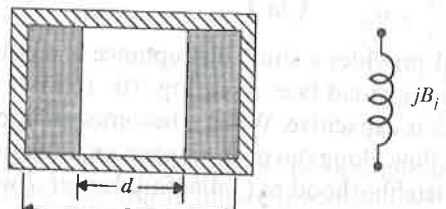
$$= 0.526 \text{ } (\text{dB/m}).$$

10-4.4 DISCONTINUITIES IN RECTANGULAR WAVEGUIDES

Just as in the case of transmission lines, it is desirable to have impedance match for wave propagation in waveguides in order to achieve maximum power transfer and to reduce local power loss due to a high standing-wave ratio. There is a need to introduce shunt susceptances at appropriate points along a waveguide. These shunt susceptances often take the form of a thin metal diaphragm with an iris such as those shown in Figs. 10-15(a) and 10-15(b). When a diaphragm with an iris is in place, the electric and magnetic fields must satisfy the additional boundary conditions on the metal surface. If the waveguide operates in the dominant TE_{10} mode, the additional boundary conditions require the presence of all higher-order modes, and the situation is vastly more complicated. However, the waveguide is usually designed so that only the dominant mode can propagate. The higher-order modes are then all cutoff modes; they are evanescent and are localized near the iris. An analytical determination of the effective shunt susceptance of an iris would necessitate the solution



(a) Capacitive iris and equivalent susceptance



(b) Inductive iris and equivalent susceptance.

FIGURE 10-15
Irises in waveguide as susceptances.

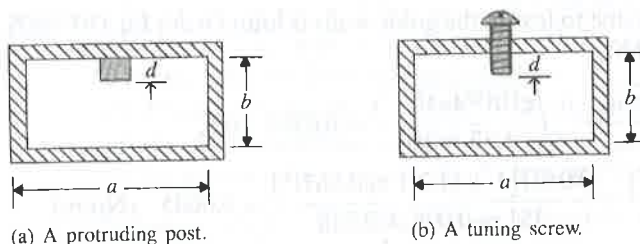


FIGURE 10-16
Post or screw in a waveguide.

of a difficult electromagnetics problem. We will offer only a qualitative discussion here and give the approximate formulas[†] for the irises in Figs. 10-15(a) and 10-15(b).

The iris in Fig. 10-15(a) is made of thin conducting diaphragms extending from one narrow wall to the other. As seen in Fig. 10-12(a), the electric field lines of the dominant TE_{10} mode in a cross section are in the y -direction, going across the narrow dimension. Reducing this dimension from b to d may be expected to have the effect of increasing this field as well as the stored electric energy locally. Consequently, the equivalent shunt susceptance is expected to be capacitive. An approximate expression for the normalized capacitive susceptance is

$$b_c = \frac{B_c}{Y_{10}} = \frac{4b}{\lambda_g} \ln \left[\csc \left(\frac{\pi d}{2b} \right) \right], \quad (10-189)$$

where Y_{10} is the reciprocal of $Z_{TE_{10}}$ from Eq. (10-57) and λ_g is the guide wavelength given in Eq. (10-39). As we have indicated before, the actual situation is much more complicated, owing to the presence of the evanescent higher-order modes near the iris. A more accurate analysis will show that b_c is not strictly proportional to (b/λ_g) . The approximate formula in Eq. (10-189) is accurate to within 5% in the normal range of operating frequencies.

The iris in Fig. 10-15(b) provides additional current paths through the conducting diaphragms in the y -direction, causing new longitudinal magnetic field to exist in the iris opening and increasing the stored mangetic energy locally. Hence the equivalent shunt susceptance is expected to be inductive. An approximate expression for the normalized inductive susceptance of the iris is

$$b_i = \frac{B_i}{Y_{10}} = -\frac{\lambda_g}{a} \cot^2 \left(\frac{\pi d}{2a} \right). \quad (10-190)$$

Another type of discontinuity that provides a shunt susceptance is a conducting post protruding into the waveguide on a broad face, as in Fig. 10-16(a). If the post length d is small, the shunt susceptance is capacitive. When d becomes an appreciable fraction of b , considerable current can flow along the post, causing an inductive effect. A resonance occurs when d is in the neighborhood of $(3/4)b$. Still longer d will result

[†] For more details, see R. E. Collin, *Field Theory of Guided Waves*, McGraw-Hill, New York, 1960, Chapter 8; C. C. Johnson, *Field and Wave Electrodynamics*, McGraw-Hill, New York, 1965, Chapter 5.

in an inductive susceptance. In practical usage the post usually takes the form of a metal screw, as shown in Fig. 10-16(b). The screw could be inserted in a slit cut axially in the center of the broad face. The center slit does not appreciably disturb the field pattern in the waveguide, and the sliding screw with a variable d can be used for tuning and matching a given load to the waveguide. This is a technique similar to the single-stub matching scheme discussed in Subsection 9-7.2.

EXAMPLE 10-11 Measurements on a WG-10 S-band waveguide ($a = 7.21 \text{ cm}$, $b = 3.40 \text{ cm}$) feeding a horn antenna show a standing-wave ratio (SWR) of 2.00 at the 3 (GHz) operating frequency, and the existence of a maximum electric field at 12 (cm) from the neck of the horn. Find the location and the dimensions of a symmetrical inductive iris necessary to achieve a perfect match. Assume the waveguide to be lossless.

Solution With $a = 7.21 \times 10^{-2} \text{ (m)}$ and $b = 3.40 \times 10^{-2} \text{ (m)}$, the cutoff frequency for the dominant TE_{10} mode is

$$f_c = \frac{c}{2a} = \frac{3 \times 10^8}{2 \times 7.21 \times 10^{-2}} = 2.08 \times 10^9 \text{ (Hz)}.$$

The guide wavelength is, from Eq. (10-39),

$$\lambda_g = \frac{\lambda}{\sqrt{1 - (f_c/f)^2}} = \frac{c}{\sqrt{f^2 - f_c^2}} = \frac{3 \times 10^8}{10^9 \sqrt{3^2 - 2.08^2}} = 0.139 \text{ (m)} = 13.9 \text{ (cm)}.$$

Thus, the measured maximum of the electric field is at a distance $12/13.9 = 0.863\lambda_g$ from the neck of the horn. At that location the normalized effective load resistance is (see Eq. 9-145)

$$r_L = \frac{R_L}{R_0} = S.$$

The corresponding normalized conductance is

$$g_L = \frac{Y_L}{Y_0} = \frac{1}{S} = \frac{1}{2.00} = 0.50.$$

The rest of the problem is that of single-stub matching discussed in Subsection 9-7.2. We use the Smith admittance chart and proceed as follows (see Fig. 10-17):

1. Enter $g_L = 0.50$ on an Smith admittance chart as P_M (point of maximum electric field).

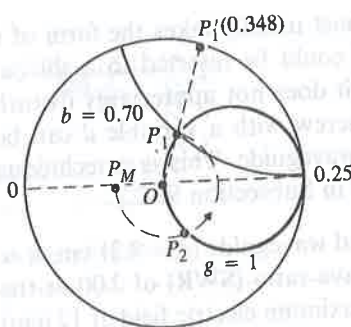


FIGURE 10-17
Construction on Smith admittance chart (Example 10-11).

2. Draw a $|\Gamma|$ -circle centered at O with radius \overline{OP}_M , intersecting the $g = 1$ circle at two points, P_1 and P_2 . Read

$$\begin{aligned} \text{at } P_1: \quad y_1 &= 1 + j0.70, \\ \text{at } P_2: \quad y_2 &= 1 - j0.70. \end{aligned}$$

Point P_2 is not useful to us because it requires a capacitive (positive) susceptance to achieve matching.

3. Draw a straight line from O through P_1 to point P'_1 on the perimeter. Read 0.348 on the "wavelength toward load" scale at P'_1 . This is $(0.863 - 0.348)\lambda_g = 7.16$ (cm) from the neck of the horn and is where an inductive iris of a normalized susceptance -0.70 should be placed.
4. Using Eq. (10-190), we determine the distance d of the required inductive iris shown in Fig. 10-15(b):

$$-0.70 = -\frac{13.9}{7.21} \cot^2 \left(\frac{\pi d}{2 \times 7.21} \right),$$

from which we find $d = 4.72$ (cm).

10-5 Circular Waveguides

Electromagnetic waves can also propagate inside round metal pipes. In this section we will study wave behaviors in circular waveguides—metal pipes having a uniform circular cross section and filled with a dielectric medium.

The basic equations to be satisfied by time-harmonic electric and magnetic field intensities in the charge-free dielectric region inside a waveguide are Eqs. (10-3) and (10-4), which are repeated below:

$$\nabla^2 \mathbf{E} + k^2 \mathbf{E} = 0 \quad (10-191)$$

and

$$\nabla^2 \mathbf{H} + k^2 \mathbf{H} = 0. \quad (10-192)$$

For a straight waveguide with a uniform circular cross section and having its axis in the z -direction, it is expedient to decompose the three-dimensional Laplacian op-

erator ∇^2 into two parts: $\nabla_{r\phi}^2$ for the transverse coordinates, and ∇_z^2 for the longitudinal z -component. Similarly, both \mathbf{E} and \mathbf{H} vectors can be written as the sum of a transverse component and an axial component:

$$\mathbf{E} = \mathbf{E}_T + \mathbf{a}_z E_z \quad (10-193)$$

and

$$\mathbf{H} = \mathbf{H}_T + \mathbf{a}_z H_z, \quad (10-194)$$

where the subscript T denotes the two-dimensional transverse component. We already know from Subsection 10-2.1 that TEM waves cannot exist in such a waveguide without an inner conductor. The propagating waves can be classified into two groups, as in rectangular waveguides: transverse magnetic (TM) and transverse electric (TE). For TM waves, $H_z = 0$, $E_z \neq 0$, and all field components can be expressed in terms of $E_z = E_z^0 e^{-\gamma z}$, where E_z^0 satisfies the homogeneous Helmholtz's equation

$$\nabla_{r\phi}^2 E_z^0 + (\gamma^2 + k^2) E_z^0 = 0 \quad (10-195)$$

or

$$\nabla_{r\phi}^2 E_z^0 + h^2 E_z^0 = 0. \quad (10-196)$$

For TE waves, $E_z = 0$, $H_z \neq 0$, and all field components can be expressed in terms of $H_z = H_z^0 e^{-\gamma z}$, where H_z^0 satisfies exactly the same homogeneous Helmholtz's equation required of E_z^0 above.

Although Eq. (10-196) is similar in form to Eq. (10-24), their solutions are quite different. We will consider the solution of Eq. (10-196) in the following subsection.

10-5.1 BESSEL'S DIFFERENTIAL EQUATION AND BESSEL FUNCTIONS

In cylindrical coordinates the expansion of Eq. (10-196) gives (see Eq. 4-8)

$$\frac{1}{r} \frac{\partial}{\partial r} \left(r \frac{\partial E_z^0}{\partial r} \right) + \frac{1}{r^2} \frac{\partial^2 E_z^0}{\partial \phi^2} + h^2 E_z^0 = 0. \quad (10-197)$$

To solve Eq. (10-197), we apply the method of separation of variables by assuming a product solution.

$$E_z^0(r, \phi) = R(r)\Phi(\phi), \quad (10-198)$$

where $R(r)$ and $\Phi(\phi)$ are functions only of r and ϕ , respectively. Substituting solution (10-198) in Eq. (10-197) and dividing by the product $R(r)\Phi(\phi)$, we obtain

$$\frac{r}{R(r)} \frac{d}{dr} \left[r \frac{dR(r)}{dr} \right] + h^2 r^2 = -\frac{1}{\Phi(\phi)} \frac{d^2 \Phi(\phi)}{d\phi^2}. \quad (10-199)$$

Now the left side of Eq. (10-199) is a function of r only, and the right side is a function of ϕ only. For Eq. (10-199) to hold for all values of r and ϕ , both sides must be equal to the same constant. Let this constant (separation constant) be n^2 . We can separate Eq. (10-199) into two ordinary differential equations:

$$\frac{d^2 \Phi(\phi)}{d\phi^2} + n^2 \Phi(\phi) = 0 \quad (10-200)$$

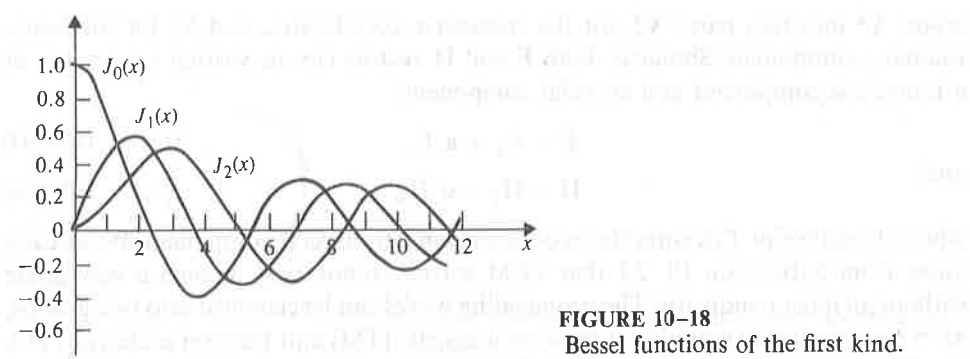


FIGURE 10-18
Bessel functions of the first kind.

and

$$\frac{r}{R(r)} \frac{d}{dr} \left[r \frac{dR(r)}{dr} \right] + h^2 r^2 = n^2$$

or

$$\boxed{\frac{d^2 R(r)}{dr^2} + \frac{1}{r} \frac{dR(r)}{dr} + \left(h^2 - \frac{n^2}{r^2} \right) R(r) = 0.} \quad (10-201)$$

Equation (10-201) is known as *Bessel's differential equation*.

A solution of Eq. (10-201) can be obtained by assuming $R(r)$ to be a power series in r with unknown coefficients,

$$R(r) = \sum_{p=0}^{\infty} C_p (hr)^p, \quad (10-202)$$

substituting it into the equation, and equating the sum of the coefficients of each power of r to zero. The actual work is tedious.[†] The result is

$$R(r) = C_n J_n(hr), \quad (10-203)$$

where C_n is an arbitrary constant, and

$$J_n(hr) = \sum_{m=0}^{\infty} \frac{(-1)^m (hr)^{n+2m}}{m!(n+m)! 2^{n+2m}} \quad (10-204)$$

is called the *Bessel function of the first kind* of n th order with an argument hr . Equation (10-204) holds only for integral values of n , which is true for cases of our interest, as we shall see later. $J_n(x)$ versus x curves of the first few orders have been plotted in Fig. 10-18. Several things are worth noting. First, $J_n(0) = 0$ for all n except when $n = 0$; for the zeroth order, $J_0(0) = 1$. Second, $J_n(x)$ are alternating functions

[†] N. W. MaLachlan, *Bessel Functions for Engineers*, 2d ed, Oxford University Press, New York, 1946.

TABLE 10-2
Zeros of $J_n(x)$, x_{np}

$p \backslash n$	$n = 0$	$n = 1$	$n = 2$
1	2.405	3.832	5.136
2	5.520	7.016	8.417

of decreasing amplitudes that cross the zero level at progressively shorter intervals. As x becomes very large, all $J_n(x)$ approach a sinusoidal form. Table 10-2 lists the values of the first several x_{np} , which denotes the p th zero of $J_n(x)$: $J_n(x_{np}) = 0$. In the next subsection we will find that the values of x_{np} determine the eigenvalues of TM modes in a circular waveguide. The eigenvalues of TE modes, on the other hand, depend on the zeros of the derivative of Bessel functions of the first kind—that is, on the values of x'_{np} , which make $J'_n(x'_{np}) = 0$ (see Subsection 10-5.3). The values of the first several x'_{np} are tabulated in Table 10-3.

So far, we have obtained only one solution—Bessel function of the first kind, $J_n(hr)$ —for the Bessel's differential equation (10-201). But Bessel's equation is a second-order equation; there should be two linearly independent solutions for each value of n . In other words, there should be another solution that is not linearly dependent on $J_n(hr)$. Such a solution exists. It is called **Bessel function of the second kind** or **Neumann function** and is usually denoted by $N_n(hr)$:

$$N_n(hr) = \frac{(\cos n\pi)J_n(hr) - J_{-n}(hr)}{\sin n\pi}. \quad (10-205)$$

The general solution of Eq. (10-201) can then be written as

$$R(r) = C_n J_n(hr) + D_n N_n(hr), \quad (10-206)$$

where C_n and D_n are arbitrary constants to be determined from boundary conditions.

A distinctive property of Bessel function of the second kind of all orders is that they become infinite when the argument is zero. When we study wave propagation in a circular waveguide, our region of interest includes the axis where $r = 0$. Since an infinite field is a physical impossibility, the solution $R(r)$ in Eq. (10-206) cannot contain a $N_n(hr)$ term. This means that the coefficient D_n must be zero for all n . Thus,

TABLE 10-3
Zeros of $J'_n(x)$, x'_{np}

$p \backslash n$	$n = 0$	$n = 1$	$n = 2$
1	3.832	1.841	3.054
2	7.016	5.331	6.706

for wave-mode problems inside a circular waveguide there is no need to be concerned with the $N_n(hr)$ term.

In the study of circular waveguides that follows, the preceding short summary of Bessel's differential equation and Bessel functions should suffice. The rest of this subsection discusses some additional aspects for completeness. It may be skipped if the material on dielectric-rod waveguides in Subsection 10-6.3 is to be omitted.

In case the region of interest of a problem in cylindrical coordinates does not include the axis where $r = 0$ (such as the problem of a coaxial waveguide with an inner conductor), the radial solution $R(r)$ in Eq. (10-206) must consist of both $J_n(hr)$ and $N_n(hr)$ terms, and the coefficients C_n and D_n are to be determined from boundary conditions. Furthermore, if a problem does not involve the entire 2π range of ϕ (such as the problem of a wedge-shaped waveguide), the constant n in Eq. (10-200) will not be an integer. Let it be denoted by v . We write the solution of the Bessel's differential equation as

$$R(r) = CJ_v(hr) + DN_v(hr). \quad (10-207)^{\dagger}$$

In some wave problems it is convenient to define linear combinations of the Bessel functions:

$$H_v^{(1)}(hr) = J_v(hr) + jN_v(hr), \quad (10-208)$$

$$H_v^{(2)}(hr) = J_v(hr) - jN_v(hr), \quad (10-209)$$

where $H_v^{(1)}$ and $H_v^{(2)}$ are called **Hankel functions** of the first and second kind, respectively. When the argument hr is very large, the asymptotic expressions for $H_v^{(1)}$ and $H_v^{(2)}$ are

$$H_v^{(1)}(hr) \rightarrow \sqrt{\frac{2}{\pi hr}} e^{j(hr - \pi/4 - v\pi/2)}, \quad (10-210)$$

$$H_v^{(2)}(hr) \rightarrow \sqrt{\frac{2}{\pi hr}} e^{-j(hr - \pi/4 - v\pi/2)}. \quad (10-211)$$

These expressions with imaginary exponential coefficients and decreasing amplitudes place in evidence the wave character of the Hankel functions. They are useful in problems of radiation.

When h^2 is negative ($h = j\zeta$), two other functions $I_v(\zeta)$ and $K_v(\zeta)$, related to J_v and $H_v^{(1)}$, respectively, are defined:

$$I_v(\zeta r) = j^{-v} J_v(j\zeta r), \quad (10-212)$$

$$K_v(\zeta r) = \frac{\pi}{2} j^{v+1} H_v^{(1)}(j\zeta r). \quad (10-213)$$

[†] The expression for $J_v(hr)$ for a nonintegral v is that given in Eq. (10-204) with $(n+m)!$ replaced by the gamma function $\Gamma(v+m+1)$.

ed to be concerned
ng short summary
ce. The rest of this
may be skipped if
to be omitted.
ordinates does not
waveguide with an
nsist of both $J_n(hr)$
ed from boundary
 2π range of ϕ (such
Eq. (10-200) will
of the Bessel's dif-

(10-207)^t

mbinations of the

(10-208)

(10-209)

second kind, respec-
ssions for $H_v^{(1)}$ and

(10-210)

(10-211)

reasing amplitudes
are useful in prob- $K_v(\zeta)$, related to J_v

(10-212)

(10-213)

 $(n+m)!$ replaced by the

I_v and K_v are called **modified Bessel functions** of the first and second kind, respectively. For large arguments the following asymptotic expressions are obtained:

$$I_v(\zeta r) \rightarrow \sqrt{\frac{1}{2\pi\zeta r}} e^{\zeta r}, \quad (10-214)$$

$$K_v(\zeta r) \rightarrow \sqrt{\frac{\pi}{2\zeta r}} e^{-\zeta r}. \quad (10-215)$$

It is seen that at large r , $K_v(\zeta r)$ shows an exponential decay with distance, characteristic of an evanescent wave. It is useful in surface-wave problems such as dielectric-rod waveguides and optical fibers. The choice of the appropriate form as a solution for the Bessel's differential equation depends on the type of the problem and on convenience.

10-5.2 TM WAVES IN CIRCULAR WAVEGUIDES

Figure 10-19 shows a circular waveguide of radius a . It consists of a metal pipe centered around the z -axis. The enclosed dielectric medium is assumed to have constitutive parameters ϵ and μ . For TM waves, $H_z = 0$. We write

$$E_z(r, \phi, z) = E_z^0(r, \phi) e^{-\gamma z}, \quad (10-216)$$

where $E_z^0(r, \phi)$ satisfies Eq. (10-196). The solution is written in the form of Eq. (10-198), in which

$$R(r) = C_n J_n(hr), \quad (10-217)$$

and $\Phi(\phi)$ is the solution of Eq. (10-200). Since all field components are periodic with respect to ϕ (period = 2π), the only admissible solution for Eq. (10-200) is $\sin n\phi$ or $\cos n\phi$, or a linear combination of the two (see Table 4-1). It is because of this requirement of periodicity that we demand n to be an integer, as indicated previously. Whether $\sin n\phi$ or $\cos n\phi$ is chosen is immaterial; it changes only the location of the

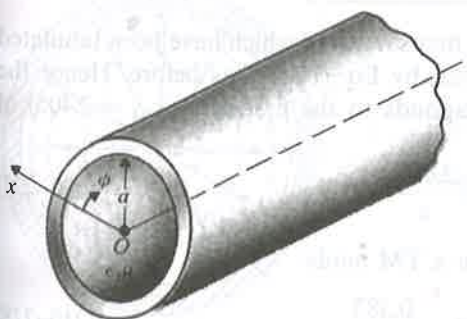


FIGURE 10-19

A circular waveguide.

reference $\phi = 0$ angle. Customarily, we write $E_z^0(r, \phi)$ for TM modes as

$$E_z^0 = C_n J_n(hr) \cos n\phi. \quad (\text{TM modes}) \quad (10-218)$$

The transverse components E_r^0 and E_ϕ^0 can be found from an adaptation of Eq. (10-29) to the cross-sectional polar coordinates (Problem P.10-26):

$$(\mathbf{E}_T^0)_{\text{TM}} = \mathbf{a}_r E_r^0 + \mathbf{a}_\phi E_\phi^0 = -\frac{\gamma}{h^2} \nabla_T E_z^0, \quad (10-219)$$

where

$$\nabla_T E_z^0 = \left(\mathbf{a}_r \frac{\partial}{\partial r} + \mathbf{a}_\phi \frac{\partial}{r \partial \phi} \right) E_z^0. \quad (10-220)$$

The magnetic field components can then be obtained by using Eq. (10-32).

We have for TM modes, in addition to E_z^0 in Eq. (10-218),

$$E_r^0 = -\frac{j\beta}{h} C_n J'_n(hr) \cos n\phi, \quad (10-221)$$

$$E_\phi^0 = \frac{j\beta n}{h^2 r} C_n J_n(hr) \sin n\phi, \quad (10-222)$$

$$H_r^0 = -\frac{j\omega\epsilon n}{h^2 r} C_n J_n(hr) \sin n\phi, \quad (10-223)$$

$$H_\phi^0 = -\frac{j\omega\epsilon}{h} C_n J'_n(hr) \cos n\phi, \quad (10-224)$$

$$H_z^0 = 0, \quad (10-225)$$

where γ has been replaced by $j\beta$, J'_n is the derivative of J_n with respect to its argument (hr), and the coefficient C_n depends on the field strength of the excitation.

The eigenvalues of TM modes (the admissible values of h) are determined from the boundary condition that E_z^0 must vanish at $r = a$; that is,

$$J_n(ha) = 0. \quad (\text{TM modes}) \quad (10-226)$$

There are infinitely many zeros of $J_n(x)$, the first several of which have been tabulated in Table 10-2. The cutoff frequency is given by Eq. (10-35) as before. Hence the eigenvalue for the TM_{01} mode that corresponds to the first zero ($x_{01} = 2.405$) of $J_0(x)$ is

$$(h)_{\text{TM}_{01}} = \frac{2.405}{a}, \quad (10-227)$$

which yields the lowest cutoff frequency for a TM mode:

$$(f_c)_{\text{TM}_{01}} = \frac{(h)_{\text{TM}_{01}}}{2\pi\sqrt{\mu\epsilon}} = \frac{0.383}{a\sqrt{\mu\epsilon}}. \quad (10-228)$$

des as

(10-218)

adaptation of Eq. 6:

(10-219)

(10-220)

(10-32).

(10-221)

(10-222)

(10-223)

(10-224)

(10-225)

ct to its argument
itation.

determined from

(10-226)

ve been tabulated
before. Hence the
($x_{01} = 2.405$) of

(10-227)

(10-228)

The phase constant β and the guide wavelength λ_g can be found from Eqs. (10-38) and (10-39), respectively.

For the TM_{01} mode ($n = 0$), E_z^0 , E_r^0 , and H_ϕ^0 are the only nonzero field components. A sketch of the electric and magnetic field lines in a typical transverse plane is given in Fig. 10-20. According to Eq. (10-224), H_ϕ^0 varies with r as $J'_0(hr)$, which equals $-J_1(hr)$. Thus the density of the magnetic field lines increases from $r = 0$ to $r = a$.

Note that in rectangular waveguides the first and second numbers of the mode index denote the number of half-wave field variations in the x - and y -directions, respectively, in a transverse xy -plane. By convention *the first number of the mode index for circular waveguides always represents the number of half-wave field variations in the ϕ -direction*, and the second number represents the number of half-wave field variations in the r -direction. Hence the transverse field pattern of the TM_{01} mode in a circular waveguide is analogous to the TM_{11} mode (instead of the TM_{01} mode, which does not exist) in a rectangular waveguide.

10-5.3 TE WAVES IN CIRCULAR WAVEGUIDES

For TE modes, $E_z = 0$, and

$$H_z(r, \phi, z) = H_z^0(r, \phi)e^{-\gamma z}, \quad (10-229)$$

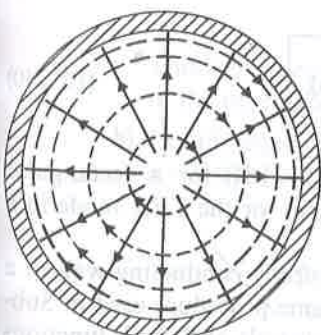
where H_z^0 satisfies the homogeneous Helmholtz's equation

$$\nabla_{r\phi}^2 H_z^0 + h^2 H_z^0 = 0. \quad (10-230)$$

Analogously to the TM case, we write the solution as

$$H_z^0 = C_n J_n(hr) \cos n\phi. \quad (\text{TE modes}) \quad (10-231)$$

From H_z^0 we find the transverse magnetic field components H_r^0 and H_ϕ^0 by using Eq. (10-53), and we find the electric field components E_r^0 and E_ϕ^0 by applying Eq. (10-55)—similar to Eq. (10-219).



— Electric field lines
- - - Magnetic field lines

FIGURE 10-20
Field lines for TM_{01} mode in a transverse plane of circular waveguide.

We have for TE modes, in addition to H_z^0 in Eq. (10-229),

$$H_r^0 = -\frac{j\beta}{h} C'_n J'_n(hr) \cos n\phi, \quad (10-232)$$

$$H_\phi^0 = \frac{j\beta n}{h^2 r} C'_n J_n(hr) \sin n\phi, \quad (10-233)$$

$$E_r^0 = \frac{j\omega\mu n}{h^2 r} C'_n J_n(hr) \sin n\phi, \quad (10-234)$$

$$E_\phi^0 = \frac{j\omega\mu}{h} C'_n J'_n(hr) \cos n\phi, \quad (10-235)$$

$$E_z^0 = 0. \quad (10-236)$$

The required boundary condition for TE waves is that the normal derivative of H_z^0 must vanish at $r = a$; that is,

$$J'_n(ha) = 0. \quad (\text{TE modes}) \quad (10-237)$$

The first several zeros of $J'_n(x)$ are listed in Table 10-3, from which we see that the smallest x'_{np} is $x'_{11} = 1.841$. This corresponds to the *smallest eigenvalue*

$$(h)_{\text{TE}_{11}} = \frac{1.841}{a}, \quad (10-238)$$

and the *lowest cutoff frequency*

$$(f_c)_{\text{TE}_{11}} = \frac{h_{\text{TE}_{11}}}{2\pi\sqrt{\mu\epsilon}} = \frac{0.293}{a\sqrt{\mu\epsilon}} \quad (\text{Hz}), \quad (10-239)$$

which is lower than $(f_c)_{\text{TM}_0}$, given in Eq. (10-228). Hence ***the TE₁₁ mode is the dominant mode in a circular waveguide.*** In an air-filled circular waveguide of radius a , the cutoff wavelength for the dominant mode is

$$(\lambda_c)_{\text{TE}_{11}} = \frac{a}{0.293} = 3.41a \quad (\text{m}). \quad (10-240)$$

It is interesting to compare Eq. (10-240) with Eq. (10-164) for a rectangular waveguide. A sketch of the electric and magnetic field lines for the TE₁₁ mode in a typical transverse plane is shown in Fig. 10-21.

The attenuation constant due to losses in the imperfectly conducting wall of a circular waveguide can be calculated by following the same procedure used in Sub-section 10-4.3 for a rectangular waveguide. However, integrals of Bessel's functions would be involved, and we shall not pursue this aspect further in this book. Suffice

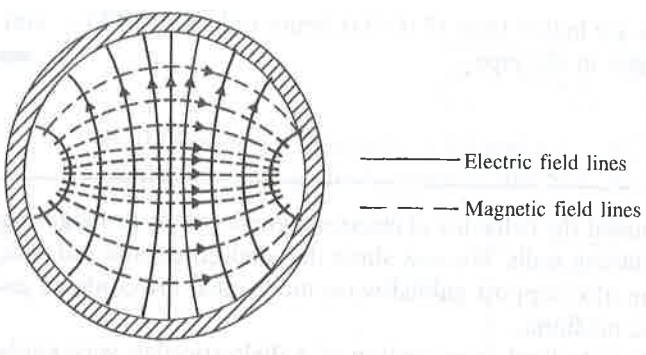


FIGURE 10-21
Field lines for TE_{11} mode in a transverse plane of a circular waveguide.

it to say that the attenuation constants of the dominant-mode propagating waves in circular and rectangular waveguides having comparable dimensions are of the same order of magnitude. A point of special interest for circular waveguides is that the attenuation constant of TE_{0p} waves decreases monotonically with frequency—the absence of a minimum point in $\alpha_c \sim f$ curves. No other waves in circular or rectangular waveguides have this property.

EXAMPLE 10-12 (a) A 10 (GHz) signal is to be transmitted inside a hollow circular conducting pipe. Determine the inside diameter of the pipe such that its lowest cutoff frequency is 20% below this signal frequency. (b) If the pipe is to operate at 15 (GHz), what waveguide modes can propagate in the pipe?

Solution

a) The cutoff frequency of the dominant mode in a circular waveguide of radius a is, from Eq. (10-239),

$$(f_c)_{\text{TE}_{11}} = \frac{0.293c}{a} = \frac{0.879}{a} \times 10^8 \text{ (Hz)}$$

$$= \frac{0.0879}{a} \text{ (GHz).}$$

This is to be equated to $0.80 \times 10 = 8$ (GHz). Hence the required inside diameter of the pipe is $2a = 2 \times (0.0879/8) = 0.022$ (m), or 2.2 (cm).

b) Cutoff frequencies for waveguide modes in a hollow circular pipe of inner radius $a = 0.011$ (m) that are lower than 15 (GHz) are, from Tables 10-1 and 10-2,

$$(f_c)_{\text{TE}_{11}} = 8 \text{ (GHz)},$$

$$(f_c)_{\text{TM}_{01}} = 8 \times \left(\frac{x_{01}}{x'_{11}} \right) = 8 \times \left(\frac{2.405}{1.841} \right) = 10.45 \text{ (GHz)},$$

$$(f_c)_{\text{TE}_{21}} = 8 \times \left(\frac{x'_{21}}{x'_{11}} \right) = 8 \times \left(\frac{3.054}{1.841} \right) = 13.27 \text{ (GHz)}.$$

The f_c of all other modes are higher than 15 (GHz); hence only TE₁₁, TM₀₁, and TE₂₁ modes can propagate in the pipe.

10-6 Dielectric Waveguides

In previous sections we discussed the behavior of electromagnetic waves propagating along waveguides with conducting walls. We now show that dielectric slabs and rods without conducting walls can also support guided-wave modes that are confined essentially within the dielectric medium.

Figure 10-22 shows a longitudinal cross section of a dielectric-slab waveguide of thickness d . For simplicity we consider this a problem with no dependence on the x -coordinate. Let ϵ_d and μ_d be the permittivity and permeability, respectively, of the dielectric slab, which is situated in free space (ϵ_0, μ_0). We assume that the dielectric is lossless and that waves propagate in the $+z$ -direction. The behavior of TM and TE modes will now be analyzed separately.

10-6.1 TM WAVES ALONG A DIELECTRIC SLAB

For transverse magnetic waves, $H_z = 0$. Since there is no x -dependence, Eq. (10-62) applies. We have

$$\frac{d^2 E_z^0(y)}{dy^2} + h^2 E_z^0(y) = 0, \quad (10-241)$$

where

$$h^2 = \gamma^2 + \omega^2 \mu \epsilon. \quad (10-242)$$

Solutions of Eq. (10-241) must be considered in both the slab and the free-space regions, and they must be matched at the boundaries.

In the slab region we assume that the waves propagate in the $+z$ -direction without attenuation (lossless dielectric); that is, we assume

$$\gamma = j\beta. \quad (10-243)$$

The solution of Eq. (10-241) in the dielectric slab may contain both a sine term and a cosine term, which are an odd and an even function, respectively, of y :

$$E_z^0(y) = E_o \sin k_y y + E_e \cos k_y y, \quad |y| \leq \frac{d}{2}, \quad (10-244)$$

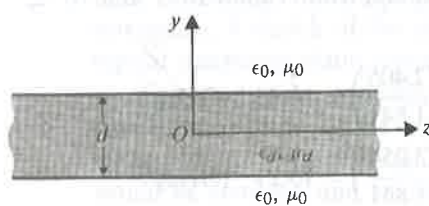


FIGURE 10-22
A longitudinal cross-section of a dielectric-slab waveguide.

/ TE₁₁, TM₀₁, and

waves propagating
electric slabs and rods
at are confined es-

tric-slab waveguide
dependence on the
respectively, of the
that the dielectric
havior of TM and

dence, Eq. (10-62)

(10-241)

(10-242)

and the free-space

+z-direction with-

(10-243)

oth a sine term and
ly, of y:

(10-244)

lectric-slab waveguide.

where

$$k_y^2 = \omega^2 \mu_d \epsilon_d - \beta^2 = h_d^2. \quad (10-245)$$

In the free-space regions ($y > d/2$ and $y < -d/2$) the waves must decay exponentially so that they are guided along the slab and do not radiate away from it. We have

$$E_z^0(y) = \begin{cases} C_u e^{-\alpha(y-d/2)}, & y \geq \frac{d}{2}, \\ C_l e^{\alpha(y+d/2)}, & y \leq -\frac{d}{2}, \end{cases} \quad (10-246a)$$

where

$$\alpha^2 = \beta^2 - \omega^2 \mu_0 \epsilon_0 = -h_0^2. \quad (10-247)$$

Equations (10-245) and (10-247) are called *dispersion relations* because they show the nonlinear dependence of the phase constant β on ω .

At this stage we have not yet determined the values of k_y and α ; nor have we found the relationships among the amplitudes E_o , E_e , C_u , and C_l . In the following, we will consider the odd and even TM modes separately.

a) *Odd TM modes.* For odd TM modes, $E_z^0(y)$ is described by a sine function that is antisymmetric with respect to the $y = 0$ plane. The only other field components, $E_y^0(y)$ and $H_x^0(y)$, are obtained from Eqs. (10-28) and (10-25), respectively.

i) In the dielectric region, $|y| \leq d/2$:

$$E_z^0(y) = E_o \sin k_y y, \quad (10-248)$$

$$E_y^0(y) = -\frac{j\beta}{k_y} E_o \cos k_y y, \quad (10-249)$$

$$H_x^0(y) = \frac{j\omega \epsilon_d}{k_y} E_o \cos k_y y. \quad (10-250)$$

ii) In the upper free-space region, $y \geq d/2$:

$$E_z^0(y) = \left(E_o \sin \frac{k_y d}{2} \right) e^{-\alpha(y-d/2)}, \quad (10-251)$$

$$E_y^0(y) = -\frac{j\beta}{\alpha} \left(E_o \sin \frac{k_y d}{2} \right) e^{-\alpha(y-d/2)}, \quad (10-252)$$

$$H_x^0(y) = \frac{j\omega \epsilon_0}{\alpha} \left(E_o \sin \frac{k_y d}{2} \right) e^{-\alpha(y-d/2)}, \quad (10-253)$$

where C_u in Eq. (10-246a) has been set to equal $E_o \sin(k_y d/2)$, which is the value of $E_z^0(y)$ in Eq. (10-248) at the upper interface, $y = d/2$.

iii) In the lower free-space region, $y \leq -d/2$:

$$E_z^0(y) = -\left(E_o \sin \frac{k_y d}{2} \right) e^{\alpha(y+d/2)}, \quad (10-254)$$

$$E_y^0(y) = -\frac{j\beta}{\alpha} \left(E_o \sin \frac{k_y d}{2} \right) e^{\alpha(y+d/2)}, \quad (10-255)$$

$$H_x^0(y) = \frac{j\omega\epsilon_0}{\alpha} \left(E_o \sin \frac{k_y d}{2} \right) e^{\alpha(y+d/2)}, \quad (10-256)$$

where C_l in Eq. (10-246b) has been set to equal $-E_o \sin(k_y d/2)$, which is the value of $E_z^0(y)$ in Eq. (10-248) at the lower interface $y = -d/2$.

Now we must determine k_y and α for a given angular frequency of excitation ω . The continuity of H_x at the dielectric surface requires that $H_x^0(d/2)$ computed from Eqs. (10-250) and (10-253) be the same. We have

$$\frac{\alpha}{k_y} = \frac{\epsilon_0}{\epsilon_d} \tan \frac{k_y d}{2} \quad (\text{Odd TM modes}). \quad (10-257)$$

By adding dispersion relations Eqs. (10-245) and (10-247) we find

$$\alpha^2 + k_y^2 = \omega^2(\mu_d \epsilon_d - \mu_0 \epsilon_0) \quad (10-258)$$

or

$$\alpha = [\omega^2(\mu_d \epsilon_d - \mu_0 \epsilon_0) - k_y^2]^{1/2}. \quad (10-259)$$

Equations (10-257) and (10-259) can be combined to give an expression in which k_y is the only unknown:

$$[\omega^2(\mu_d \epsilon_d - \mu_0 \epsilon_0) - k_y^2]^{1/2} = \frac{\epsilon_0}{\epsilon_d} k_y \tan \frac{k_y d}{2}. \quad (10-260)$$

Unfortunately, the transcendental equation, Eq. (10-260), cannot be solved analytically. But for a given ω and given values of ϵ_d , μ_d , and d of the dielectric slab, both the left and the right sides of Eq. (10-260) can be plotted versus k_y . The intersections of the two curves give the values of k_y for odd TM modes, of which there are only a finite number, indicating that there are only a finite number of possible modes. This is in contrast with the infinite number of modes possible in waveguides with conducting walls.

We note from Eq. (10-248) that $E_z^0 = 0$ for $y = 0$. Hence a perfectly conducting plane may be introduced to coincide with the $y = 0$ plane without affecting the existing fields. It follows that the characteristics of odd TM waves propagating along a dielectric-slab waveguide of thickness d are the same as those of the corresponding TM modes supported by a dielectric slab of a thickness $d/2$ that is backed by a perfectly conducting plane.

The *surface impedance* looking down from above on the surface of dielectric slab is

$$Z_s = -\frac{E_z^0}{H_x^0} = j \frac{\alpha}{\omega \epsilon_0} \quad (\text{TM modes}), \quad (10-261)$$

which is an inductive reactance. Thus a TM surface wave can be supported by an inductive surface.

(10-255)

(10-256)

$(k_y d/2)$, which is
 $= -d/2$.
 Frequency of excitation
 $H_x^0(d/2)$ computed

(10-257)

find

(10-258)

(10-259)

pression in which

(10-260)

cannot be solved
 d of the dielectric
 plotted versus k_y .
 odd TM modes, of
 only a finite num-
 ber of modes pos-

perfectly conduct-
 without affecting
 waves propagating
 those of the cor-
 cekness $d/2$ that is

surface of dielectric

(10-261)

e supported by an

b) *Even TM modes.* For even TM modes, $E_z^0(y)$ is described by a cosine function that is symmetric with respect to the $y = 0$ plane:

$$E_z^0(y) = E_e \cos k_y y, \quad |y| \leq \frac{d}{2}. \quad (10-262)$$

The other nonzero field components, E_y^0 and H_x^0 , both inside and outside the dielectric slab can be obtained in exactly the same manner as in the case of odd TM modes (see Problem P.10-33). Instead of Eq. (10-257), the characteristic relation between k_y and α now becomes

$$\frac{\alpha}{k_y} = -\frac{\epsilon_0}{\epsilon_d} \cot \frac{k_y d}{2} \quad (\text{Even TM modes}), \quad (10-263)$$

which can be used in conjunction with Eq. (10-259) to determine the transverse wavenumber k_y and the transverse attenuation constant α . The several solutions correspond to the several even TM modes that can exist in the dielectric slab waveguide of thickness d . Of course, in this case a conducting plane *cannot* be placed at $y = 0$ without disturbing the whole field structure.

From Eqs. (10-245) and (10-247) it is easy to see that the phase constant, β , of propagating TM waves lies between the intrinsic phase constant of the free space, $k_0 = \omega \sqrt{\mu_0 \epsilon_0}$, and that of the dielectric, $k_d = \omega \sqrt{\mu_d \epsilon_d}$; that is,

$$\omega \sqrt{\mu_0 \epsilon_0} < \beta < \omega \sqrt{\mu_d \epsilon_d}.$$

As β approaches the value of $\omega \sqrt{\mu_0 \epsilon_0}$, Eq. (10-247) indicates that α approaches zero. An absence of attenuation means that the waves are no longer bound to the slab. The limiting frequencies under this condition are called the *cutoff frequencies* of the dielectric waveguide. From Eq. (10-245) we have $k_y = \omega_c \sqrt{\mu_d \epsilon_d - \mu_0 \epsilon_0}$ at cutoff. Substitution into Eqs. (10-257) and (10-263) with α set to zero yields the following relations for TM modes. At cutoff:

Odd TM Modes	Even TM Modes
$\tan \left(\frac{\omega_{co} d}{2} \sqrt{\mu_d \epsilon_d - \mu_0 \epsilon_0} \right) = 0$ $\pi f_{co} d \sqrt{\mu_d \epsilon_d - \mu_0 \epsilon_0} = (n - 1)\pi, \quad n = 1, 2, 3, \dots$	$\cot \left(\frac{\omega_{ce} d}{2} \sqrt{\mu_d \epsilon_d - \mu_0 \epsilon_0} \right) = 0$ $\pi f_{ce} d \sqrt{\mu_d \epsilon_d - \mu_0 \epsilon_0} = (n - \frac{1}{2})\pi, \quad n = 1, 2, 3, \dots$
$f_{co} = \frac{(n - 1)}{d \sqrt{\mu_d \epsilon_d - \mu_0 \epsilon_0}} \quad (10-264)$	$f_{ce} = \frac{(n - \frac{1}{2})}{d \sqrt{\mu_d \epsilon_d - \mu_0 \epsilon_0}} \quad (10-265)$

It is seen that $f_{co} = 0$ for $n = 1$. This means that the lowest-order odd TM mode can propagate along a dielectric-slab waveguide regardless of the thickness of the slab.

As the frequency of a given TM wave increases beyond the corresponding cutoff frequency, α increases and the wave clings more tightly to the slab.

10-6.2 TE WAVES ALONG A DIELECTRIC SLAB

For transverse electric waves, $E_z = 0$, and Eq. (10-82) applies

$$\frac{d^2 H_z^0(y)}{dy^2} + h^2 H_z^0(y) = 0, \quad (10-266)$$

where h^2 is the same as that given in Eq. (10-242). The solution for $H_z^0(y)$ may also contain both a sine term and a cosine term:

$$H_y^0(y) = H_o \sin k_y y + H_e \cos k_y y, \quad |y| \leq \frac{d}{2}, \quad (10-267)$$

where k_y has been defined in Eq. (10-245). In the free-space regions ($y > d/2$ and $y < -d/2$) the waves must decay exponentially. We write

$$H_z^0(y) = \begin{cases} C'_u e^{-\alpha(y-d/2)}, & y \geq \frac{d}{2}, \\ C'_l e^{\alpha(y+d/2)}, & y \leq -\frac{d}{2}, \end{cases} \quad (10-268a)$$

$$H_z^0(y) = \begin{cases} C'_u e^{-\alpha(y-d/2)}, & y \geq \frac{d}{2}, \\ C'_l e^{\alpha(y+d/2)}, & y \leq -\frac{d}{2}, \end{cases} \quad (10-268b)$$

where α is defined in Eq. (10-247). Following the same procedure as used for TM waves, we consider the odd and even TE modes separately. Besides $H_z^0(y)$, the only other field components are $H_y^0(y)$ and $E_x^0(y)$, which can be obtained from Eqs. (10-50) and (10-51).

a) Odd TE modes.

i) In the dielectric region, $|y| \leq d/2$:

$$H_z^0(y) = H_o \sin k_y y, \quad (10-269)$$

$$H_y^0(y) = -\frac{j\beta}{k_y} H_o \cos k_y y, \quad (10-270)$$

$$E_x^0(y) = -\frac{j\omega\mu_d}{k_y} H_o \cos k_y y. \quad (10-271)$$

ii) In the upper free-space region, $y \geq d/2$:

$$H_z^0(y) = \left(H_o \sin \frac{k_y d}{2} \right) e^{-\alpha(y-d/2)}, \quad (10-272)$$

$$H_y^0(y) = -\frac{j\beta}{\alpha} \left(H_o \sin \frac{k_y d}{2} \right) e^{-\alpha(y-d/2)}, \quad (10-273)$$

$$E_x^0(y) = -\frac{j\omega\mu_0}{\alpha} \left(H_o \sin \frac{k_y d}{2} \right) e^{-\alpha(y-d/2)}. \quad (10-274)$$

nding cutoff fre-

(10-266)

 $H_z^0(y)$ may also

(10-267)

ns ($y > d/2$ and

(10-268a)

(10-268b)

e as used for TM
es $H_z^0(y)$, the only
from Eqs. (10-50)

(10-269)

(10-270)

(10-271)

(10-272)

(10-273)

(10-274)

iii) In the lower free-space region, $y \leq -d/2$:

$$H_z^0(y) = -\left(H_o \sin \frac{k_y d}{2}\right) e^{\alpha(y+d/2)}, \quad (10-275)$$

$$H_y^0(y) = -\frac{j\beta}{\alpha} \left(H_o \sin \frac{k_y d}{2}\right) e^{\alpha(y+d/2)}, \quad (10-276)$$

$$E_x^0(y) = -\frac{j\omega\mu_0}{\alpha} \left(H_o \sin \frac{k_y d}{2}\right) e^{\alpha(y+d/2)}. \quad (10-277)$$

A relation between k_y and α can be obtained by equating $E_x^0(y)$, given in Eqs. (10-271) and (10-274), at $y = d/2$. Thus,

$$\frac{\alpha}{k_y} = \frac{\mu_0}{\mu_d} \tan \frac{k_y d}{2} \quad (\text{Odd TE modes}), \quad (10-278)$$

which is seen to be closely analogous to the characteristic equation, Eq. (10-257), for odd TM modes. Equations (10-259) and (10-278) can be combined in the manner of Eq. (10-260) to find k_y graphically. From k_y , α can be found from Eq. (10-259).

From a position of looking down from above, the surface impedance of the dielectric slab is

$$Z_s = \frac{E_x^0}{H_z^0} = -j \frac{\omega\mu_0}{\alpha} \quad (\text{TE modes}), \quad (10-279)$$

which is a capacitive reactance. Hence a TE surface wave can be supported by a capacitive surface.

b) Even TE modes. For even TE modes, $H_z^0(y)$ is described by a cosine function that is symmetric with respect to the $y = 0$ plane.

$$H_z^0(y) = H_e \cos k_y y, \quad |y| \leq d/2. \quad (10-280)$$

The other nonzero field components, H_y^0 and E_x^0 , both inside and outside the dielectric slab can be obtained in the same manner as for odd TE modes (see Problem P.10-35). The characteristic relation between k_y and α is closely analogous to that for even TM modes as given in Eq. (10-263):

$$\frac{\alpha}{k_y} = -\frac{\mu_0}{\mu_d} \cot \frac{k_y d}{2} \quad (\text{Even TE modes}). \quad (10-281)$$

It is easy to see that the expressions for the cutoff frequencies given in Eqs. (10-264) and (10-265) apply also to TE modes. Like the lowest-order ($n = 1$) TM mode, the lowest-order odd TE mode has no cutoff frequency. The characteristic relations for all the propagating modes along a dielectric-slab waveguide of a thickness d are listed in Table 10-4.

TABLE 10-4
Characteristic Relations for Dielectric-Slab Waveguide[†]

Mode		Characteristic Relation	Cutoff Frequency
TM	Odd	$(\alpha/k_y) = (\epsilon_0/\epsilon_d) \tan(k_y d/2)$	$f_{co} = (n - 1)/d \sqrt{\mu_d \epsilon_d - \mu_0 \epsilon_0}$
	Even	$(\alpha/k_y) = -(\epsilon_0/\epsilon_d) \cot(k_y d/2)$	$f_{ce} = (n - \frac{1}{2})/d \sqrt{\mu_d \epsilon_d - \mu_0 \epsilon_0}$
TE	Odd	$(\alpha/k_y) = (\mu_0/\mu_d) \tan(k_y d/2)$	$f_{co} = (n - 1)/d \sqrt{\mu_d \epsilon_d - \mu_0 \epsilon_0}$
	Even	$(\alpha/k_y) = -(\mu_0/\mu_d) \cot(k_y d/2)$	$f_{ce} = (n - \frac{1}{2})/d \sqrt{\mu_d \epsilon_d - \mu_0 \epsilon_0}$

[†] $\alpha = [\omega^2(\mu_d \epsilon_d - \mu_0 \epsilon_0) - k_y^2]^{1/2}$.

EXAMPLE 10-13 A dielectric-slab waveguide with constitutive parameters $\mu_d = \mu_0$ and $\epsilon_d = 2.50\epsilon_0$ is situated in free space. Determine the minimum thickness of the slab so that a TM or TE wave of the even type at a frequency 20 GHz may propagate along the guide.

Solution The lowest TM and TE waves of the even type have the same cutoff frequency along a dielectric-slab waveguide:

$$f_c = \frac{n - \frac{1}{2}}{d \sqrt{\mu_d \epsilon_d - \mu_0 \epsilon_0}}.$$

Letting $n = 1$, we have

$$f_c = \frac{c}{2d \sqrt{\frac{\mu_d \epsilon_d}{\mu_0 \epsilon_0} - 1}}.$$

Therefore,

$$\begin{aligned} d_{\min} &= \frac{c}{2f_c \sqrt{\frac{\mu_d \epsilon_d}{\mu_0 \epsilon_0} - 1}} \\ &= \frac{3 \times 10^8}{2 \times 20 \times 10^9 \sqrt{2.5 - 1}} = 6.12 \times 10^{-3} \text{ (m)} \text{ or } 6.12 \text{ (mm)}. \end{aligned}$$

EXAMPLE 10-14 (a) Obtain an approximate expression for the decaying rate of the dominant TM surface wave outside of a very thin dielectric-slab waveguide. (b) Find the time-average power per unit slab width transmitted along the guide. (c) What is the time-average power transmitted in the transverse direction?

Solution

- a) The dominant TM wave is the odd mode having a zero cutoff frequency— $f_{co} = 0$ for $n = 1$, independent of the slab thickness (see Table 10-4). With a slab that

is very thin in comparison to the operating wavelength, $k_y d/2 \ll 1$, $\tan(k_y d/2) \cong k_y d/2$, and Eq. (10-257) becomes

$$\alpha \cong \frac{\epsilon_0}{2\epsilon_d} k_y^2 d. \quad (10-282)$$

Using Eq. (10-258), Eq. (10-282) can be written approximately as

$$\alpha \cong \frac{\epsilon_0}{2\epsilon_d} \omega^2 (\mu_d \epsilon_d - \mu_0 \epsilon_0) d \quad (\text{Np/m}). \quad (10-283)$$

In Eq. (10-283) it has been assumed that $\alpha d/2 \ll \epsilon_d/\epsilon_0$.

b) The time-average Poynting vector in the $+z$ -direction in the dielectric slab is

$$\mathcal{P}_{av} = \frac{1}{2} \Re e(-\mathbf{a}_y E_y \times \mathbf{a}_x H_x).$$

Using Eqs. (10-249) and (10-250), we have $\mathbf{P}_{av} = \mathbf{a}_z P_{av}$ and

$$\begin{aligned} P_{av} &= 2 \int_0^{d/2} \mathcal{P}_{av} dy = \frac{\omega \epsilon_d \beta}{k_y^2} E_o^2 \int_0^{d/2} \cos^2(k_y y) dy \\ &= \frac{\omega \epsilon_d \beta}{4k_y^2} E_o^2 \left[d + \frac{1}{k_y} \sin(k_y d) \right] \quad (\text{W/m}), \end{aligned} \quad (10-284)$$

where

$$k_y \cong \omega \sqrt{\mu_d \epsilon_d - \mu_0 \epsilon_0} \quad (10-284a)$$

and

$$\beta \cong \omega \sqrt{\mu_0 \epsilon_0}. \quad (10-284b)$$

c) The time-average Poynting vector in the transverse direction is calculated from

$$\mathcal{P}_{av} = \frac{1}{2} \Re e(\mathbf{a}_z E_z \times \mathbf{a}_x H_x).$$

From Subsection 10-6.1 we see that the expressions of E_z^0 and H_x^0 are 90° out of time phase. Their product has no real part, yielding a zero \mathcal{P}_{av} . Hence no average power is transmitted in the transverse direction normal to the reactive surface.

10-6.3 ADDITIONAL COMMENTS ON DIELECTRIC WAVEGUIDES

In the preceding subsection we studied the characteristics of electromagnetic waves guided by dielectric slabs with an analysis based on Maxwell's equations and the associated boundary conditions. We can gain some physical insight from the concept of total reflection in plane-wave theory that we discussed in Section 8-10.

Consider the dielectric slab in Fig. 10-23. From Section 8-10 we know that if a plane wave in the slab with a permittivity $\epsilon_d > \epsilon_0$ is incident obliquely on the lower

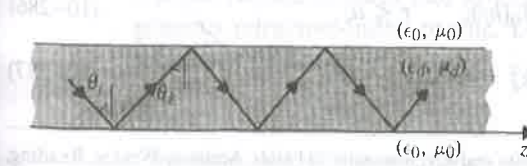


FIGURE 10-23
Bouncing-wave interpretation of propagating waves along a dielectric waveguide.

boundary at an angle of incidence θ_i greater than the critical angle (see Eq. 8-188)

$$\theta_c = \sin^{-1} \sqrt{\frac{\epsilon_0}{\epsilon_d}}, \quad (10-285)$$

it will be totally reflected toward the upper boundary. Moreover, an evanescent wave exists along the interface (in z -direction) that is attenuated exponentially in the transverse direction outside of the boundary. The reflected wave from the lower boundary will be incident on the upper boundary at the same angle of incidence $\theta_i > \theta_c$ and will be similarly totally reflected. This process will continue so that there will be two sets of multiply reflected waves: one set going from the upper boundary toward the lower boundary, and the other set from the lower boundary toward the upper boundary. Under the condition that the points on the same wavefront have the same phase, each set of reflected waves forms a single uniform plane wave. We then have two interfering uniform plane waves, giving rise to an interference pattern, which is the mode pattern of the propagating wave. It is clear that the phase requirements at both reflecting boundaries depend on the angle of incidence θ_i , since θ_i determines the phase shifts caused by total internal reflections. Analysis shows that the required phase conditions correspond precisely to the dispersion and characteristic relations obtained in the preceding section.[†] Thus the results based on Maxwell's equations and boundary conditions can be interpreted by bouncing waves due to total internal reflections.

So far our attention has been directed toward the wave behavior in dielectric-slab waveguides. Similar analyses apply to round dielectric-rod waveguides. In particular, they can be used to study the transmission of light waves along quartz or glass fibers that form optical waveguides. Optical fiber waveguides are of great importance as transmission media for communication or control systems because of their low-attenuation and large-bandwidth properties. They also are extremely compact and flexible. A study of circular dielectric waveguides necessitates the use of cylindrical coordinates that lead to Bessel's differential equation and Bessel functions. The study is complicated by the fact that pure TM or TE modes are possible only if the fields are circularly symmetrical; that is, if the fields are independent of the angle coordinate ϕ . When the fields are dependent on ϕ , separation into TM and TE modes is no longer possible, and it is necessary to assume the existence of both E_z and H_z components simultaneously and study the so-called **hybrid modes**.

As a simple example, consider the circularly symmetrical TM modes for a round dielectric rod of radius a and permittivity ϵ_d , situated in air. The transverse distribution of the axial component of electric field intensity, E_z^0 , in the dielectric rod ($r \leq a$) is, from Eq. (10-218) by setting $n = 0$,

$$E_{zi}^0 = C_0 J_0(hr), \quad r \leq a, \quad (10-286)$$

where

$$h^2 = \gamma^2 + k_d^2 = \omega^2 \mu_0 \epsilon_d - \beta^2. \quad (10-287)$$

[†] S. R. Seshadri, *Fundamentals of Transmission Lines and Electromagnetic Fields*, Addison-Wesley, Reading, Mass., 1971, Chapter 8.

(see Eq. 8-188)

(10-285)

evanescent wave
ally in the trans-
lower boundary
ence $\theta_i > \theta_c$ and
here will be two
ary toward the
e upper bound-
the same phase,
en have two in-
n, which is the
gements at both
determines the
at the required
eristic relations
well's equations
o total internal

or in dielectric-
guides. In par-
long quartz or
re of great im-
ems because of
extremely com-
ates the use of
essel functions.
e possible only
ndependent of the
n into TM and
istence of both
TM modes.

des for a round
verse distribu-
tric rod ($r \leq a$)

(10-286)

(10-287)

Wesley, Reading,

The corresponding $H_{\phi i}^0$ is, from Eq. (10-224),

$$H_{\phi i}^0 = -\frac{j\omega\epsilon_d}{h} C_0 J'_0(hr), \quad r \leq a. \quad (10-288)$$

Outside the dielectric rod, the fields are required to be evanescent and must decrease exponentially with distance. An appropriate choice for E_{zo}^0 is $K_0(\zeta r)$, the modified Bessel function of the second kind of order zero, whose asymptotic expansion for large arguments is given in Eq. (10-215). We write

$$E_{zo}^0 = D_0 K_0(\zeta r), \quad r \geq a, \quad (10-289)$$

where

$$\zeta^2 = \beta^2 - k_0^2 = \beta^2 - \omega^2 \mu_0 \epsilon_0, \quad (10-290)$$

and D_0 is a constant. The corresponding $H_{\phi o}^0$ is

$$H_{\phi o}^0 = \frac{j\omega\epsilon_0}{\zeta} D_0 K'_0(\zeta r), \quad r \geq a. \quad (10-291)$$

The field components E_z^0 and H_ϕ^0 must be continuous at $r = a$, which requires

$$C_0 J_0(ha) = D_0 K_0(\zeta a) \quad (10-291)$$

and

$$\frac{\epsilon_d}{h} C_0 J'_0(ha) = -\frac{\epsilon_0}{\zeta} D_0 K'_0(\zeta a). \quad (10-292)$$

Combination of Eqs. (10-291) and (10-292) gives the following characteristic equation for circularly symmetrical TM modes:

$$\frac{J_0(ha)}{J'_0(ha)} = -\frac{\epsilon_d \zeta}{\epsilon_0 h} \frac{K_0(\zeta a)}{K'_0(\zeta a)}, \quad (10-293)$$

where ζ and h are related through Eqs. (10-287) and (10-290):

$$h^2 + \zeta^2 = \omega^2 \mu_0 (\epsilon_d - \epsilon_0). \quad (10-294)$$

Equations (10-293) and (10-294) can be solved for h and ζ either graphically or on a computer. Once the eigenvalues have been found, the cutoff frequencies and other properties of the corresponding circularly symmetrical TM modes can be determined.

In the above example we discussed only the analysis procedure for circularly symmetrical TM modes in an unclad homogeneous optical fiber. In practice, commercially available optical fibers are mainly of two types: step-index fibers that consist of a central homogeneous dielectric core and an outer sheath of a material having a lower refractive index and graded-index fibers whose center core has a nonhomogeneous refractive-index profile. Detailed studies of these types do not fall into the scope of this book.[†]

[†] See, for instance, D. Marcuse, *Theory of Dielectric Waveguides*, Academic Press, New York, 1974; A. W. Snyder and J. D. Love, *Optical Waveguide Theory*, Methuen Inc., New York, 1984.

10-7 Cavity Resonators

We have previously pointed out that at UHF (300 MHz to 3 GHz) and higher frequencies, ordinary lumped-circuit elements such as R , L , and C are difficult to make, and stray fields become important. Circuits with dimensions comparable to the operating wavelength become efficient radiators and will interfere with other circuits and systems. Furthermore, conventional wire circuits tend to have a high effective resistance both because of energy loss through radiation and as a result of skin effect. To provide a resonant circuit at UHF and higher frequencies, we look to an enclosure (a cavity) completely surrounded by conducting walls. Such a shielded enclosure confines electromagnetic fields inside and furnishes large areas for current flow, thus eliminating radiation and high-resistance effects. These enclosures have natural resonant frequencies and a very high Q (quality factor), and are called *cavity resonators*. In this section we will study the properties of rectangular and circular cylindrical cavity resonators.

10-7.1 RECTANGULAR CAVITY RESONATORS

Consider a rectangular waveguide with both ends closed by a conducting wall. The interior dimensions of the cavity are a , b , and d , as shown in Fig. 10-24. Let us disregard for the moment the probe-excitation part of the figure. Since both TM and TE modes can exist in a rectangular guide, we expect TM and TE modes in a rectangular resonator too. However, the designation of TM and TE modes in a resonator is *not unique* because we are free to choose x or y or z as the "direction of propagation"; that is, there is no unique "longitudinal direction." For example, a TE mode with respect to the z -axis could be a TM mode with respect to the y -axis.

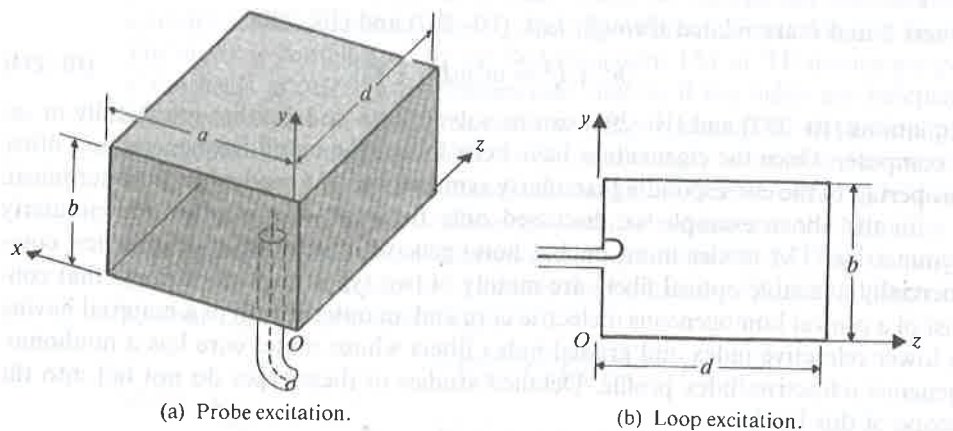


FIGURE 10-24
Excitation of cavity modes by a coaxial line.

and higher frequencies difficult to make, due to the opposite circuits high effective skin effect. Due to an enclosed enclosure current flow, thus the natural **cavity resonators**. For cylindrical

wall. The 0-24. Let us both TM and modes in a rectangular resonator of propagation, a TE mode axis.

For our purposes we choose the z-axis as the reference "direction of propagation." In actuality the existence of conducting end walls at $z = 0$ and $z = d$ gives rise to multiple reflections and sets up standing waves; no wave propagates in an enclosed cavity. A three-symbol (mnp) subscript is needed to designate a TM or TE standing wave pattern in a cavity resonator.

TM_{mnp} Modes The expressions for the transverse variations of the field components for TM_{mn} modes in a waveguide have been given in Eqs. (10-132) and (10-134) through (10-137). Note that the longitudinal variation for a wave traveling in the +z-direction is described by the factor $e^{-\gamma z}$ or $e^{-j\beta z}$, as indicated in Eq. (10-121). This wave will be reflected by the end wall at $z = d$; and the reflected wave, going in the -z-direction, is described by a factor $e^{j\beta z}$. The superposition of a term with $e^{-j\beta z}$ and another of the same amplitude[†] with $e^{j\beta z}$ results in a standing wave of the $\sin \beta z$ or $\cos \beta z$ type. Which should it be? The answer to this question depends on the particular field component.

Consider the transverse component $E_y(x, y, z)$. Boundary conditions at the conducting surfaces require that it be zero at $z = 0$ and $z = d$. This means that (1) its z-dependence must be of the $\sin \beta z$ type, and that (2) $\beta = p\pi/d$. The same argument applies to the other transverse electric field component $E_x(x, y, z)$.

Recalling that the appearance of the factor $(-\gamma)$ in Eqs. (10-134) and (10-135) is the result of a differentiation with respect to z , we conclude that the other components $E_z(x, y, z)$, $H_x(x, y, z)$, and $H_y(x, y, z)$, which do not contain the factor $(-\gamma)$, must vary according to $\cos \beta z$. We have then, from Eqs. (10-132) and (10-134) through (10-137), the following *phasors* of the field components for TM_{mnp} modes in a rectangular cavity resonator:

$$E_z(x, y, z) = E_0 \sin\left(\frac{m\pi}{a}x\right) \sin\left(\frac{n\pi}{b}y\right) \cos\left(\frac{p\pi}{d}z\right), \quad (10-295)$$

$$E_x(x, y, z) = -\frac{1}{h^2} \left(\frac{m\pi}{a}\right) \left(\frac{p\pi}{d}\right) E_0 \cos\left(\frac{m\pi}{a}x\right) \sin\left(\frac{n\pi}{b}y\right) \sin\left(\frac{p\pi}{d}z\right), \quad (10-296)$$

$$E_y(x, y, z) = -\frac{1}{h^2} \left(\frac{n\pi}{b}\right) \left(\frac{p\pi}{d}\right) E_0 \sin\left(\frac{m\pi}{a}x\right) \cos\left(\frac{n\pi}{b}y\right) \sin\left(\frac{p\pi}{d}z\right), \quad (10-297)$$

$$H_x(x, y, z) = \frac{j\omega\epsilon}{h^2} \left(\frac{n\pi}{b}\right) E_0 \sin\left(\frac{m\pi}{a}x\right) \cos\left(\frac{n\pi}{b}y\right) \cos\left(\frac{p\pi}{d}z\right), \quad (10-298)$$

$$H_y(x, y, z) = -\frac{j\omega\epsilon}{h^2} \left(\frac{m\pi}{a}\right) E_0 \cos\left(\frac{m\pi}{a}x\right) \sin\left(\frac{n\pi}{b}y\right) \cos\left(\frac{p\pi}{d}z\right), \quad (10-299)$$

where

$$h^2 = \left(\frac{m\pi}{a}\right)^2 + \left(\frac{n\pi}{b}\right)^2. \quad (10-300)$$

[†] The reflection coefficient at a perfect conductor is -1.

It is clear that the integers m , n , and p denote the number of half-wave variations in the x -, y -, and z -direction, respectively.

From Eq. (10-138) we obtain the following expression for the resonant frequency:

$$\omega_{mnp} = \frac{1}{\sqrt{\mu\epsilon}} \sqrt{\left(\frac{m\pi}{a}\right)^2 + \left(\frac{n\pi}{b}\right)^2 + \left(\frac{p\pi}{d}\right)^2}$$

or

$$f_{mnp} = \frac{u}{2} \sqrt{\left(\frac{m}{a}\right)^2 + \left(\frac{n}{b}\right)^2 + \left(\frac{p}{d}\right)^2} \quad (\text{Hz}) \quad (10-301)$$

Equation (10-301) states the obvious fact that the resonant frequency increases as the order of a mode becomes higher.

TE_{mnp} Modes For TE_{mnp} modes ($E_z = 0$) the phasor expressions for the standing-wave field components can be written from Eqs. (10-158) and (10-159) through (10-162). We follow the same rules as those we used for TM_{mnp} modes; namely, (1) the transverse (tangential) electric field components must vanish at $z = 0$ and $z = d$, and (2) the factor γ indicates a negative partial differentiation with respect to z . The first rule requires a $\sin(p\pi z/d)$ factor in $E_x(x, y, z)$ and $E_y(x, y, z)$, as well as in $H_z(x, y, z)$; and the second rule indicates a $\cos(p\pi z/d)$ factor in $H_x(x, y, z)$ and $H_y(x, y, z)$, and the replacement of γ by $-(p\pi/d)$. Thus,

$$H_z(x, y, z) = H_0 \cos\left(\frac{m\pi}{a}x\right) \cos\left(\frac{n\pi}{b}y\right) \sin\left(\frac{p\pi}{d}z\right), \quad (10-302)$$

$$E_x(x, y, z) = \frac{j\omega\mu}{h^2} \left(\frac{n\pi}{b}\right) H_0 \cos\left(\frac{m\pi}{a}x\right) \sin\left(\frac{n\pi}{b}y\right) \sin\left(\frac{p\pi}{d}z\right), \quad (10-303)$$

$$E_y(x, y, z) = -\frac{j\omega\mu}{h^2} \left(\frac{m\pi}{a}\right) H_0 \sin\left(\frac{m\pi}{a}x\right) \cos\left(\frac{n\pi}{b}y\right) \sin\left(\frac{p\pi}{d}z\right), \quad (10-304)$$

$$H_x(x, y, z) = -\frac{1}{h^2} \left(\frac{m\pi}{a}\right) \left(\frac{p\pi}{d}\right) H_0 \sin\left(\frac{m\pi}{a}x\right) \cos\left(\frac{n\pi}{b}y\right) \cos\left(\frac{p\pi}{d}z\right), \quad (10-305)$$

$$H_y(x, y, z) = -\frac{1}{h^2} \left(\frac{n\pi}{b}\right) \left(\frac{p\pi}{d}\right) H_0 \cos\left(\frac{m\pi}{a}x\right) \sin\left(\frac{n\pi}{b}y\right) \cos\left(\frac{p\pi}{d}z\right), \quad (10-306)$$

The value of h^2 has been given in Eq. (10-300). The expression for resonant frequency, f_{mnp} , remains the same as that obtained for TM_{mnp} modes in Eq. (10-301). Different modes having the same resonant frequency are called **degenerate modes**. Thus TM_{mnp} and TE_{mnp} modes are always degenerate if none of the mode indices is zero. The mode with the lowest resonant frequency for a given cavity size is referred to as the **dominant mode** (see Example 10-15).

Examination of the field expressions, Eqs. (10-295) through (10-299), for TM modes in a cavity reveals that the longitudinal and transverse electric field compo-

nents are in time phase with one another and in time quadrature with the magnetic field components. Hence the time-average Poynting vector and time-average power transmitted in any direction are zero, as they should be in a lossless cavity. This is in contrast to the field expressions Eqs. (10-132) and (10-134) through (10-137) for TM modes in a waveguide, where the transverse electric field components are in time phase with the transverse magnetic field components, resulting in a time-average power flow in the direction of wave propagation. The same contrasting phase relationships between electric and magnetic field components for TE modes in a cavity resonator (Eqs. 10-302 through 10-306) and those in a waveguide (Eqs. 10-158 through 10-162) are also in evidence.

A particular mode in a cavity resonator (or a waveguide) may be excited from a coaxial line by means of a small probe or loop antenna. In Fig. 10-24(a) a probe is shown that is the tip of the inner conductor of a coaxial cable and protrudes into a cavity at a location where the electric field is a maximum for the desired mode. The probe is, in fact, an antenna that couples electromagnetic energy into the resonator. Alternatively, a cavity resonator may be excited through the introduction of a small loop at a place where the magnetic flux of the desired mode linking the loop is a maximum. Figure 10-24(b) illustrates such an arrangement. Of course, the source frequency from the coaxial line must be the same as the resonant frequency of the desired mode in the cavity.

As an example, for the TE_{101} mode in an $a \times b \times d$ rectangular cavity, there are only three nonzero field components:

$$(10-302)$$

$$E_y = -\frac{j\omega\mu a}{\pi} H_0 \sin\left(\frac{\pi}{a}x\right) \sin\left(\frac{\pi}{d}z\right), \quad (10-307)$$

$$(10-303)$$

$$H_x = -\frac{a}{d} H_0 \sin\left(\frac{\pi}{a}x\right) \cos\left(\frac{\pi}{d}z\right), \quad (10-308)$$

$$(10-304)$$

$$H_z = H_0 \cos\left(\frac{\pi}{a}x\right) \sin\left(\frac{\pi}{d}z\right). \quad (10-309)$$

$$(10-305)$$

$$(10-306)$$

This mode may be excited by a probe inserted in the center region of the top or bottom face where E_y is maximum, as shown in Fig. 10-24(a), or by a loop to couple a maximum H_x placed inside the front or back face, as shown in Fig. 10-24(b). The best location of a probe or a loop is affected by the impedance-matching requirements of the microwave circuit of which the resonator is a part.

A commonly used method for coupling energy from a waveguide to a cavity resonator is the introduction of a hole or iris at an appropriate location in the cavity wall. The field in the waveguide at the hole must have a component that is favorable in exciting the desired mode in the resonator.

EXAMPLE 10-15 Determine the dominant modes and their frequencies in an air-filled rectangular cavity resonator for (a) $a > b > d$, (b) $a > d > b$, and (c) $a = b = d$, where a , b , and d are the dimensions in the x -, y -, and z -directions, respectively.

Solution With the z -axis chosen as the reference “direction of propagation”: First, for TM_{mnp} modes, Eqs. (10–295) through (10–299) show that neither m nor n can be zero, but that p can be zero; second, for TE_{mnp} modes, Eqs. (10–302) through (10–306) show that either m or n (but not both m and n) can be zero, but that p cannot be zero. Thus the modes of the lowest orders are

$$\text{TM}_{110}, \quad \text{TE}_{011}, \quad \text{and } \text{TE}_{101}.$$

The resonant frequency for both TM and TE modes is given by Eq. (10–301).

- a) For $a > b > d$: The lowest resonant frequency is

$$f_{110} = \frac{c}{2} \sqrt{\frac{1}{a^2} + \frac{1}{b^2}}, \quad (10-310)$$

where c is the velocity of light in free space. Therefore TM_{110} is the dominant mode.

- b) For $a > d > b$: The lowest resonant frequency is

$$f_{101} = \frac{c}{2} \sqrt{\frac{1}{a^2} + \frac{1}{d^2}}, \quad (10-311)$$

and TE_{101} is the dominant mode.

- c) For $a = b = d$, all three of the lowest-order modes (namely, TM_{110} , TE_{011} , and TE_{101}) have the same field patterns. The resonant frequency of these degenerate modes is

$$f_{110} = \frac{c}{\sqrt{2}a}. \quad (10-312)$$

10-7.2 QUALITY FACTOR OF CAVITY RESONATOR

A cavity resonator stores energy in the electric and magnetic fields for any particular mode pattern. In any practical cavity the walls have a finite conductivity; that is, a nonzero surface resistance, and the resulting power loss causes a decay of the stored energy. The **quality factor**, or Q , of a resonator, like that of any resonant circuit, is a measure of the bandwidth of the resonator and is defined as

$$Q = 2\pi \frac{\text{Time-average energy stored at a resonant frequency}}{\text{Energy dissipated in one period of this frequency}}. \quad (10-313)$$

(Dimensionless)

Let W be the total time-average energy in a cavity resonator. We write

$$W = W_e + W_m, \quad (10-314)$$

where W_e and W_m denote the energies stored in the electric and magnetic fields, respectively. If P_L is the time-average power dissipated in the cavity, then the energy

gation": First, n nor n can be through (10-306) p cannot be

Eq. (10-301).

(10-310)

the dominant

(10-311)

TE_{010} , TE_{011} , and these degenerate

(10-312)

any particular cavity; that is, a fraction of the stored energy circuit, is a

(10-313)

(10-314)

magnetic fields, en the energy

dissipated in one period is P_L divided by frequency, and Eq. (10-313) can be written as

$$Q = \frac{\omega W}{P_L} \quad (\text{Dimensionless}). \quad (10-315)$$

In determining the Q of a cavity at a resonant frequency, it is customary to assume that the loss is small enough to allow the use of the field patterns without loss.

We will now find the Q of an $a \times b \times d$ cavity for the TE_{101} mode that has three nonzero field components given in Eqs. (10-307), (10-308), and (10-309). The time-average stored electric energy is

$$\begin{aligned} W_e &= \frac{\epsilon_0}{4} \int |E_y|^2 dv \\ &= \frac{\epsilon_0 \omega^2 \mu_0^2 \pi^2}{4h^4 a^2} H_0^2 \int_0^d \int_0^b \int_0^a \sin^2\left(\frac{\pi}{a}x\right) \sin^2\left(\frac{\pi}{d}z\right) dx dy dz \\ &= \frac{\epsilon_0 \omega_{101}^2 \mu_0^2 a^2}{4\pi^2} H_0^2 \left(\frac{a}{2}\right) b \left(\frac{d}{2}\right) = \frac{1}{4} \epsilon_0 \mu_0^2 a^3 b d f_{101}^2 H_0^2, \end{aligned} \quad (10-316)$$

where we have used $h^2 = (\pi/a)^2$ from Eq. (10-300). The total time-average stored magnetic energy is

$$\begin{aligned} W_m &= \frac{\mu_0}{4} \int \{|H_x|^2 + |H_z|^2\} dv \\ &= \frac{\mu_0}{4} H_0^2 \int_0^d \int_0^b \int_0^a \left\{ \frac{\pi^4}{h^4 a^2 d^2} \sin^2\left(\frac{\pi}{a}x\right) \cos^2\left(\frac{\pi}{d}z\right) \right. \\ &\quad \left. + \cos^2\left(\frac{\pi}{a}x\right) \sin^2\left(\frac{\pi}{d}z\right) \right\} dx dy dz \\ &= \frac{\mu_0}{4} H_0^2 \left\{ \frac{a^2}{d^2} \left(\frac{a}{2}\right) b \left(\frac{d}{2}\right) + \left(\frac{a}{2}\right) b \left(\frac{d}{2}\right) \right\} = \frac{\mu_0}{16} abd \left(\frac{a^2}{d^2} + 1\right) H_0^2. \end{aligned} \quad (10-317)$$

From Eq. (10-311) the resonant frequency for the TE_{101} mode is

$$f_{101} = \frac{1}{2\sqrt{\mu_0 \epsilon_0}} \sqrt{\frac{1}{a^2} + \frac{1}{d^2}}. \quad (10-318)$$

Substitution of f_{101} from Eq. (10-318) in Eq. (10-316) proves that, at the resonant frequency, $W_e = W_m$. Thus,

$$W = 2W_e = 2W_m = \frac{\mu_0 H_0^2}{8} abd \left(\frac{a^2}{d^2} + 1\right). \quad (10-319)$$

To find P_L , we note that the power loss per unit area is

$$\mathcal{P}_{av} = \frac{1}{2} |J_s|^2 R_s = \frac{1}{2} |H_t|^2 R_s, \quad (10-320)$$

where $|H_t|$ denotes the magnitude of the tangential component of the magnetic field at the cavity walls. The power loss in the $z = d$ (back) wall is the same as that in the $z = 0$ (front) wall. Similarly, the power loss in the $x = a$ (left) wall is the same as that in the $x = 0$ (right) wall; and the power loss in the $y = b$ (upper) wall is the same as that in the $y = 0$ (lower) wall. We have

$$\begin{aligned} P_L &= \oint \mathcal{P}_{av} ds = R_s \left\{ \int_0^b \int_0^a |H_x(z=0)|^2 dx dy + \int_0^d \int_0^b |H_z(x=0)|^2 dy dz \right. \\ &\quad \left. + \int_0^d \int_0^a |H_x|^2 dx dz + \int_0^d \int_0^a |H_z|^2 dx dz \right\} \\ &= \frac{R_s H_0^2 a}{2} \left\{ \frac{a^2}{d} \left(\frac{b}{d} + \frac{1}{2} \right) + d \left(\frac{b}{a} + \frac{1}{2} \right) \right\}. \end{aligned} \quad (10-321)$$

Using Eqs. (10-319) and (10-321) in Eq. (10-315), we obtain

$$Q_{101} = \frac{\pi f_{101} \mu_0 a b d (a^2 + d^2)}{R_s [2b(a^3 + d^3) + ad(a^2 + d^2)]} \quad (\text{TE}_{101} \text{ mode}), \quad (10-322)$$

where f_{101} has been given in Eq. (10-318).

EXAMPLE 10-16 (a) What should be the size of a hollow cubic cavity made of copper in order for it to have a dominant resonant frequency of 10 (GHz)? (b) Find the Q at that frequency.

Solution

- a) For a cubic cavity, $a = b = d$: From Example 10-15 we know that TM_{110} , TE_{011} , and TE_{101} are degenerate dominant modes having the same field patterns and that

$$f_{101} = \frac{3 \times 10^8}{\sqrt{2}a} = 10^{10} \text{ (Hz).}$$

Therefore,

$$\begin{aligned} a &= \frac{3 \times 10^8}{\sqrt{2} \times 10^{10}} = 2.12 \times 10^{-2} \text{ (m)} \\ &= 21.2 \text{ (mm)}. \end{aligned}$$

- b) The expression of Q in Eq. (10-322) for a cubic cavity reduces to

$$Q_{101} = \frac{\pi f_{101} \mu_0 a}{3 R_s} = \frac{a}{3} \sqrt{\pi f_{101} \mu_0 \sigma}. \quad (10-323)$$

For copper, $\sigma = 5.80 \times 10^7 \text{ (S/m)}$, we have

$$Q_{101} = \left(\frac{2.12}{3} \times 10^{-2} \right) \sqrt{\pi 10^{10} (4\pi 10^{-7}) (5.80 \times 10^7)} = 10,700.$$

magnetic field
as that in the
same as that
is the same as

$$^2 dy dz$$

$$(10-321)$$

$$(10-322)$$

vity made of
Hz)? (b) Find

M_{110} , TE_{011} ,
patterns and

$$(10-323)$$

The Q of a cavity resonator is thus extremely high in comparison with that obtainable from lumped L-C resonant circuits. In practice, the preceding value is somewhat lower owing to losses through feed connections and surface irregularities.

10-7.3 CIRCULAR CAVITY RESONATOR

In a manner similar to the construction of a rectangular cavity resonator from a rectangular waveguide, a circular cylindrical resonator can be formed by placing conducting walls at both ends of a cylindrical waveguide. For simplicity, let us consider the TM_{01} mode in a circular waveguide of radius a at cutoff so that there is no variation in the z -direction. The ends of the waveguide are shorted by conducting plates at a distance d ($< 2a$) apart, forming a circular cylindrical cavity. The field components inside the cavity are, from Eqs. (10-218) and (10-224) by setting $n = 0$ and recalling Eq. (10-227),

$$E_z = C_0 J_0(hr) = C_0 J_0\left(\frac{2.405}{a}r\right), \quad (10-324)$$

$$H_\phi = -\frac{jC_0}{\eta_0} J'_0(hr) = \frac{jC_0}{\eta_0} J_1\left(\frac{2.405}{a}r\right), \quad (10-325)$$

where the relation $J'_0(hr) = -J_1(hr)$ has been used. The electric and magnetic field patterns for the TM_{010} mode in the circular cavity in both transverse and longitudinal sections are sketched in Fig. 10-25. Note from Eqs. (10-324) and (10-325) again that

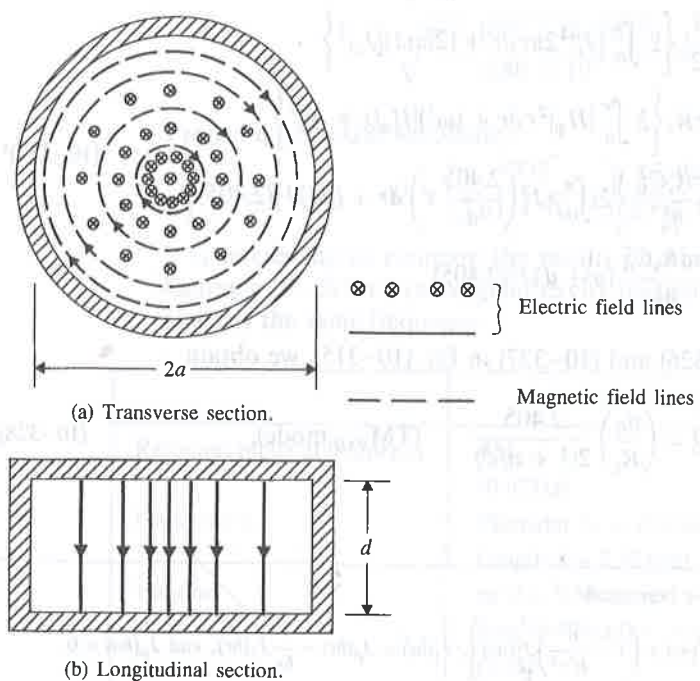


FIGURE 10-25
 TM_{010} field patterns in a circular cylindrical cavity resonator.

the electric and magnetic fields are in time quadrature, resulting in no power loss in the cavity walls.

In actuality the cavity walls do have a finite conductivity and a nonzero surface resistance. There will be power loss in the walls, and the cavity Q is not infinite. To calculate the cavity Q , we apply Eq. (10-315) and follow the same procedure as that used in the preceding subsection for the rectangular resonator. We will assume that the field intensities inside a low-loss cavity remain approximately the same as those for a lossless cavity.

Let us find the Q of a circular cylindrical cavity of radius a and length d for the TM_{010} mode. The field components have been given in Eqs. (10-324) and (10-325). The time-average stored energy is

$$\begin{aligned} W &= 2W_e = \frac{\epsilon_0}{2} \int_V |E_z|^2 dv \\ &= \frac{\epsilon_0 C_0^2}{2} (2\pi d) \int_0^a J_0^2\left(\frac{2.405}{a} r\right) r dr \\ &= (\pi \epsilon_0 d) C_0^2 \left[\frac{a^2}{2} J_1^2(2.405) \right]. \end{aligned} \quad (10-326)$$

The average power loss per unit area is given by Eq. (10-320). Here $H_t = H_\phi$, and there are radial surface currents J_r on the flat end faces and uniform longitudinal surface currents J_z on the inside of the cylindrical walls. We have

$$\begin{aligned} P_L &= \frac{R_s}{2} \left\{ 2 \int_0^a |J_r|^2 2\pi r dr + (2\pi ad) |J_z|^2 \right\} \\ &= \pi R_s \left\{ 2 \int_0^a |H_\phi|^2 r dr + (ad) |H_\phi(r=a)|^2 \right\} \\ &= \frac{\pi R_s C_0^2}{\eta_0^2} \left\{ 2 \int_0^a r J_1^2\left(\frac{2.405}{a} r\right) dr + (ad) J_1^2(2.405) \right\} \\ &= \frac{\pi a R_s C_0^2}{\eta_0^2} (a+d) J_1^2(2.405). \end{aligned} \quad (10-327)^{\dagger}$$

Substituting Eqs. (10-326) and (10-327) in Eq. (10-315), we obtain

$$Q = \left(\frac{\eta_0}{R_s} \right) \frac{2.405}{2(1+a/d)} \quad (\text{TM}_{010} \text{ mode}), \quad (10-328)$$

[†] The following relations have been used:

$$\int J_n^2(hr) r dr = \frac{r^2}{2} \left[J_n^2(hr) + \left(1 - \frac{n^2}{h^2 r^2} \right) J_n^2(hr) \right], \quad J'_1(hr) = J_0(hr) - \frac{1}{hr} J_1(hr), \quad \text{and} \quad J_0(ha) = 0.$$

no power loss
nonzero surface
not infinite. To
procedure as that
ill assume that
same as those

length d for the
(10-325).

$H_t = H_\phi$, and
m longitudinal

(10-327)[†]

(10-328)

$J_0(ha) = 0$.

where $R_s = \sqrt{\pi f \mu_0 / \sigma}$ is to be calculated at the resonant frequency for the TM_{010} mode, which is, from Eqs. (10-227) and (10-228),

$$(f)_{\text{TM}_{010}} = \frac{2.405}{2\pi a \sqrt{\mu_0 \epsilon_0}} = \frac{0.115}{a} \quad (\text{GHz}). \quad (10-329)$$

EXAMPLE 10-17 A hollow circular cylindrical cavity resonator is to be constructed of copper such that its length d equals its diameter $2a$. (a) Determine a and d for a resonant frequency of 10 (GHz) at the TM_{010} mode. (b) Find the Q of the cavity at resonance.

Solution

a) From Eq. (10-329) we have

$$\frac{0.115}{a} = 10,$$

or

$$a = 1.15 \times 10^{-2} \text{ (m)} = 1.15 \text{ (cm)}.$$

Thus,

$$d = 2a = 2.30 \text{ (cm)}.$$

$$\begin{aligned} \text{b)} \quad R_s &= \sqrt{\frac{\pi f \mu_0}{\sigma}} \\ &= \sqrt{\frac{\pi \times 10^{10} \times (4\pi 10^{-7})}{5.80 \times 10^7}} = 2.61 \times 10^{-2} \text{ (\Omega)}. \end{aligned}$$

From Eq. (10-328) we obtain

$$Q = \left(\frac{377}{2.61 \times 10^{-2}} \right) \frac{2.405}{2(1 + 1/2)} = 11,580.$$

It is interesting to compare the results of this example with those obtained in Example 10-16 for a rectangular cavity resonator of a comparable size that resonates at the same frequency.

	Circular Cavity	Rectangular Cavity
Resonant mode at frequency	TM_{010} 10 (GHz)	TE_{101} 10 (GHz)
Dimensions	Diameter $2a = 2.30$ (cm) Length $d = 2.30$ (cm)	$a = b = d = 2.12$ (cm)
Volume	$\pi a^2 d = 9.56$ (cm^3)	$a \times b \times d = 9.53$ (cm^3)
Total area	$2(\pi a^2) + (2\pi ad) = 24.93$ (cm^2)	$6a^2 = 26.97$ (cm^2)
Q	11,580	10,700

We see that these two cavities have approximately the same volume, but the total surface area of the rectangular cavity is about 8.2% larger. The larger surface area leads to a higher power loss and a lower Q . The Q of the circular cavity is approximately 8.2% higher.

Review Questions

- R.10-1** Why are the common types of transmission lines not useful for the long-distance signal transmission at microwave frequencies in the TEM mode?
- R.10-2** What is meant by a *cutoff frequency* of a waveguide?
- R.10-3** Why are lumped-parameter elements connected by wires not useful as resonant circuits at microwave frequencies?
- R.10-4** What is the governing equation for electric and magnetic field intensity phasors in the dielectric region of a straight waveguide with a uniform cross section?
- R.10-5** What are the three basic types of propagating waves in a uniform waveguide?
- R.10-6** Define *wave impedance*.
- R.10-7** Explain why single-conductor hollow or dielectric-filled waveguides cannot support TEM waves.
- R.10-8** Discuss the analytical procedure for studying the characteristics of TM waves in a waveguide.
- R.10-9** Discuss the analytical procedure for studying the characteristics of TE waves in a waveguide.
- R.10-10** What are *eigenvalues* of a boundary-value problem?
- R.10-11** Can a waveguide have more than one cutoff frequency? On what factors does the cutoff frequency of a waveguide depend?
- R.10-12** What is an *evanescent mode*?
- R.10-13** Is the guide wavelength of a propagating wave in a waveguide longer or shorter than the wavelength in the corresponding unbounded dielectric medium?
- R.10-14** In what way does the wave impedance in a waveguide depend on frequency:
 - For a propagating TEM wave?
 - For a propagating TM wave?
 - For a propagating TE wave?
- R.10-15** What is the significance of a purely reactive wave impedance?
- R.10-16** Can one tell from an $\omega-\beta$ diagram whether a certain propagating mode in a waveguide is dispersive? Explain.
- R.10-17** Explain how one determines the phase velocity and the group velocity of a propagating mode from its $\omega-\beta$ diagram.
- R.10-18** What is meant by an *eigenmode*?
- R.10-19** On what factors does the cutoff frequency of a parallel-plate waveguide depend?
- R.10-20** What is meant by the *dominant mode* of a waveguide? What is the dominant mode of a parallel-plate waveguide?

- R.10-21** Can a TM or TE wave with a wavelength 3 (cm) propagate in a parallel-plate waveguide whose plate separation is 1 (cm)? 2 (cm)? Explain.
- R.10-22** Compare the cutoff frequencies of TM_0 , TM_n , TM_m ($m > n$), and TE_n modes in a parallel-plate waveguide.
- R.10-23** Define *energy-transport velocity*.
- R.10-24** Does the attenuation constant due to dielectric losses increase or decrease with frequency for TM and TE modes in a parallel-plate waveguide?
- R.10-25** Discuss the essential differences in the frequency behavior of the attenuation caused by finite plate conductivity in a parallel-plate waveguide for TEM, TM, and TE modes.
- R.10-26** State the boundary conditions to be satisfied by E_z for TM waves in a rectangular waveguide.
- R.10-27** Which TM mode has the lowest cutoff frequency of all the TM modes in a rectangular waveguide?
- R.10-28** State the boundary conditions to be satisfied by H_z for TE waves in a rectangular waveguide.
- R.10-29** Which mode is the dominant mode in a rectangular waveguide if (a) $a > b$, (b) $a < b$, and (c) $a = b$?
- R.10-30** What is the cutoff wavelength of the TE_{10} mode in a rectangular waveguide?
- R.10-31** Which are the nonzero field components for the TE_{10} mode in a rectangular waveguide?
- R.10-32** Discuss the frequency-dependence of the attenuation constant caused by losses in the dielectric medium in a waveguide.
- R.10-33** Discuss the general attenuation behavior caused by wall losses as a function of frequency for the TE_{10} mode in a rectangular waveguide.
- R.10-34** Discuss the general attenuation behavior caused by wall losses as a function of frequency for the TM_{11} mode in a rectangular waveguide.
- R.10-35** Discuss the factors that affect the choice of the linear dimensions a and b for the cross section of a rectangular waveguide.
- R.10-36** What type of conducting diaphragm with an iris in a waveguide can provide a shunt capacitive susceptance? A shunt inductive susceptance? Explain.
- R.10-37** Under what circumstances does a Bessel's differential equation arise?
- R.10-38** Describe some general properties of Bessel functions of the first kind.
- R.10-39** Why are Bessel functions of the second kind not useful in the analysis of wave propagation in a hollow circular waveguide?
- R.10-40** Which mode is the dominant mode in a circular waveguide?
- R.10-41** It is claimed that the TE_{11} wave of a given frequency will propagate in a circular cylindrical pipe having a diameter only 76.5% of that required to support a TM_{01} wave of the same frequency. Explain.
- R.10-42** What is the distinctive characteristic of the attenuation constant of TE_{0n} modes in a circular waveguide?
- R.10-43** Why is it necessary that the permittivity of the dielectric slab in a dielectric waveguide be larger than that of the surrounding medium?

- R.10-44** What are dispersion relations?
- R.10-45** Can a dielectric-slab waveguide support an infinite number of discrete TM and TE modes? Explain.
- R.10-46** What kind of surface can support a TM surface wave? A TE surface wave?
- R.10-47** What is the dominant mode in a dielectric-slab waveguide? What is its cutoff frequency?
- R.10-48** Does the attenuation of the waves outside a dielectric slab waveguide increase or decrease with slab thickness?
- R.10-49** How does the time-average power transmitted in the transverse direction of a dielectric waveguide depend on the propagating mode in the guide?
- R.10-50** What kinds of Bessel functions are appropriate in the analysis of wave behavior in and around optical fibers? Explain.
- R.10-51** What are cavity resonators? What are their most desirable properties?
- R.10-52** Are the field patterns in a cavity resonator traveling waves or standing waves? How do they differ from those in a waveguide?
- R.10-53** In terms of field patterns, what does the TM_{110} mode signify? The TE_{123} mode?
- R.10-54** What is the expression for the resonant frequency of TM_{mnp} modes in a rectangular cavity resonator of dimensions $a \times b \times d$? Of TE_{mnp} modes?
- R.10-55** What is meant by *degenerate modes*?
- R.10-56** What are the modes of the lowest orders in a rectangular cavity resonator?
- R.10-57** Define the quality factor, Q , of a resonator.
- R.10-58** What fundamental assumption is made in the derivation of the formulas for the Q of cavity resonators?
- R.10-59** What field components exist in a circular cylindrical cavity operating in the TM_{010} mode?
- R.10-60** Will the Q of a circular cylindrical cavity resonator be higher or lower by increasing its length? Explain by physical reasoning.
- R.10-61** Explain why the measured Q of a cavity resonator is lower than the calculated value.

Problems

P.10-1 In studying the wave behavior in a straight waveguide having a uniform but arbitrary cross section it is expedient to find general formulas expressing the transverse field components in terms of their longitudinal components. We write

$$\mathbf{E} = \mathbf{E}_T + \mathbf{a}_z E_z,$$

$$\mathbf{H} = \mathbf{H}_T + \mathbf{a}_z H_z,$$

$$\nabla = \nabla_T + \mathbf{a}_z \frac{\partial}{\partial z},$$

where the subscript T denotes "transverse." Prove the following relations for time-harmonic excitation:

a) $\mathbf{E}_T = -\frac{1}{h^2} (\gamma \nabla_T E_z - \mathbf{a}_z j\omega \mu \times \nabla_T H_z)$ (10-330)

b) $\mathbf{H}_T = -\frac{1}{h^2} (\gamma \nabla_T H_z + \mathbf{a}_z j\omega \epsilon \times \nabla_T E_z),$ (10-331)

where h^2 is that given in Eq. (10-15).

P.10-2 For rectangular waveguides, use appropriate relations in Section 10-2 to:

- plot the universal circle diagrams relating u_g/u and β/k versus $f_c/f,$
- plot the universal graphs of $u/u_p, \beta/k,$ and λ_g/λ versus $f/f_c,$
- find $u_p/u, u_g/u, \beta/k,$ and λ_g/λ at $f = 1.25f_c.$

P.10-3 Sketch the $\omega-\beta$ diagrams of a parallel-plate waveguide separated by a dielectric slab of thickness b and constitutive parameters (ϵ, μ) for $TM_1, TM_2,$ and TM_3 modes. Discuss

- how b and the constitutive parameters affect the diagrams,
- whether the same curves apply to TE modes.

P.10-4 Obtain the expressions for the surface charge density and the surface current density for TM_n modes on the conducting plates of a parallel-plate waveguide. Do the currents on the two plates flow in the same direction or in opposite directions?

P.10-5 Obtain the expressions for the surface current density for TE_n modes on the conducting plates of a parallel-plate waveguide. Do the currents on the two plates flow in the same direction or in opposite directions?

P.10-6 Sketch the electric and magnetic field lines for (a) the TM_2 mode and (b) the TE_2 mode in a parallel-plate waveguide.

P.10-7 Determine the energy-transport velocity of the TE_n mode in a lossless parallel-plate waveguide in terms of its cutoff frequency.

P.10-8 A waveguide is formed by two parallel copper sheets— $\sigma_c = 5.80 \times 10^7$ (S/m)—separated by a 5 (cm) thick lossy dielectric— $\epsilon_r = 2.25, \mu_r = 1, \sigma = 10^{-10}$ (S/m). For an operating frequency of 10 (GHz), find $\beta, \alpha_d, \alpha_e, u_p, u_g,$ and λ_g for (a) the TEM mode, (b) the TM_1 mode, and (c) the TM_2 mode.

P.10-9 Repeat Problem P.10-8 for (a) the TE_1 mode and (b) the TE_2 mode.

P.10-10 For a parallel-plate waveguide,

- find the frequency (in terms of the cutoff frequency f_c) at which the attenuation constant due to conductor losses for the TM_n mode is a minimum,
- obtain the formula for this minimum attenuation constant,
- calculate this minimum α_c for the TM_1 mode if the parallel plates are made of copper and spaced 5 (cm) apart in air.

P.10-11 A parallel-plate waveguide made of two perfectly conducting infinite planes spaced 3 (cm) apart in air operates at a frequency 10 (GHz). Find the maximum time-average power that can be propagated per unit width of the guide without a voltage breakdown for

- the TEM mode,
- the TM_1 mode,
- the TE_1 mode.

P.10-12 Without deriving any new equations, roughly sketch the electric and magnetic field lines in a typical xy -plane of a rectangular waveguide for

- TM_{21} mode by an extension of Fig. 10-11(a).
- TE_{11} mode by an extension of Fig. 10-12(a).

The densities of the field lines should show the proper sine or cosine variations.

P.10-13 For an $a \times b$ rectangular waveguide operating at the TM_{11} mode,

- a) derive the expressions for the surface current densities on the conducting walls,
- b) sketch the surface currents on the walls at $x = 0$ and at $y = b$.

P.10-14 A standard air-filled S-band rectangular waveguide has dimensions $a = 7.21$ (cm) and $b = 3.40$ (cm). What mode types can be used to transmit electromagnetic waves having the following wavelengths?

- a) $\lambda = 10$ (cm)
- b) $\lambda = 5$ (cm)

P.10-15 Determine the energy-transport velocity of the TE_{10} mode in a lossless $a \times b$ rectangular waveguide in terms of its cutoff frequency.

P.10-16 Calculate and list in ascending order the cutoff frequencies (in terms of the cutoff frequency of the dominant mode) of an $a \times b$ rectangular waveguide for the following modes: TE_{01} , TE_{10} , TE_{11} , TE_{02} , TE_{20} , TM_{11} , TM_{12} , and TM_{22} (a) if $a = 2b$ and (b) if $a = b$.

P.10-17 An air-filled $a \times b$ ($b < a < 2b$) rectangular waveguide is to be constructed to operate at 3 (GHz) in the dominant mode. We desire the operating frequency to be at least 20% higher than the cutoff frequency of the dominant mode and also at least 20% below the cutoff frequency of the next higher-order mode.

- a) Give a typical design for the dimensions a and b .
- b) Calculate for your design β , u_p , λ_g , and the wave impedance at the operating frequency.

P.10-18 Calculate and compare the values of β , u_p , u_g , λ_g , and $Z_{\text{TE}_{10}}$ for a 2.5 (cm) \times 1.5 (cm) rectangular waveguide operating at 7.5 (GHz)

- a) if the waveguide is hollow,
- b) if the waveguide is filled with a dielectric medium characterized by $\epsilon_r = 2$, $\mu_r = 1$ and $\sigma = 0$.

P.10-19 An air-filled rectangular waveguide made of copper and having transverse dimensions $a = 7.20$ (cm) and $b = 3.40$ (cm) operates at a frequency 3 (GHz) in the dominant mode. Find (a) f_c , (b) λ_g , (c) α_c , and (d) the distance over which the field intensities of the propagating wave will be attenuated by 50%.

P.10-20 An average power of 1 (kW) at 10 (GHz) is to be delivered to an antenna at the TE_{10} mode by an air-filled rectangular copper waveguide 1 (m) long and having sides $a = 2.25$ (cm) and $b = 1.00$ (cm). Find

- a) the attenuation constant due to conductor losses,
- b) the maximum values of the electric and magnetic field intensities within the waveguide,
- c) the maximum value of the surface current density on the conducting walls,
- d) the total amount of average power dissipated in the waveguide.

P.10-21 Find the maximum amount of 10 (GHz) average power that can be transmitted through an air-filled rectangular waveguide— $a = 2.25$ (cm), $b = 1.00$ (cm)—at the TE_{10} mode without a breakdown.

P.10-22 Determine the value of (f/f_c) at which the attenuation constant due to conductor losses in an $a \times b$ rectangular waveguide for the TE_{10} mode is a minimum. What is the minimum obtainable α_c in a 2 (cm) \times 1 (cm) guide? At what frequency?

P.10-23 Derive Eq. (10-188), the formula for the attenuation constant due to conductor losses in an $a \times b$ rectangular waveguide for the TM_{11} mode. Determine the value of (f/f_c) at which this attenuation constant is a minimum.

P.10-24 Measurements at 10 (GHz) on an X-band air-filled rectangular waveguide ($a = 2.29$ cm, $b = 1.02$ cm) connected to an unknown load indicate a minimum electric field at 6 (cm) from the load and a standing-wave ratio (SWR) of 1.80. Find the location and the dimensions of a symmetrical capacitive iris required to bring the SWR to unity.

P.10-25 A solution of the Bessel's differential equation

$$\frac{d^2 R(r)}{dr^2} + \frac{1}{r} \frac{dR(r)}{dr} + R(r) = 0 \quad (10-332)$$

can be obtained by assuming $R(r)$ to be a power series in r as in Eq. (10-202), substituting it in the equation, and equating the sum of the coefficients of each power of r to zero. Find the solution and verify that it is consistent with $J_0(r)$ given in Eq. (10-204).

P.10-26 Starting from Maxwell's curl equations in simple media, verify Eq. (10-219) for TM modes in a circular waveguide.

P.10-27 Without deriving any new equations, roughly sketch the electric and magnetic field lines in a typical transverse plane of a circular waveguide

- a) for TM₁₁ mode by an extension of Fig. 10-20, and
- b) for TE₀₁ mode.
- c) Determine the cutoff frequencies for TM₁₁ and TE₀₁ modes in an air-filled circular waveguide of radius a .

P.10-28 Sketch the $\omega-\beta$ diagrams for TE₁₁ and TM₀₁ modes in a hollow circular waveguide of radius a . Discuss how the diagrams will be affected

- a) if a is doubled,
- b) if the waveguide is filled with a nonmagnetic medium having a dielectric constant ϵ_r .

P.10-29 For a straight waveguide with a semicircular cross section shown in Fig. 10-26,

- a) write the appropriate expression of E_z^0 for TM modes,
- b) write the appropriate expression of H_z^0 for TE modes.
- c) Explain how the eigenvalues of the respective modes can be determined.

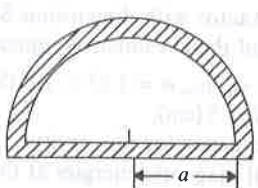


FIGURE 10-26
Cross section of a semicircular waveguide
(Problem P.10-29).

P.10-30 Show that electromagnetic waves propagate along a dielectric waveguide with a velocity between that of plane-wave propagation in the dielectric medium and that in the medium outside.

P.10-31 Find the solutions of Eq. (10-260) for k_y by plotting Eqs. (10-257) and (10-258) with $\alpha d/2$ versus $k_y d/2$ for $d = 1$ (cm) and $\epsilon_r = 3.25$ if (a) $f = 200$ (MHz), and (b) $f = 500$ (MHz). Determine β and α for the lowest-order odd TM modes at the two frequencies.

P.10-32 Repeat problem P.10-31 using Eq. (10-263). What can you conclude about the even TM modes?

P.10-33 For an infinite dielectric-slab waveguide of thickness d situated in air, obtain the instantaneous expressions of all the nonzero field components for even TM modes in the slab, as well as in the upper and lower free-space regions.

P.10-34 When the slab thickness of a dielectric-slab waveguide is very small in terms of the operating wavelength, the field intensities decay very slowly away from the slab surface, and the propagation constant is nearly equal to that of the surrounding medium.

- Show that if $k_y d \ll 1$, the following relations hold approximately for the dominant TE mode:

$$\beta \approx k_0,$$

$$\alpha \approx \frac{\mu_0 d}{2\mu_d} (k_d^2 - k_0^2),$$

where $k_d = \omega \sqrt{\mu_d \epsilon_d}$ and $k_0 = \omega \sqrt{\mu_0 \epsilon_0}$.

- For a slab of thickness 5 (mm) and dielectric constant 3, estimate the distance from the slab surface at which the field intensities have decayed to 36.8% of their values at the surface for an operating frequency of 300 (MHz).

P.10-35 For an infinite dielectric-slab waveguide of thickness d situated in free space, obtain the instantaneous expressions of all the nonzero field components for even TE modes in the slab, as well as in the upper and lower free-space regions. Derive Eq. (10-281).

P.10-36 A waveguide consists of an infinite dielectric slab (ϵ_d, μ_d) of thickness d that is sitting on a perfect conductor.

- What are the propagating modes and what are their cutoff frequencies?
- Obtain the phasor expressions for the surface current and surface charge densities on the conducting base for the propagating modes.

P.10-37 A round dielectric-rod waveguide of radius a , permittivity ϵ_1 , and permeability μ_1 is enveloped in a homogeneous medium characterized by permittivity ϵ_2 and permeability μ_2 .

- Write the expressions of all the field amplitudes for circularly symmetrical TE modes.
- Obtain the characteristic equation for these modes.

P.10-38 Given an air-filled lossless rectangular cavity resonator with dimensions 8 (cm) \times 6 (cm) \times 5 (cm), find the first twelve lowest-order modes and their resonant frequencies.

P.10-39 An air-filled rectangular cavity with brass walls— $\epsilon_0, \mu_0, \sigma = 1.57 \times 10^7$ (S/m)—has the following dimensions: $a = 4$ (cm), $b = 3$ (cm), and $d = 5$ (cm).

- Determine the dominant mode and its resonant frequency for this cavity.
- Find the Q and the time-average stored electric and magnetic energies at the resonant frequency, assuming H_0 to be 0.1 (A/m).

P.10-40 If the rectangular cavity in Problem P.10-39 is filled with a lossless dielectric material having a dielectric constant 2.5, find

- the resonant frequency of the dominant mode,
- the Q ,
- the time-average stored electric and magnetic energies at the resonant frequency, assuming H_0 to be 0.1 (A/m).

P.10-41 A rectangular cavity resonator of length d is constructed from an $a \times b$ rectangular waveguide. It is to be operated at the TE_{101} mode.

- For a fixed b , determine the relative magnitudes of a and d such that the cavity Q is maximized.
- Obtain an expression for Q as a function of a/b under the above conditions.

air, obtain the modes in the
slab surface, dium.
the dominant

distance from
of their values

free space,
or even TE modes
(10-281).

cess d that is

ies?
charge densities

permeability μ_1
l permeability μ_2 ,
electrical TE

nsions 8 (cm) \times
requencies.
 $\times 10^7$ (S/m)—

cavity.
ies at the

ss dielectric

nt frequency,

$a \times b$

at the cavity Q
nditions.

P.10-42 For an air-filled rectangular copper cavity resonator,

- calculate its Q for the TE_{101} mode if its dimensions are $a = d = 1.8b = 3.6$ (cm),
- determine how much b should be increased in order to make Q 20% higher.

P.10-43 Derive an expression for the Q of an air-filled $a \times b \times d$ rectangular resonator for the TM_{110} mode.

P.10-44 For an air-filled cylindrical cavity resonator of radius a and length d :

- Write the general expressions for the resonant frequencies and the corresponding wavelengths for TM_{mnp} and TE_{mnp} modes.
- For $d = a$, list the first seven modes that have the lowest resonant frequencies.

P.10-45 In some microwave applications, ring-shaped cavity resonators with a very narrow center part are used. A cross section of such a resonator is shown in Fig. 10-27, in which d is very small in comparison with the resonant wavelength. Assuming that this resonator can be represented approximately by a parallel combination of the capacitance of the narrow center part and the inductance of the rest of the structure, find

- the approximate resonant frequency,
- the approximate resonant wavelength.

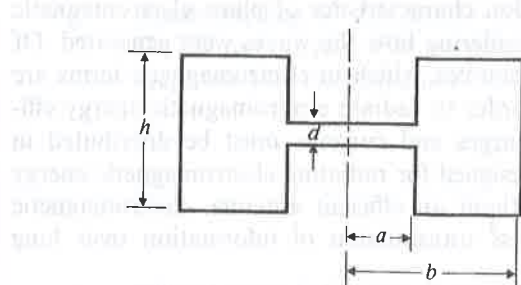


FIGURE 10-27
A ring-shaped resonator with a narrow center part (Problem P.10-45).